ADVANCES IN PHYSICS

A QUARTERLY SUPPLEMENT of the PHILOSOPHICAL MAGAZINE

EDITOR
PROFESSOR N. F. MOTT, M.A., D.Sc., F.R.S.

EDITORIAL BOARD
SIR LAWRENCE BRAGG, O.B.E., M.C., M.A., D.Sc., F.R.S.
SIR GEORGE THOMSON, M.A., D.Sc., F.R.S.
PROFESSOR A. M. TYNDALL, C.B.E., D.Sc., F.R.S.

UNIVERSITY OF HAWAII
LIBRARY
MAY 26 '58

VOLUME 7 APRIL 1958 NUMBER 26

PRICE per part £1
PRICE per annum £3 15*s.* 0*d.* post free

PRINTED AND PUBLISHED BY TAYLOR & FRANCIS LTD
RED LION COURT, FLEET ST., LONDON E.C.4

QC1
A36

A new International Journal

ERGONOMICS

HUMAN FACTORS IN WORK, MACHINE CONTROL AND EQUIPMENT DESIGN

General Editor

A. T. WELFORD

University of Cambridge, Psychological Laboratory, Downing Place, Cambridge

Editorial Board

H. Bastenier, *Belgium*; R. Bonnardel, Bernard Metz, *France*; E. A. Müller, *Germany*; M. G. Bennett, W. F. Floyd, W. E. Hick, Sir Charles Lovatt Evans, L. G. Norman, *Great Britain*; F. H. Bonjer, *Netherlands*; S. P. M. Forssman, *Sweden*; E. Grandjean, *Switzerland*; H. S. Belding, P. M. Fitts, *U.S.A.*

Contents of February, 1958

The Strength of the Lifting Action in Man. By R. J. Whitney, Medical Research Council Unit for Research on Climate and Working Efficiency, Department of Human Anatomy, University Museum, Oxford

Physiological Methods for Estimating the Physical Work Capacity in Workers especially of the Older Age Groups. By Irma Åstrand, Department of Physiology, Central Gymnastic Institute, Stockholm

Use of Competitive Tests as a Method of Performance Research. By M. J. Karvonen, Institute of Occupational Health, Helsinki

Research on Human Factors in Road Transport. By G. Grime, Road Research Laboratory, Department of Scientific and Industrial Research, Harmondsworth, Middlesex, England

Headlight Design. By R. L. Moore, Road Research Laboratory, Department of Scientific and Industrial Research, Harmondsworth, Middlesex, England

Simplifying the Operator's Task as a Controller. By A. W. Bailey, U.S. Naval Research Laboratory

The Relationship between Dial Size, Reading Distance and Reading Accuracy. By K. F. H. Murrell, W. D. Laurie and C. McCarthy, Naval Motion Study Unit

Price £1 5s. 0d. per part, plus postage
Subscription price per volume £4 15s. 0d. post free, payable in advance

Printed and Published by

TAYLOR & FRANCIS LTD

RED LION COURT, FLEET STREET, LONDON, E.C.4

Orders originating in U.S.A., and Canada should be sent to the Academic Press Inc., 111 Fifth Avenue, New York, 3, N.Y., U.S.A.

Journal of Electronics and Control

A Philosophical Magazine Associated Journal

Editor:
J. THOMSON, M.A., D.Sc., M.I.E.E., F.Inst.P.

Assistant Editor:
J. R. DAY, B.Sc.

Consultant Editor:
Professor N. F. MOTT, F.R.S.

Editorial Board:
Professor P. AIGRAIN (France)
Professor H. B. G. CASIMIR (Holland)
J. F. COALES (U.K.)
D. W. FRY (U.K.)
Dr. W. KLEIN (Germany)
Dr. R. KOMPFNER (U.S.A.)

Contents of March, 1958

Electronics Section

On the Space-Charge Divergence of an Axially Symmetric Beam. By E. R. Harrison, Atomic Energy Research Establishment, Harwell

The Transverse Magnetoresistance Effect in Indium Antimonide. By C. H. Champness Research Department, Metropolitan-Vickers Electrical Co. Ltd.

Non-Linear Phenomenological Theory of Plasma Oscillations. By Louis Gold, Lincoln Laboratory, Massachusetts Institute of Technology, Lexington, Massachusetts

A High Frequency Germanium Drift Transistor by Post Alloy Diffusion. By J. S. Lamming, Communication from the Staff of the Research Laboratories of The General Electric Company Limited, Wembley, England

The Negative Glow and Cathode Spots in Low Pressure Arcs. By M. A. Cayless, Research Laboratory, The British Thomson-Houston Co. Ltd., Rugby

Control Section

B.S.I.R.A. Open Days Address. Nuclear Instrumentation. By Sir John Cockcroft, Atomic Energy Research Establishment, Harwell

Circuit Analogues of Suhl-type Masers. By K. W. H. Stevens, University of Nottingham

Amplification using a Precessing Magnetic Moment. By K. W. H. Stevens, University of Nottingham

Price per part £1 5s. plus postage
Price per volume £7 post free, payable in advance
6 monthly issues per volume

Printed and Published by

TAYLOR & FRANCIS LTD
RED LION COURT, FLEET STREET, LONDON, E.C.4

Orders originating in U.S.A. and Canada should be sent to the Academic Press Inc., 111 Fifth Avenue, New York, 3, N.Y., U.S.A.

A HISTORY OF MATHEMATICS

from antiquity to the early nineteenth century

by J. F. SCOTT, B.A., D.Sc., Ph.D.
Vice-Principal of St. Mary's College, Strawberry Hill, Twickenham, Middlesex

Author of *The Scientific Work of René Descartes* (1596–1650), *Mathematical Work of John Wallis, D.D., F.R.S.* (1616–1703), and other works

CONTENTS: Mathematics in Antiquity—Greek Mathematics—The Invention of Trigonometry—Decline of Alexandrian Science and the Revival in Europe—Mathematics in the Orient—Progress of Mathematics during the Renaissance—New Methods in Geometry—The Rise of Mechanics—The Invention of Decimal Fractions and of Logarithms—Newton and the Calculus—Taylor and Maclaurin, the Bernoullis and Euler, Related Advances—The Calculus of Variations, Probability, Projective Geometry, Non-Euclidean Geometry—Theory of Numbers—Lagrange, Legendre, Laplace, Gauss.

This volume is intended primarily to help students who desire to have a knowledge of the development of the subject but who have too little leisure to consult original works and documents. The author has availed himself of the facilities afforded by The Royal Society and other learned Societies to reproduce extracts from manuscripts and many scarce works.

$9\frac{3}{4} \times 6\frac{3}{4}$

Price 3 guineas

Printed and Published by

TAYLOR & FRANCIS LTD.
RED LION COURT, FLEET STREET, LONDON, E.C.4



THE MATHEMATICAL WORKS OF JOHN WALLIS, D.D., F.R.S.

by

J. F. SCOTT, Ph.D., B.A.

"His work will be indispensable to those interested in the early history of The Royal Society. I commend to all students of the Seventeenth Century, whether scientific or humane, this learned and lucid book."—Extract from foreword by Prof. E. N. da C. Andrade, D.Sc., Ph.D., F.R.S.

Recommended for publication by University of London

12/6 net

Printed and Published by

TAYLOR & FRANCIS, LTD.
RED LION COURT, FLEET STREET, LONDON, E.C.4.

The Philosophical Magazine

First Published in 1798

Editor:
PROFESSOR N. F. MOTT, M.A., D.Sc., F.R.S.

Editorial Board:
SIR LAWRENCE BRAGG, O.B.E., M.C., M.A., D.Sc., F.R.S.
SIR GEORGE THOMSON, M.A., D.Sc., F.R.S.
PROFESSOR A. M. TYNDALL, C.B.E., D.Sc., F.R.S.

Contents of April, 1958

The Magnetic Susceptibility and Electrical Resistivity of Some Transition Metal Silicides. By D. A. Robins, Research Laboratories of The General Electric Company, Limited, Wembley, England

$\pi^{\pm} \rightarrow \pi^{0} + e^{\pm} + \nu + 8m_e c^2$? By E. Feenberg and H. Primakoff, Washington University, St. Louis, Missouri, U.S.A.

The Decoration of Dislocations in Crystals of Silver Chloride with Gold. By J. T. Bartlett and J. W. Mitchell, H. H. Wills Physical Laboratory, University of Bristol

The Thermal and Electrical Resistivity of Bismuth and Antimony at Low Temperatures. By G. K. White and S. B. Woods, Division of Pure Physics, National Research Council, Ottawa, Canada

The Polarization of Luminescence in Diamond. By R. J. Elliott, I. G. Matthews and E. W. J. Mitchell, Physics Research Laboratory, The University of Reading

On a Feature of Galactic Radio Emission. By Harriet Tunmer, Cavendish Laboratory, Cambridge

Observations on Extensive Air Showers. V. The Size Spectrum of Showers containing 3×10^6–3×10^8 Particles. By T. E. Cranshaw, J. de Beer, W. Galbraith and N. A. Porter, Atomic Energy Research Establishment, Harwell

Plastic Deformation of Nickel Single Crystals at Low Temperatures. By Peter Haasen, Institute for the Study of Metals, University of Chicago, U.S.A., and Max-Planck-Institut für Metallforschung, Stuttgart, Germany

Price per part £1 5s.

Price per annum £13 10s. post free, payable in advance

Printed and Published by

TAYLOR & FRANCIS LTD

RED LION COURT, FLEET STREET, LONDON, E.C.4

Physics in Medicine and Biology

A Taylor and Francis International Journal published in association with the Hospital Physicists' Association

Editor: J. E. ROBERTS, D.Sc.
Consultant Editor: Professor N. F. MOTT, F.R.S.

Editorial Board

R. BONET-MAURY
J. DAINTY
H. E. JOHNS
W. A. LANGMEAD
D. A. MCDONALD
J. S. MITCHELL
G. J. NEARY
B. RAJEWSKY
J. ROTBLAT
S. ROWLANDS
H. P. SCHWAN
R. SIEVERT
F. W. SPIERS
J. F. TAIT
A. J. H. VENDRIK

Contents of January, 1958

The Relative Performances of Large Volume Plastic and Liquid Scintillators. By P. M. Bird, M.Sc., Ph.D., Department of National Health and Welfare, Ottawa, Ontario, Canada and P. R. J. Burch, M.A., Ph.D., Department of Medical Physics, University of Leeds, The General Infirmary, Leeds, 1, England

Selection of Gamma-Ray Emitting Isotopes as Permanent Implants in the Treatment of Cancer. By Lionel Cohen, General Hospital, Johannesburg, South Africa

Determination of the Stopping Power of Some Light Elements for 14·5 MEV Electrons. By G. W. Dolphin, B.Sc., Ph.D., Physics Department, St. Bartholomew's Hospital Medical College, London, E.C.1

The Assay of Mixtures of Sodium-24 and Potassium-42 in Clinical Tracer Studies; with Particular Reference to the Measurement of Exchangeable Sodium and Potassium. By D. S. Munro, M.D., M.R.C.P., H. Rensehler, M.D., and G. M. Wilson, M.D., F.R.C.P., Department of Pharmacology and Therapeutics, University of Sheffield

The Half-Life of Iodine-131. By L. Burkinshaw, Ph.D., Department of Radiotherapeutics, University of Cambridge

The Breakage of Tradescantia Chromatids by Ionizing Radiations. By John Read, Ph.D., The Hugh Adam Research Department of the Medical School and the New Zealand Branch of the British Empire Cancer Campaign, University of Otago, Dunedin, New Zealand

An Electrical Impedance Method for the Determination of Vascular Changes in the Terminal Vascular Bed of Membranous Structures. By Frederick M. Liebman and Sam Bagno, from the Department of Physiology, Graduate School of Arts and Science, New York University and the Murry and Leonie Guggenheim Foundation Institute for Dental Research, New York University, College of Dentistry, New York City

The Calibration of Infra-Red Gas Analysers for use in the Estimation of Carbon Dioxide. By P. W. Ramwell, B.Sc. and J. B. Dawson, Ph.D., University of Leeds

Subscription price per volume £3 10s. post free, payable in advance
4 parts per volume—£1 per part plus postage

Printed and Published by
TAYLOR & FRANCIS LTD
RED LION COURT, FLEET STREET, LONDON, E.C.4

Orders originating in U.S.A. and Canada should be sent to the Academic Press Inc., 111 Fifth Avenue, New York, 3, N.Y., U.S.A.

CONTENTS

The Physics of Water and Ice. By B. J. Mason, Warren Research Fellow of the Royal Society, Imperial College, London i

The Structure of Ice–I, as Determined by X-Ray and Neutron Diffraction Analysis. By P. G. Owston, Imperial Chemical Industries Ltd., Akers Research Laboratories, The Frythe, Welwyn, Herts. . . 171

Electron Diffraction Investigations into the Cubic and other Structural Forms of Ice. By M. Blackman and N. D. Lisgarten, Physics Department, Imperial College, London, S.W.7 189

The Infra-Red and Raman Spectra of Ice. By Nathan Ockman, Department of Chemistry, Harvard University 199

The Supercooling and Nucleation of Water. By B. J. Mason, Warren Research Fellow of The Royal Society, Imperial College, London 221

The Growth of Ice Crystals from the Vapour and the Melt. By B. J. Mason, Warren Research Fellow of the Royal Society, Imperial College, London 235

The Mechanical Properties of Ice. I. The Plastic Properties of Ice. By J. W. Glen, Physics Department, University of Birmingham 254

The Mechanical Properties of Ice. II. The Elastic Constants and Mechanical Relaxation of Single Crystal Ice. By R. W. B. Stephens, Physics Department, Imperial College, London . . 266

Thermal Conductivities and Expansion Coefficients of Water and Ice. By R. W. Powell, National Physical Laboratory, Teddington . 276

ADVANCES IN PHYSICS

A QUARTERLY SUPPLEMENT
of the
PHILOSOPHICAL MAGAZINE

VOLUME 7 APRIL 1958 NUMBER 26

INTRODUCTORY NOTE

The Physics of Water and Ice

By B. J. MASON
Warren Research Fellow of the Royal Society, Imperial College, London

ALTHOUGH water, in its solid, liquid and vapour phases, is the most common and the most vital of all natural substances, much concerning its structure, properties and behaviour has yet to be properly investigated and explained. Many of its anomalous characteristics, such as the liquid having a greater density than the solid, with a maximum value at 4°C, the solid and liquid having very high values of latent heat, specific heat and dielectric constant, the high thermal conductivity of the liquid and its properties as an ionizing solvent *par excellence*, have yet to be satisfactorily interpreted in terms of the arrangement of the molecules and the forces between them.

It is the aim of this series of articles to provide an up-to-date account of our knowledge concerning the structure, formation and growth of ice crystals, and of their mechanical, thermal and electrical properties.

The atomic arrangement in ice, at different temperatures, being fundamental to a study of its properties, is discussed in the first three papers which review the information provided by x-ray, neutron and electron diffraction, by infra-red and Raman spectra, for both ordinary and heavy ice. All the evidence tends to confirm, for hexagonal ice-I, Pauling's statistical picture of two 'half-hydrogen atoms' lying along each oxygen–oxygen bond. The convergence of opinion towards this view, which has very important theoretical implications, is perhaps one of the most satisfactory results of recent work. That water may condense, at temperatures below about −120°C, into a diamond-type cubic lattice, and

into an amorphous, non-crystalline structure at temperatures below about $-140°C$, is now firmly established; the thermodynamic status of these new forms of ice is of considerable interest.

The supercooling of water which, for micron-size droplets, may be extended to $-40°C$, and the onset of both homogeneous and heterogeneous nucleation, have been extensively studied of late largely because of their fundamental importance in the physics of rain formation. The rather clear-cut experimental relationships which have recently emerged for water may provide a valuable guide to the behaviour of other systems, for example the solidification of metals.

The fact that ice crystals, growing from the vapour, exhibit a remarkable five-fold change of habit over the temperature range 0°C to $-25°C$, apart from its importance in the study of snow-crystal development, provides a difficult and fascinating problem in crystal physics.

As for the mechanical, thermal and electrical properties of ice, the fundamental need here is for accurate, reliable and reproducible experimental data on such parameters as elastic constants and mechanical relaxation, thermal expansion and conductivity, electrical conductivity and dielectric measurements, especially for single crystals where anisotropic effects will be of particular interest. The papers by Glen and Stephens, and by Powell, besides summarizing the present position, point clearly to the need for further measurements. This survey was to have included a contribution on dielectric constant and electrical conductivity measurements for single-crystalline ice and their theoretical interpretation in terms of the existence defects in the ice lattice, but this will now appear in a later issue. It is hoped that later reviews will deal with water in the liquid state.

The Structure of Ice–I, as Determined by X-Ray and Neutron Diffraction Analysis

by P. G. Owston
Imperial Chemical Industries Ltd., Akers Research Laboratories, The Frythe, Welwyn, Herts.

§ 1. Introduction

It is at first sight surprising that the structure of ice, which is chemically so simple, should present a difficult problem. Ice was studied by x-ray methods very early in the history of x-ray crystallography (Rinne 1917), and the geometrical arrangement of the oxygen atoms, which are the principal diffracting centres for x-rays, was correctly deduced by W. H. Bragg in 1922. There has nevertheless remained much uncertainty about the details of the structure, and much of the knowledge we have, especially so far as the hydrogen atoms are concerned, has until recently come less from diffraction studies than from infra-red spectra and dielectric and other physical measurements. This was partly because of the experimental difficulties of preparing and handling ice crystals suitable for x-ray work, but still more because x-ray analytical methods were for long inadequate to deal with the hydrogen atoms. It was not until about 1948 that it was generally recognized that hydrogen atoms could be detected at all by x-ray methods. It is often not important if the hydrogen atoms are neglected, for instance in molecular organic compounds, but in hydroxy compounds and especially in ice the hydrogen atoms have such structural importance that they cannot be neglected.

More recently it has become apparent that neutron diffraction is of special usefulness in detecting hydrogen atoms, and its contribution is considered later in this review. It is first necessary to consider the various structures that have been proposed for ice, together with the evidence for them, both summarizing and extending a previous review by the author (Owston 1951 a).

§ 2. The Crystal Symmetry of Ice

In the interpretation of the diffraction patterns of crystals, whether due to x-rays, electrons, or neutrons, it is important to know the symmetry of the crystal. This can sometimes be deduced from the symmetry of the patterns themselves, but by no means always. X-ray photographs of ice are a particularly unreliable guide because the hydrogen atoms scatter x-rays so weakly, and the evidence must therefore come from other observations.

There has been a consequent lack of unanimity regarding the crystal symmetry of ice, and this has resulted in a number of structures being postulated, each having one of the various proposed symmetries. Laue photographs have always been found to have the hexagonal symmetry $6/mmm(D_{6h})$ (Rinne 1917, Barnes 1929, Lonsdale and Owston 1948, Owston 1949). An apparent exception is given by Seljakov (1936 a, b, 1937) who found that some of his specimens gave trigonal Laue patterns, and was thus led to postulate the existence of two polymorphic forms of ice. It has since been shown that the trigonal patterns were almost certainly due to hexagonal crystals set in a particular orientation in which a Laue pattern of deceptively trigonal appearance is obtained (Lonsdale and Owston 1948, Berger and Saffer 1953).

The external shape of crystals often allows the crystal class to be determined, but the shapes of ice crystals are so varied that no reliable conclusion can be reached. Most snow crystals which have a regular shape have the full holohedral hexagonal symmetry, though crystals of several less symmetrical forms have occasionally been reported (Dorsey 1940). Recent work has shown how the shapes of ice crystals can be changed by small amounts of impurities (Schaefer 1949, Hallett and Mason 1958), and even more remarkably by small variations in the temperature and degree of supersaturation of the atmosphere (see Mason's article in this volume). Even under comparatively constant conditions the shapes of crystals differ, and, for instance, pyramidal and prismatic crystals can grow side by side (Adams 1930 ; Shaw and Mason 1955).

From these last observations on crystals grown in the laboratory one of three results follows: either ice has the full dihexagonal bipyramidal symmetry $6/mmm(D_{6h})$, the other pyramidal or uniterminal crystals being due to accidental causes during crystal growth: or conversely the true symmetry is dihexagonal pyramidal $6mm(C_{6v})$, the prismatic crystals being twins: or thirdly, both are true forms, and ice is polymorphic. From the fact that the two forms occur together, and that there is no sharp discontinuity in any of the physical properties of ice or supercooled water, certainly at temperatures above about $-40°C$, polymorphism is improbable except at very low temperatures or very high pressures.

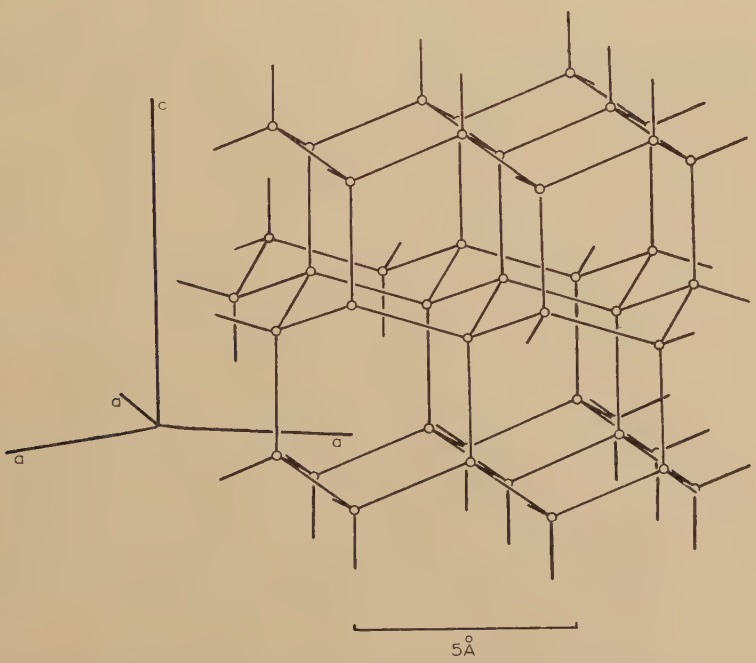
If the second conclusion is correct, and ice crystals have a uniterminal axis they should show pyro- and piezo-electric properties. Pyroelectricity has never been observed in ice (Wooster 1933, Mason and Owston 1952), and whilst some workers claim to have observed piezoelectricity (Rossmann 1950, Kumm 1951) the most recent and sensitive measurements leave no doubt that ice is not measurably piezo-electric (Mason and Owston 1952, Steinemann 1953, Rossberg and Magun 1957).

It seems probable that ice is centrosymmetric, belonging to the dihexagonal bipyramidal class $6/mmm(D_{6h})$. There remains a possibility, though a small one, that it has a lower symmetry but there is at present no reliable evidence for this, and any structure which requires a lower symmetry must, unless supported by other evidence, be regarded as doubtful.

§ 3. The Structure of Ice

Much of the discussion on ice has been based on the work of Barnes (1929) who studied single crystals of ice by x-ray methods. When the indices of the reflections were listed, some were seen to be absent; this is due to the regular arrangement of the atoms in the unit cell, and in this case the absences fall systematically into two groups. The first group is characteristic of the group-space symmetries $P6_3/mmc(D^4_{6h})$ and $P\bar{6}2c(D^4_{3h})$ with four molecules per unit cell, whilst from the second group the exact positions of the oxygen atoms, which are the principal diffracting centres for x-rays, can be found. Two assumptions are necessary for this: the first, which is explicitly stated by Barnes, is that no two oxygen atoms can be less than 1·20 Å apart, as in other crystal structures; the second, which was only implicitly assumed, is that hydrogen atoms do not scatter x-rays.

Fig. 1



The arrangement of the oxygen atoms in ice in layers perpendicular to the hexagonal axis, showing the tetrahedral coordination.

In this way the structure shown in fig. 1 was deduced; it has the symmetry $P6_3/mmc$, though exactly the same result is obtained if one begins by assuming the lower symmetry $P\bar{6}2c(D^4_{3h})$; this is true also of $P6_322(D^6_6)$, a possible space-group which was overlooked by Barnes. The principal characteristic of this arrangement is that each molecule is at the centre of a regular tetrahedron with four molecules, each 2·76 Å away, at the apices.

It shares this characteristic with the cubic low-temperature form of ice, an important difference being that in the hexagonal form the molecules are all concentrated close to planes which are perpendicular to the principal, hexagonal, axis. This layer structure is responsible for many of the physical properties of ice, such as its ready cleavage, the flow of glaciers which occurs by the gliding of the layers over each other, and the ease with which it forms large sheets on water, the layers being parallel to the surface (Bragg 1922, 1938, Owston 1951 b).

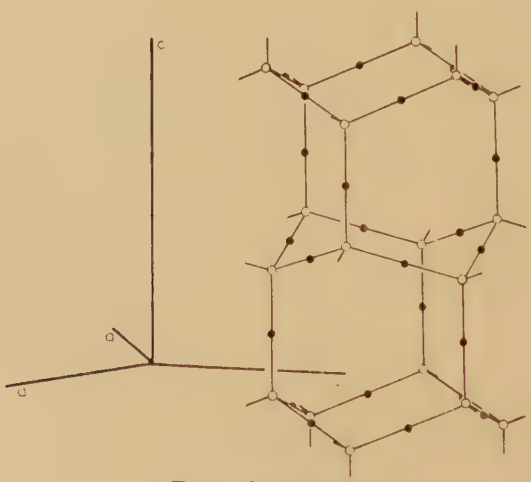
Having established the positions of the atoms by considering the reflections which were absent, Barnes confirmed them by showing that the intensities of the reflections which were present agreed with the calculated values. He also attempted to use the intensities to decide whether the oxygen atoms are present as atoms or as ions $O^{=}$, but obtained no conclusive result.

§ 4. The Positions of the Hydrogen Atoms

4.1. *Barnes' Structure*

Though there was no evidence from these diffraction experiments alone about the positions of the hydrogen atoms, it seemed reasonable to suppose

Fig. 2

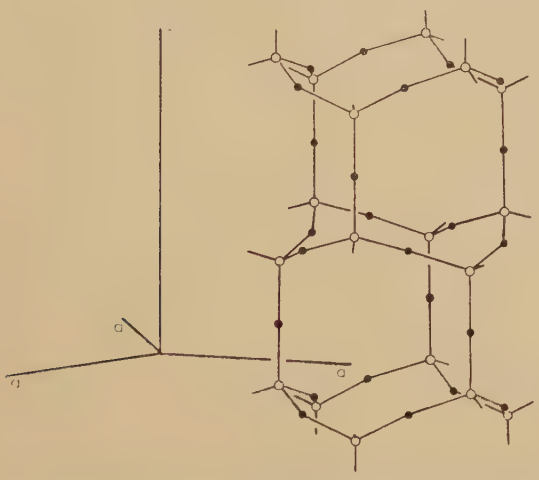


Barnes' structure.

that the forces which hold the oxygen atoms in this highly symmetrical configuration will affect the placing of the hydrogen atoms. The positions of the hydrogen atoms should then be related to the symmetry of the oxygen atom lattice and this would be most simply accomplished by placing a hydrogen atom midway between each pair of oxygen atoms (fig. 2). Since the distance between neighbouring oxygen atoms, 2·76 Å, is only a little greater than the normal distance between oxygen ions, this is

a possible structure, if it is assumed that in ice the water molecule is ionized to form $2H^+ + O^=$, and that the hydrogen ions occupy a negligible volume in the crystal. In this structure, usually known as Barnes' structure, the symmetry remains as $P6_3/mmc$. Alternatively, the hydrogen ions might be slightly displaced from the oxygen–oxygen line, but still equidistant from the two oxygen atoms, resulting in the alternative symmetry $P\bar{6}2c$ (fig. 3). There appears to be no physical reason why they should occupy these positions, however, since they would then be in an unsymmetrical electrostatic field.

Fig. 3



Barnes' alternative structure, with the hydrogen atoms displaced from the O–O line.

Various objections have been raised to Barnes' structure. The first, mainly of a geometrical nature, was put forward by Brandenberger (1930), who pointed out that the theory of symmetry permits several other structures, though all are less symmetrical than that of fig. 2; here also it was assumed that hydrogen atoms have no effect on the x-ray diffraction patterns. A second objection (Kinsey and Sponsler 1933) is that crystals composed of ions usually melt at a high temperature, and the melt has a high electrical conductivity; it is improbable, therefore, that ice consists of ions.

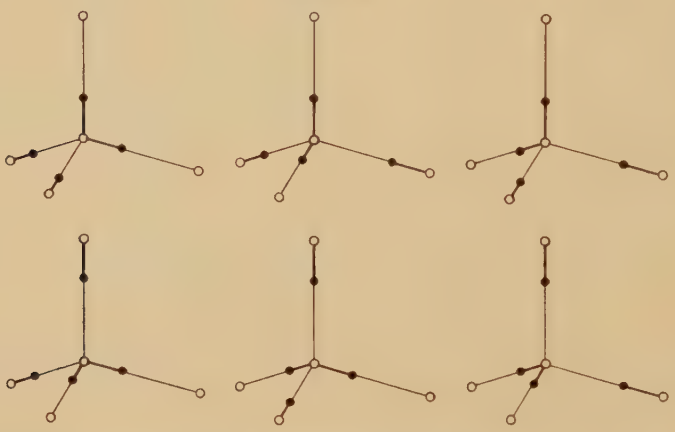
4.2. *Bernal and Fowler's Structure*

The problem was reviewed in 1933 by Bernal and Fowler, who pointed out that the Raman and infra-red spectra of steam show that it consists of molecules of water, with the hydrogen atoms 0·96 Å from the oxygen atoms. The spectra of water and ice are essentially similar to those of steam, apart from some line-broadening due to interaction of the molecules; this has since been confirmed and amplified by the work of Fox and Martin

(1940) and Dennison (1940). It follows that ice also consists of molecules and does not contain hydrogen ions (apart from the very small concentration due to slight ionization, as in water). The same conclusion was reached by comparing the dielectric properties of ice and water.

The dielectric measurements also showed that in ice near 0°C most of the water molecules are not free to rotate, but are held in fixed orientations by fairly strong forces—comparable in fact with the forces which hold the crystal together, as estimated from the heat of sublimation of ice. This can only occur if the hydrogen atoms are in fixed positions, the most stable position being, again, along the lines joining the centres of the oxygen atoms, 0·96 Å from one oxygen atom and 1·80 Å from the other; each oxygen atom then has two hydrogen atoms 0·96 Å away, and two others 1·80 Å away, one from each of two neighbouring molecules (fig. 4).

Fig. 4

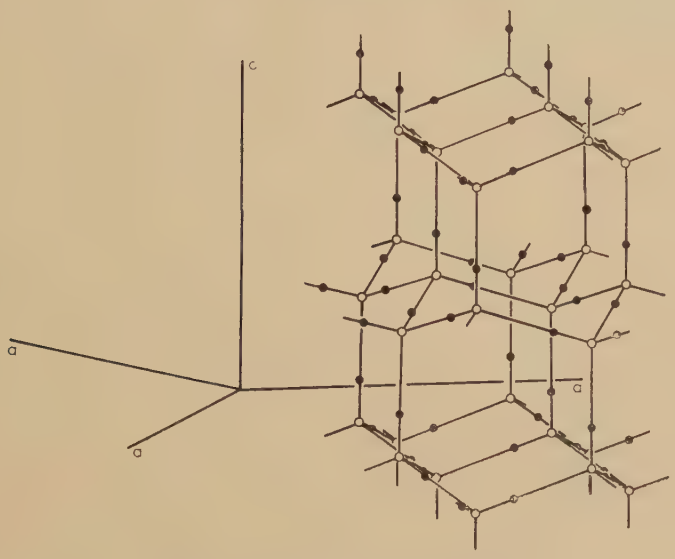


The six possible arrangements of the hydrogen atoms on the four bonds round each oxygen atom.

The number of possible arrangements of molecules bound together by these unsymmetrical links is very large indeed, though most of them have no regularly repeating unit of structure. Some are regular, and one of them, usually known as the Bernal–Fowler structure, is shown in fig. 5. This is the simplest structure with the hydrogen atoms in fixed positions which has hexagonal symmetry (space-group $P6_3cm(C_{6v}^3)$). The unit cell contains twelve H_2O molecules, being three times larger than Barnes' unit cell. The arrangement of the oxygen atoms is exactly the same as in Barnes' model, the lower symmetry being due to the less symmetrical placing of the hydrogen atoms. The numerical values of the variable y and z coordinates for the hydrogen atoms given by Bernal and Fowler are incorrect, leading to an O H bond-length of 0·82 Å rather than the correct value of about 0·96 Å, but this does not affect the principles of their discussion.

This proposed structure is polar, and should lead to piezo- and pyro-electric properties. Since these are probably absent in ice, Bernal and Fowler advanced the structure with reservations, observing that so regular an arrangement is unlikely to be the correct structure, at least at temperatures just below the melting-point. They considered that the

Fig. 5



Bernal and Fowler's structure.

most probable structure is one of the non-regular ones, "crystalline only in the position of its molecules [i.e. in the positions of the oxygen atoms], but glass-like in their orientation [i.e. in the arrangement of the hydrogen atoms]".

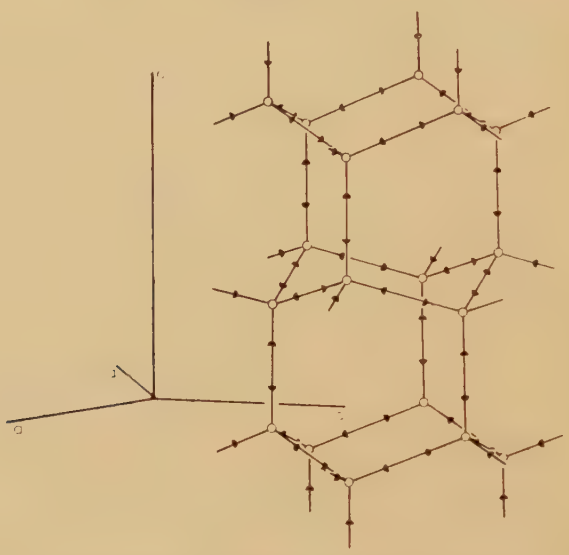
4.3. *The Statistical Structure*

In the 'glass-like' arrangements, the positions of all the atoms in the crystals must be stated in order to specify the structure, and it can be shown that a crystal containing N molecules can have any of $(\frac{3}{2})^N$ possible structures, including the small number of regular structures (Pauling 1935, Slater 1941, Bjerrum 1951). In deriving this number it is assumed that N is very large and that boundary conditions can be ignored. Since the immediate surroundings of all the molecules are the same whatever the molecular orientation (see fig. 4), all the molecules have the same potential energy, and the energy of all the possible structures is the same. All the structures are thus equally probable and it follows that ice should have a residual entropy of $k \ln (\frac{3}{2})^N = R \ln (\frac{3}{2}) = 0{\cdot}806$ cal/mole degree.

This has been confirmed experimentally, the values found being $0{\cdot}82 \pm 0{\cdot}15$ cal/mole degree for ordinary ice, and $0{\cdot}77 \pm 0{\cdot}10$ cal/mole degree for 'heavy' ice (D_2O) (Giauque and Ashley 1933, Giauque and Stout 1936, Long and Kemp 1936).

The dielectric properties of ice (Auty and Cole 1952) show that the orientation of the molecules is constantly changing at temperatures above about $-60°$C, and that the crystal is therefore constantly changing from one of the $(\frac{3}{2})^N$ configurations to another; the exact mechanism of the changes has been much discussed, but will not be considered in this

Fig. 6



The Statistical or Half-hydrogen Structure.

review. The diffraction effects produced by a dynamically irregular structure like this will be the same as would be given by the mean structure, statistically averaged in time and over the whole volume of the crystal (Lonsdale 1946). This mean structure, known variously as the Statistical, Half-hydrogen, or Pauling structure, consists of molecules containing one oxygen atom with four 'half-hydrogen' atoms arranged tetrahedrally round it (fig. 6). The unit cell of this structure contains four molecules, is the same size as that of Barnes' structure, and has the symmetry $P6_3/mmc$. The diffraction evidence for this and the other structures described will be considered later.

4.4. *Other Model Structures*

The Statistical structure was deduced on the assumption that the immediate surroundings of all the molecules are identical, whatever the molecular orientation. This has been criticised by Bjerrum (1951) on

two grounds. Firstly he points out that if the tetrahedral arrangement of the molecules is exactly regular, the axial ratio of the unit cell should be $c/a = \sqrt{(8/3)} = 1{\cdot}633$. Accurate measurements on both ice (H_2O ice) and heavy ice (D_2O ice) suggest that at temperatures between 0°C and −66°C the ratio is considerably less than this (Megaw 1934, Truby 1955), though at temperatures of −110°C and lower the ratio is close to the theoretical value (Vegard and Hillesund 1942, Blackman and Lisgarten 1957, see table 1). If the ratio is less than 1·633 the intermolecular bonds

Table 1. The Cell-Dimensions of Ice (Å)

a	c	c/a	Temp. °C	Reference
H_2O Ice				
4·5239 ± 0·0014	7·3690 ± 0·0012	1·629	0	Megaw (1934)
4·5071 ± 0·0005	7·3327 ± 0·0009	1·627	−46	Truby (1955)
4·5189 ± 0·002	7·355 ± 0·0035	1·628	−66	Megaw (1934)
4·493 ± 0·004	7·337 ± 0·006	1·633	−110	Blackman and Lisgarten (1957)†
4·480 ± 0·004	7·310 ± 0·002	1·632	−185	Vegard and Hillesund (1942)
D_2O Ice				
4·5279 ± 0·0014	7·3721 ± 0·0012	1·628	4	Megaw (1934)
4·5269 ± 0·0014	7·3706 ± 0·0012	1·628	0	
4·5159 ± 0·002	7·355 ± 0·0035	1·629	−66	
4·495 ± 0·004	7·335 ± 0·007	1·632	−110	Blackman and Lisgarten (1957)†
4·483 ± 0·003	7·318 ± 0·010	1·632	−185	Vegard and Hillesund (1942)

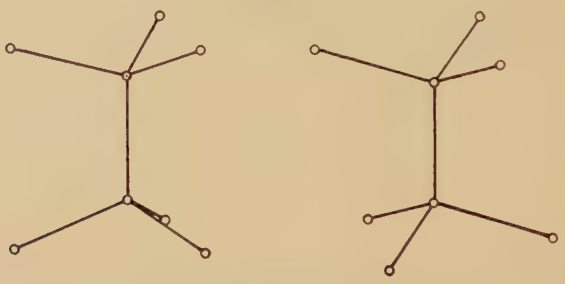
†These results are from electron diffraction experiments ; all others are from x-ray work.

parallel to the hexagonal axis are slightly shorter than those which are inclined at 109° 28′ to it; i.e. the bonds between the layers (see fig. 1) are shorter than the bonds within the layers.

Bjerrum's second objection to the Statistical structure is that the surroundings of the molecules are not independent of the orientation when all the hydrogen atoms on the neighbouring molecules are taken into account. He points out that the bonds parallel to the c-axis are mirror-symmetric, whilst the bonds inclined to the c-axis are centro-symmetric

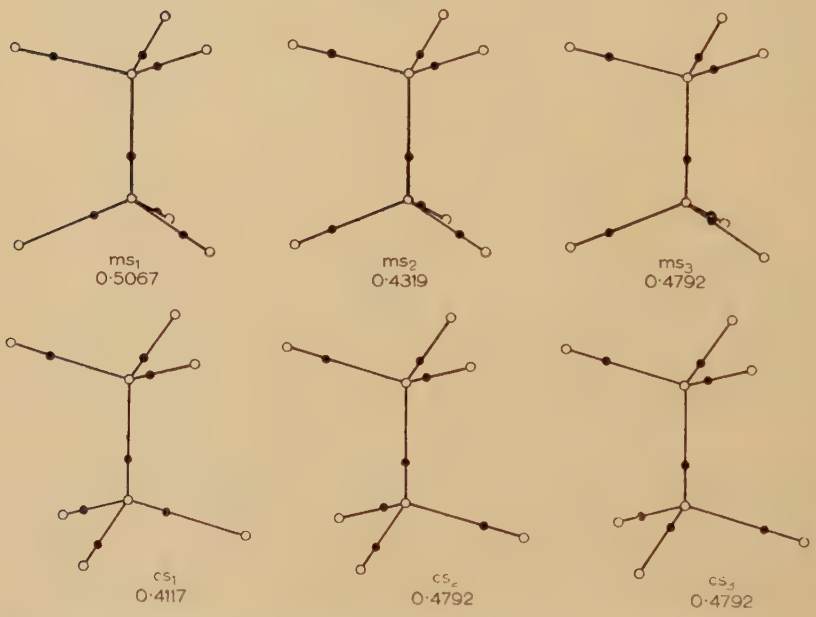
(fig. 7). It proves to be more straightforward to calculate the energies of the bonds, rather than the potential energies of the molecules, and when this is done six different cases are distinguished (fig. 8). Three of these, ms_1, cs_2 and cs_3, are more stable than the others and Bjerrum

Fig. 7



The mirror-symmetric and centro-symmetric types of bond.

Fig. 8



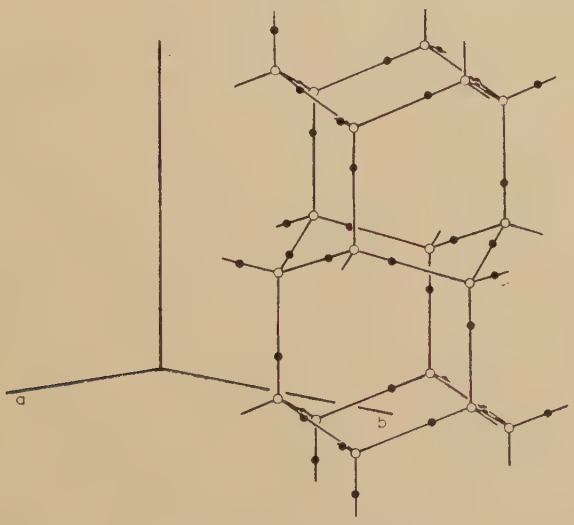
The six different bond configurations, with their electrostatic energies as calculated by Bjerrum.

suggests that ice is hexagonal rather than cubic because of the special stability of the ms_1 arrangement, which does not occur in cubic ice.

If any of the $(3/2)^N$ possible arrangements can contain a larger-than-average proportion of these more stable bonds, the residual entropy will

be much less than $R \ln (3/2)$. Owston (1953) has in fact derived a group of twelve equivalent structures which contain only these three most stable types. One of these is shown in fig. 9; the oxygen atoms are in the same positions as in Barnes' structure, but because of the unsymmetrical placing of the hydrogen atoms the total symmetry is monoclinic, space group $Pc(C_s^2)$, with eight molecules in the unit cell and the cell dimensions $a = 4{\cdot}15$ Å, $b = a\sqrt{3} = 7{\cdot}81$ Å, $c = 7{\cdot}35$ Å, $\beta = 90°$. This is the smallest unit cell possible if the hydrogen atoms are in fixed positions. If this were the correct structure, ice at low temperatures should be pyro- and piezo-electric and have no residual entropy. It is certainly not the correct structure at higher temperatures (i.e. above about $-60°$C) where molecular

Fig. 9



The Monoclinic structure.

movements are large, and if ice were to assume this structure at low temperatures there would be a specific heat anomaly at the transition temperature. There is, however, no reliable evidence of any such anomaly.

There is some doubt about the validity of Bjerrum's work and the conclusions drawn from it. It has already been mentioned that at lower temperatures the axial ratio of ice approaches the theoretical value, and it is not entirely certain how far this ratio departs from the theoretical value at higher temperatures. The results given in table 1 cannot be plotted on smooth curves, and it is clear that at least some of them are less accurate than their authors supposed them to be, though which of them is incorrect is not known.

The confirmation of the existence of the cubic form of ice at temperatures below approximately $-110°$C (König 1942, 1943, Blackman and Lisgarten 1957, Shallcross and Carpenter 1957) conflicts with Bjerrum's conclusion

that the stability of the hexagonal form should become increasingly greater than that of the cubic form as the temperature is reduced. Finally Pitzer and Polissar (1956) have pointed out that Bjerrum omitted certain important interactions in calculating the stabilities of the six arrangements in fig. 8. When these interactions are taken into account the differences in stability become extremely small, and an ordered structure can then form only at very low temperatures, if indeed it forms at all. To this might be added the observation that all calculations of energies in molecular models are inexact and caution is necessary in interpreting the significance of small differences in energy, whether the differences appear considerable, as found by Bjerrum, or negligible, as found by Pitzer and Polissar.

Although Bjerrum's work is open to criticism, the fact that ice above about $-70°$C is hexagonal rather than cubic may nevertheless be connected with the difference between the observed and theoretical axial ratios. Any explanation of this possible relationship must also take into account the observation that over the narrow temperature range where hexagonal and cubic ice can co-exist the hexagonal form has an axial ratio very close to the theoretical value.

A number of suggestions have been made by Rundle (1953, 1954, 1955) in attempts to devise a partly ordered, partly disordered model structure, which would be polar and would also explain the observed residual entropy. He was unable to find any satisfactory solution, however (see also Lipscomb 1954), and concluded that the Statistical structure must be considered the most probable, though some of the evidence for it was still subject to challenge.

§ 5. Recent X-Ray Diffraction Work

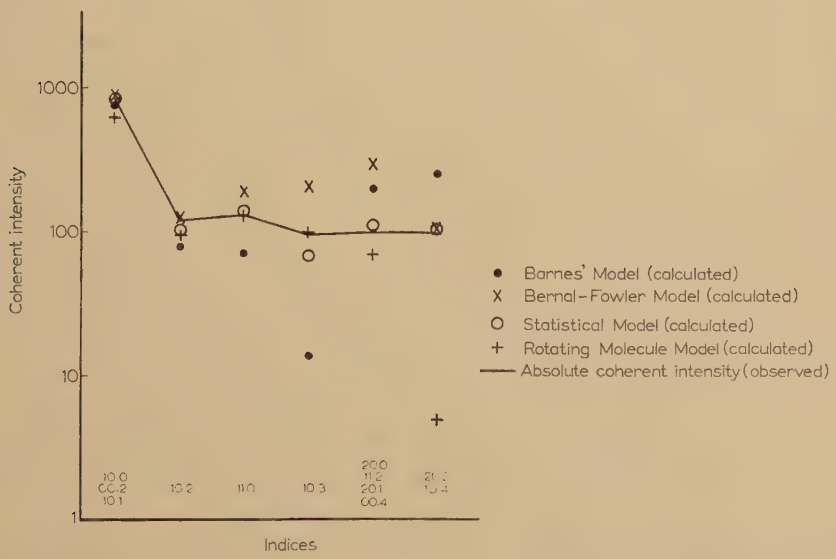
It is now well established that the positions of hydrogen atoms can be determined by modern x-ray analytical methods in molecules which also contain carbon and oxygen atoms (see, e.g. Cochran 1951). Some results of a study of ice have been given by Owston (1953), though full details were not published, and the refinement process was incomplete. The diffraction patterns contained only reflections characteristic of a hexagonal unit cell, identical with that found by Barnes. There were no additional reflections or superlattice lines, which would indicate a lower symmetry or a larger unit cell. The space-group was therefore taken to be $P6_3/mmc$, though in the work which followed (a study of the structure as projected down the a-axis) any space-group with the symmetry pgm for the [10.0] projection would give the same result. The coordinates of the oxygen atoms were taken to be $\pm(\frac{1}{3}, \frac{2}{3}, \frac{1}{16})$, $\pm(\frac{1}{3}, \frac{2}{3}, \frac{7}{16})$, as found by Barnes, and the electron density distribution due to the hydrogen atoms only was calculated from the observed intensities. It agreed closely with the distribution which would be given by the Statistical structure, with two 'half-hydrogen atoms' along each O O line. The half hydrogen atoms along the centro-symmetric bonds appear to be slightly displaced from the O–O lines, but in view of the difficulties of

obtaining accurate coordinates for these extremely light 'atoms' (the accuracy claimed was estimated at $\pm 0{\cdot}3$ Å) this deviation from the ideal Statistical structure may not be significant. An improvement in the accuracy could probably be obtained from further refinement of this work, but the results as they stand show that the Statistical structure is, in essentials, correct.

§ 6. Neutron Diffraction Studies of Ice

Although it is possible to detect hydrogen atoms by x-ray methods it is not easy to find their positions accurately because their scattering power is small; at low scattering angles the scattering powers of hydrogen and oxygen are in the ratio 1 : 8, and at higher angles the ratio is still smaller. Neutron diffraction has a great advantage here, though the hydrogen

Fig. 10



The intensity of coherent neutron diffraction for various models (the intensities on a logarithmic scale, redrawn from the results of Wollan *et al.* 1949).

atoms cause a strong diffuse scattering (due to spin incoherence) and must be replaced by deuterium for best results: the ratio of the scattering powers for neutrons is then 5 : 4. Apart from the need to use deuterated compounds, the experimental difficulties of neutron diffraction are very great, especially when single crystals are used. The difficulties can be overcome by using recently developed techniques, but most earlier work was done with polycrystalline and powdered specimens.

The first measurements on ice were carried out by Wollan *et al.* (1949) who used a specimen of D_2O ice at $-90°$C. The resolution of their apparatus was low, and only six separate powder lines could be distinguished.

These results were sufficient however to show that some of the proposed model structures cannot be correct. The models considered were Barnes' and Bernal and Fowler's structures, a model suggested by Wollan *et al.* in which the hydrogen atoms rotate round the oxygen atom, and the Statistical structure. Of these only the Statistical structure required lines with the same intensities as those which were found experimentally (fig. 10).

More recently Peterson and Levy (1957) have studied the diffraction of neutrons by single crystals of D_2O ice at $-50°$c and $-150°$c. With their apparatus complete resolution was possible and a detailed interpretation of their results could confidently be made. This confirms

Table 2. Interatomic Distances and Angles in D_2O Ice, with their Standard Deviations†

Distance (Å)	−50°c	−150°c
O–O′	2·752 ± 0·008	2·755 ± 0·006
O–O″	2·765 ± 0·0002	2·746 ± 0·0002
$O–D_1$ (uncorr.)	1·000 ± 0·009	0·997 ± 0·007
$O–D_2$ (uncorr.)	1·007 ± 0·005	0·997 ± 0·004
$O–D_1$ (corr.)	1·011	1·008
$O–D_2$ (corr.)	1·015	1·009
Angles		
O′–O–O″	109° 33′ ± 9′	109° 18′ ± 7′
O″–O–O‴	109° 24′ ± 1′	109° 38′ ± 1′
$D_2'–O–D_2$	109° 52′ ± 16′	109° 54′ ± 15′
$D_1–O–D_2$	109° 6′ ± 18′	109° 11′ ± 13′

Note : the uncorrected values O–D are the observed distances between maxima in the Fourier distribution : they are shorter than the true interatomic distances because of the effect of the rotary oscillations of the deuterium atoms round the oxygen atoms.

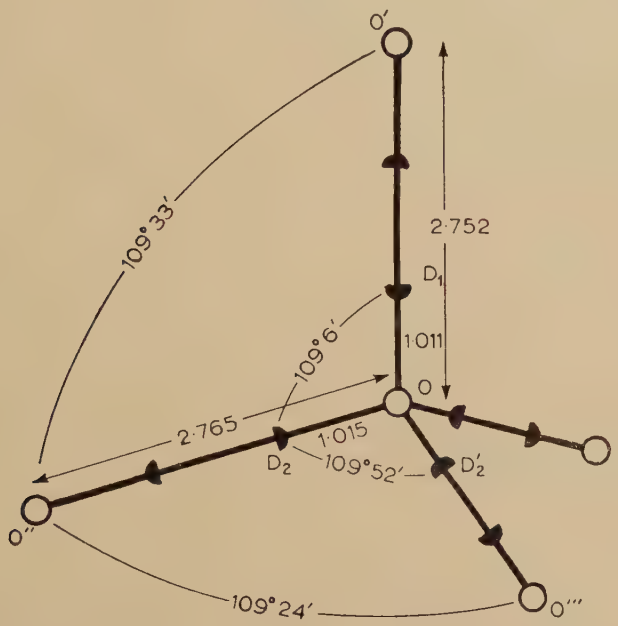
† Peterson and Levy (1957).

and greatly amplifies the x-ray results, and provides much more accurate values of the parameters of the structure. No superlattice lines of any kind were found, and this alone rules out the Bernal and Fowler and monoclinic structures, together with any other ordered asymmetrical arrangement and any regular structure with a unit cell containing more than four molecules. The reflections which were observed were all consistent with the space group $P6_3/mmc(D_{6h}^4)$, which is the symmetry of Barnes' structure, the Statistical structure and one of Rundle's partly-ordered arrangements. The intensities of the $\{Okl\}$ zone of reflections were measured and found to agree well with those expected from the Statistical structure, and when the refinement was complete the mean

difference between the observed and calculated structure amplitudes was only 3·55%. The bond-lengths and angles which were obtained are given in table 2, and those at −50°C are also shown in fig. 11; the axial lengths used were obtained by interpolation from the data of Megaw (1934) and Vegard and Hillesund (1942), and their accuracy is rather uncertain.

The conclusions to be drawn from this work leave less ground for discussion than most previous results on ice. They are, briefly, that within the small experimental errors (i) the statistical, or half-hydrogen structure is correct, (ii) the deuterium atoms are collinear with the oxygen atoms, and (iii) the average arrangement of hydrogen and oxygen atoms round each oxygen atom is a regular tetrahedron; only the angles D_2'–O–D_2

Fig. 11



Molecular dimensions in D_2O ice at −50°C (Peterson and Levy 1957).

and D_1–O–D_2 differ from the tetrahedral value more than might be expected, and even this difference is barely significant.

It seems possible, for reasons given later, that Peterson and Levy underestimated the effects of extinction in their work. It is nevertheless unlikely that the atomic positions are seriously in error, since most of the atoms are clearly resolved from each other in this projection. The estimates of the standard deviations, however, would be altered, together with the thermal parameters mentioned in § 7. The changes in the O–O bond distances on cooling from −50° to −150°C, namely an expansion of 0·003 Å in one case and a contraction of 0·019 Å in the other, suggest

that the errors may be larger than is indicated. It may be, on the other hand, that this discrepancy is due to the use of inaccurate axial lengths.

In view of these doubts the evidence that the environment of each water molecule is exactly tetrahedral is not completely reliable, though the departure from regularity cannot be great.

§ 7. Atomic Movements in Ice

It has already been mentioned that the molecules in ice are, at temperatures near the melting point, in constant motion, and it is possible from diffraction experiments to estimate the amplitudes of these thermal vibrations. The atomic movements affect both the coherent scattering, or Bragg reflections, and the incoherent background scattering.

For relatively simple compounds the amplitude of the scattering from atoms at rest, i.e. at 0°K, can be calculated reasonably accurately. At higher temperatures the amplitude for each atom is reduced by the factor $\exp[-B\sin^2\theta/\lambda^2]$, where θ is the Bragg angle for the plane hkl, λ is the wavelength of the radiation, and B is proportional to the mean square displacement of the atom from its mean position along the normal to the crystal plane hkl being considered. By applying this formula to the intensities of a sufficient number of reflections at the experimental temperature the root mean square amplitudes of vibration of the different atoms can be found.

This has been done for ordinary ice using x-ray diffraction results and the r.m.s. amplitude for the H_2O molecule (assumed to vibrate as a single rigid unit) was found to be approximately 0·44 Å at −10°C. This agrees reasonably well with the value of 0·41 Å at 0°C calculated from the specific heat of ice at very low temperatures, using Debye's theory (Owston 1951 a, 1953).

A much more thorough analysis was carried out on heavy ice by Peterson and Levy (1957) using their neutron diffraction results. They found the r.m.s. amplitudes to be: for the oxygen atoms 0·30 Å at −50°C and 0·24 Å at −150°C, the vibration being almost isotropic; for the deuterium atoms 0·35 Å at −50°C and 0·29 Å at −150°C, the vibration being appreciably anisotropic. These values are considerably lower than those for H_2O ice. The specific heat measurements of Long and Kemp (1936) lead to a characteristic Debye temperature of approximately 163°K for D_2O ice, which is rather lower than that for H_2O ice, 197°K, and approximate calculations lead to the values 0·42 Å at −50°C and 0·33 Å at −150°C for the r.m.s. amplitudes of vibration of the molecules. The difference between the values obtained by the two methods is too great to be explained by the approximate nature of Debye's theory. A possible explanation is that Peterson and Levy underestimated the effect of extinction in measuring the intensities of neutron diffraction, for ice is known to form exceptionally perfect crystals in which extinction effects are large (Lonsdale 1947).

Incoherent, diffuse, scattering in ice is of three kinds. First there is the effect of waves of vibrations of the acoustic type, which cause the

appearance of weak, diffuse reflections close to the positions of the Bragg reflections when the Bragg law $n\lambda = 2d \sin\theta$ is not exactly obeyed. In crystals near the melting point these reflections may be quite strong even when the crystal is several degrees away from the reflecting position. The shapes and intensities of these diffuse spots can be calculated from the elastic constants, giving moderate agreement with experiment. The second kind of diffuse scattering consists of diffuse streaks which join some of the diffuse spots. These may be due to vibrations in the ' optical ' modes, with very high frequencies and short wavelengths, but the theory of crystal lattice dynamics is as yet inadequate to explain them. Both these types of diffuse scattering appear on the x-ray photographs taken by Barnes (1929) though he did not comment on them; they were later recognized by Lonsdale (1946) and studied in detail by Owston (1949). It has been suggested that the diffuse streaks have their origin in movements of the hydrogen atoms, e.g. in the ' proton jumps ' and molecular rotations which have been much discussed (see, e.g. Bjerrum 1951). It is true that these streaks are very strong in x-ray photographs of ice, but this is probably because the ice was near the melting-point, where all vibrations have large amplitudes. They are equally strong, for instance, in Laue photographs of sodium, and cannot therefore be due to any type of vibration or atomic movement peculiar to ice. It has not yet been possible to study these two types of diffuse scattering by neutron diffraction.

The third type of diffuse scattering is due not to atomic movements, but to the random placing of the hydrogen atoms: at any instant only half the possible hydrogen atom sites are occupied. In x-ray diffraction experiments the diffuse scattering due to this disorder is very weak, but should be much stronger in neutron diffraction. Wollan *et al.* (1949) were able to measure its intensity at least approximately and show that it agreed with the value calculated for the Statistical structure, thus providing further confirmation of this structure.

§ 8. Conclusion

Although in this review the results of x-ray and neutron diffraction have received special attention, many of the general ideas on the structure of ice have come from other measurements. Discussions on the structure of ice have always been remarkable for the number of threads of evidence which have, of necessity, been brought in. The subject had been so thoroughly studied in the past that the powerful new method of neutron diffraction appears at first to be able to do little more than confirm what was already regarded as almost certain. There is room for more accurate work, however, and in particular a comparison of the detailed structures of cubic and hexagonal ice would be most interesting.

Acknowledgment

I am indebted to Miss J. M. Tolliday for her valuable assistance in correcting the manuscript of this review and in preparing the diagrams.

References

Adams, J. M., 1930, *Proc. roy. Soc.* A, **128,** 588.
Auty, R. P., and Cole, R. H., 1952, *J. chem. Phys.*, **20,** 1309.
Barnes, W. H., 1929, *Proc. roy. Soc.* A, **125,** 670.
Berger, C., and Saffer, C. M., 1953, *Science*, **118,** 521.
Bernal, J. D., and Fowler, R. H., 1933, *J. chem. Phys.*, **1,** 515.
Bjerrum, N., 1951, *Dan. Mat. Phys. Medd.*, **27,** No. 1.
Blackman, M., and Lisgarten, N. D., 1957, *Proc. roy. Soc.* A, **239,** 93.
Bragg, W. H., 1922, *Proc. phys. Soc. Lond.*, **34,** 98 ; 1938, *Proc. roy. Inst.*, **30,** 283.
Brandenberger, E., 1930, *Z. Krist.*, **73,** 429.
Cochran, W., 1951, *Acta cryst.*, **4,** 376.
Dennison, D. M., 1940, *Rev. mod. Phys.*, **12,** 188.
Dorsey, N. E., 1940, *The Properties of Ordinary Water Substance* (New York : Rheinhold Publishing Corp.).
Fox, J. J., and Martin, A. E., 1940, *Proc. roy. Soc. A*, **174,** 234.
Giauque, W. F., and Ashley, M. F., 1933, *Phys. Rev.*, **43,** 81.
Giauque, W. F., and Stout, J. W., 1936, *J. Amer. chem. Soc.*, **58,** 1144.
Hallett, J., and Mason, B. J., 1958, *Nature, Lond.*, **181,** 467.
Kinsey, E. L., and Sponsler, O. L., 1933, *Proc. phys. Soc. Lond.*, **45,** 768.
König, H., 1942, *Nachr. Akad. Wiss. Göttingen*, No. 1, 1 ; 1943, *Z. Krist.*, **105,** 279.
Kumm, A., 1951, *Arch. Met., Wien* A, **3,** 382.
Lipscomb, W. N., 1954, *J. chem. Phys.*, **22,** 344.
Long, E. A., and Kemp, J. D., 1936, *J. Amer. chem. Soc.*, **58,** 1829.
Lonsdale, K., 1946, *Nature, Lond.*, 158, 582 ; 1947, *Phil. Trans.*, **240,** 219.
Lonsdale, K., and Owston, P. G., 1948, *J. Glaciol*, **1,** 118.
Mason, B. J., and Owston, P. G., 1952, *Phil. Mag.*, **43,** 911.
Megaw, H. D., 1934, *Nature, Lond.*, **134.** 900.
Owston, P. G., 1949, *Acta Cryst.*, **2,** 222 ; 1951 a, *Quart. Rev. Chem. Soc.*, **5,** 344 ; 1951 b, *J. Glaciol.*, **1,** 571 ; 1953, *J. Chim. phys.*, **50,** C 13.
Pauling, L., 1935, *J. Amer. chem. Soc.*, **57,** 2680.
Peterson, S. W., and Levy, H., 1957, *Acta cryst.*, **10,** 70.
Pitzer, K. S., and Polissar, J., 1956, *J. phys. Chem.*, **60,** 1140.
Rinne, F., 1917, *Ges. Wiss. Math. Phys.*, **69,** 57.
Rossberg, D., and Magun, S., 1957, *Naturwissenschaften*, **44,** 58.
Rossmann, F., 1950, *Experientia*, 6, 182 ; 1950, *Probl. kosm. Phys.*, **25,** 71.
Rundle, R. E., 1953, *J. chem. Phys.*, **21,** 1311 ; 1954, *Ibid.*, **22,** 344 ; 1955, *J. phys. Chem.*, **59,** 680.
Seljakov, N., 1936 a, *C. R. Acad. Sci. U.R.S.S.*, **10,** 293 ; 1936 b, *Ibid.*, **11,** 227 ; 1937, *Ibid.*, **14,** 181.
Schaefer, V. J., 1949, *Chem. Rev.*, **44,** 291.
Shallcross, F. V., and Carpenter, G. B., 1957, *J. chem. Phys.*, **26,** 782.
Shaw, D., and Mason, B. J., 1955, *Phil. Mag.*, **46,** 249.
Slater, J. C., 1941, *J. chem. Phys.*, **9,** 16.
Steinemann, S., 1953, *Experientia*, **9,** 135.
Truby, F. K., 1955, *Science*, **121,** 404.
Vegard, L., and Hillesund, S., 1942, *Arb. norske VidenskAkad.* No. 8, 1.
Wollan, E. O., Davidson, W. L., and Shull, C. G., 1949, *Phys. Rev.*, **75,** 1348.
Wooster, W. A., 1933, quoted by Bernal and Fowler (1933).

Electron Diffraction Investigations into the Cubic and other Structural Forms of Ice

By M. Blackman and N. D. Lisgarten
Physics Department, Imperial College, London, S.W.7

§ 1. Electron Diffraction Experiments

The first attempt to investigate the structure of ice by electron diffraction seems to have been made by Mongan (1935). The specimens used consisted of a more or less random aggregate of crystallites deposited on a supporting metal grid at the end of a glass dewar which could be inserted into the electron diffraction camera. The dewar vessel was first filled with liquid air to obtain an ice deposit and placed in the camera, which was then evacuated. This somewhat crude procedure did not provide particularly good diffraction patterns, the rings tending to be rather diffuse and the background very high. It was, however, possible to establish that the main rings were consistent with the normal hexagonal form of ice, though the absence of certain rings, e.g. (100), showed that there was preferential orientation in the deposit. The most interesting aspect of Mongan's work lies in his emphasis on the importance of the contribution of the hydrogen atoms to the intensity of the diffraction rings ; as the work was published only in thesis form, Mongan's contribution on this point has been largely overlooked.

The first comprehensive study of the structure of deposits of water vapour was carried out by König (1942, 1943). In this work a low temperature unit was used which was specifically designed for transmission experiments. The specimen base, a collodion film, was almost completely enclosed by a copper housing into which were screwed two small copper tubes. These permitted the entry and exit of the electron beam. A poor thermal conductor (porcelain) was interposed between the collodion film and the copper housing attached to the glass dewar containing the refrigerant. This allowed a large thermal gradient to be maintained during the cooling down process which ensured that condensible vapours would be preferentially deposited on the surroundings of the specimen base. An electrical heater was provided within the cold unit, so that the temperature of the specimen base could be raised when desired. In the initial experiments the diffraction patterns were analysed into two ring systems. One of these was ascribed to an orthorhombic system and attributed to condensed grease vapours. The use of the small copper tubes was found to prevent the formation of the grease film. The other ring system which formed at the lowest temperatures used (about $-170°$C) consisted of diffuse rings which on heating to about $-150°$C changed into a sharp ring pattern consistent with a cubic structure

of the diamond type. The use of phosphorous pentoxide to dry the interior of the camera was found to delay the appearance of the deposit. König concluded that the deposit was formed by water vapour and that the diamond-type pattern was produced by a new crystalline form of ice. On heating the deposit above $-150°$c it was found that a change took place at about $-80°$c ; this consisted in the appearance of additional rings and the complete ring system was then that to be expected from hexagonal ice. The deposit appeared to start evaporating in this region of temperature and at $-70°$c the ice pattern disappeared completely.

The transition between the cubic and the hexagonal form appeared to be a slow one, at any rate no sudden change was observed. The lattice constant of the cubic form was measured and found to be $6{\cdot}36 \pm 0{\cdot}01$ Å (at $-100°$c), the volume per molecule being the same, within experimental error, as in the hexagonal form. König in fact compares the two forms with the corresponding forms for silicon dioxide, namely β crystabolite and β tridymite.

The work of König was followed by two independent investigations carried out almost simultaneously (Honjo *et al.* 1956, Lisgarten and Blackman 1956, Blackman and Lisgarten 1957). In both of these, the effect of water vapour introduced from outside the camera was studied, whereas in König's work the residual water vapour in the camera was used to produce the deposit. The low temperature unit designed by the Japanese physicists, consisting of a dewar vessel and a system of controls, is mounted on the side of the electron diffraction camera so that one end of the dewar system protrudes into the vacuum. This end carries a 20 watt heater coil and the specimen holder, which is enclosed by a cylindrical shield. This shield is provided with apertures which are normally closed, but which can be opened to allow the entry and exit of the electron beam. Despite this, a number of precautions were needed to avoid the effects of residual water vapour and other contamination.

The water vapour was admitted to the specimen region from a side glass tube fitted with a stopcock. This glass tube contained silica gel which had been allowed to absorb a certain amount of water.

The results reported by Honjo *et al.* are of a preliminary nature. They agree fairly closely with those found by König. Patterns of hexagonal ice were formed at $-80°$c, and the cubic pattern was obtained from a deposit at $-150°$c. Below $-160°$c the deposit gave only diffuse haloes ; on warming to $-150°$c the haloes developed rapidly into sharp rings of the cubic pattern. The chief difference with the work of König appears to lie in the observation of the (222) ring in the cubic pattern and the (00·4) ring in the hexagonal pattern. Both of these would be absent, in the limit where the total scattering is weak, if the hydrogen atoms did not contribute significantly to the scattering of the electrons.

In all the work, which appeared to be confined to the transmission case, the base used was collodion as in König's work. The intensities

of the diffraction rings of the cubic ice were measured and it was concluded that these intensities agreed well with those to be expected on the Pauling model (Pauling 1935) for the positions of the hydrogen atoms.

A more detailed study of the nature of the deposits formed at various temperatures has been given by Blackman and Lisgarten (1957). The low temperature unit differs from those previously described in the literature in that it is completely enclosed within the vacuum of the camera. A large refrigerant capacity is employed, the specimen being surrounded by several hundred square centimetres of cold surface. A powerful heater coil was incorporated in the system which makes it possible to maintain the specimen at a relatively high temperature while the remainder of the unit can be cooled down to the temperature of the refrigerant. This procedure was of considerable help in preventing the formation of unwanted ice and other deposits from the residual vapour. It was found possible to operate successfully without having to keep the specimen almost completely enclosed.

Table 1. Deposition Experiments

Temperature of base (°C)	Type of pattern
−180 to −140	Diffuse rings.
−140 to −120	Sharp rings of the cubic form.
−120 to −100	Sharp rings of both hexagonal and cubic forms.
−100	Sharp rings of the hexagonal form.

Specimens were examined both in reflection and in transmission. These were formed on suitable bases via a glass injection system, the vapour being provided by pure ice kept in one of the limbs of the injection system, usually at the temperature of solid carbon dioxide. The vapour was admitted via an external stopcock ; it was ascertained that the Apiezon grease used here was not a source of contamination by a special experiment in which the use of the stopcock was dispensed with, the flow of vapour being cut off by cooling the source with liquid air. In later work a double injection system was used, in which either heavy or ordinary ice could be used as the vapour sources. In general the rate of deposition was such that a diffraction pattern of suitable intensity was obtained in about five minutes. By varying the temperature of the bath surrounding the water vapour source, this time could be varied from a few seconds to fifteen minutes.

Three types of ring patterns were observed in the deposition experiments. The data are given in table 1 for a slow rate of deposition (see also figs. 1, 2, Pl. 14, fig. 3, Pl. 15. These results are based on both transmission and reflection experiments, the thickness of the deposit being

approximately the same in the two types of experiments. Most of the observations were taken in the transmission experiments. The bases used in these experiments were : formvar, collodion, amorphous germanium and amorphous silica. In the reflection work well oriented films of silver formed on mica were mainly used, but in some experiments cleaved galena was employed. The results found were independent of the nature of the base or the type of experiment. In these films the deposit always appeared to consist of random crystallites ; where thicker films were investigated, as could be done with reflection specimens, these showed a tendency to a fibrous orientation, this tendency increasing with thickness.

It was found that deposits could not be formed satisfactorily above about $-110°$C as they evaporated very quickly ; the patterns were, however, obtained by increasing the vapour pressure in the injection unit and allowing the temperature of the base to fall quickly during deposition.

All the diffraction rings found could be satisfactorily indexed with respect to either the normal hexagonal structure or the cubic diamond-type structure. It was found that the (222) ring of the cubic system was present on several plates though its relative intensity seemed rather variable. On occasion it was clearly visible, in other cases it seemed very faint. Faint traces of the (00·4) ring of the hexagonal system were also observed.

A series of experiments was made (in transmission) to study the transformation on heating of the deposits formed below $-140°$C. It was known that the pattern changed from one of diffuse rings to one of sharp (cubic) rings, but the temperature range over which this happens is not given, e.g. in König's work. A series of exposures taken on photographic film at a rate of heating of 2°C per minute (see fig. 4, Pl. 16) showed that the complete transition takes place in a temperature interval of from two to four degrees. The transition temperature is about $-120°$C. On further heating the cubic pattern was maintained until the deposit evaporated completely at about $-105°$C. All deposits formed by deposition (except those which were deliberately made thick) evaporated at about this temperature independent of the base used.

The results for deposits made using heavy water vapour were very similar to those from ordinary water vapour. Using the double injection unit, experiments on the two forms were alternated. With heavy water the diffuse, cubic and hexagonal patterns were found at temperatures which appeared to be slightly higher (by three or four degrees). The temperature to which a deposit could be heated before evaporation became appreciable also appeared to be somewhat higher. This is to be expected as heavy ice has a lower vapour pressure than ordinary ice. Experiments were carried out using the reflection technique as well as in transmission. Figure 5, Pl. 17 shows a reflection pattern from a thick layer of the cubic form of heavy ice.

§ 2. Comparison of Results

While all experiments made on deposits formed at low temperature agree on the occurrence of deposits which give three types of diffraction patterns, there do appear to be discrepancies when one examines the details of the results.

One such result is the fact that König was able to heat his deposits to a temperature above $-80°$C, where he observed in transmission experiments the transition from the cubic to the hexagonal form ; whereas in experiments described above, the deposit evaporated completely at about $-105°$C. The measurements of Tschudin (1946) on the rate of evaporation of ice in vacuum shows that a coherent ice layer vaporizes at a rate of 6×10^{-6} g cm^{-2} s^{-1} at $-80°$C, of 3×10^{-5} g cm^{-2} s^{-1} at $-70°$C. This corresponds to a loss of about 600 Å/s at $-80°$C and 3000 Å/s at $-70°$C. Since the thickness of the layers used in the electron diffraction experiments should hardly exceed 3000 Å, it would be expected that in slow heating experiments the layer will have evaporated well before $-80°$C is reached. A repeat of König's work was carried out by Blackman and Lisgarten using layers formed on collodion from the residual vapour in the camera. In this case it was sometimes possible to retain the deposit at $-80°$C and occasionally at higher temperatures. The appearance of some hexagonal rings at about $-80°$C was also observed in one case. Deposits of this type were found, however, only with collodion and with formvar. With other bases (amorphous germanium and amorphous silica in transmission experiments and silver in reflection experiments) the corresponding deposits behaved as in the injection experiments. A number of subsidiary experiments suggested that the effect was associated with part of the pumping line as well as with the particular organic bases used, but no clear-cut explanation could be obtained.

It should, however, be pointed out that Honjo and his collaborators did apparently form deposits of hexagonal ice at $-80°$C, which were then cooled to $-150°$C. While it is not stated what the rate of cooling was, it would appear that there is still some doubt as to the highest temperature at which a satisfactory deposit of ice can be formed in deposition work.

There also appears to be a difference in the temperature at which the deposit giving a diffuse pattern transforms, on heating, to one giving a sharp (cubic) pattern. König and Honjo *et al.* give this temperature as $-150°$C, whereas Blackman and Lisgarten find $-120°$C.

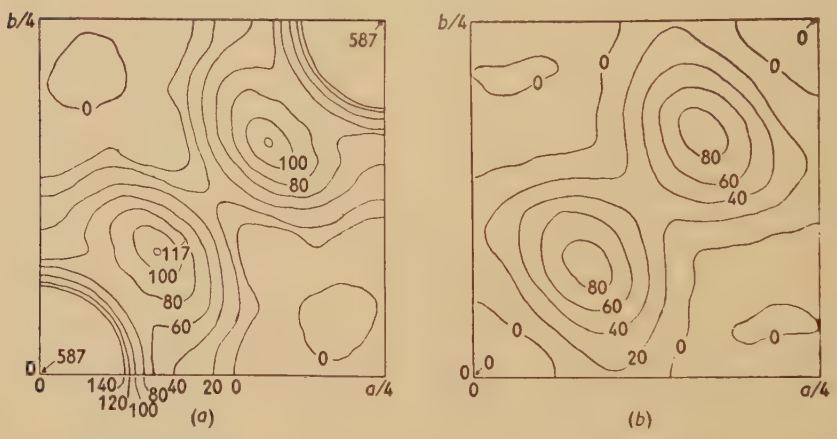
Discrepancies also appear to exist on the intensities of certain rings in the diffraction patterns : the (222) ring in the cubic pattern and the (00·4) in the hexagonal pattern. The (222) does not appear to have been observed by König, and though it is found in Blackman and Lisgarten's work, the relative intensity with which it appears seems to be variable. The (00·4) ring was also found but only as a faint trace. Both these rings were found in the work of Honjo *et al.* with presumably

satisfactory reproducibility. This is an important point as the rings would be forbidden in sufficiently thin deposits if the scattering from the hydrogens were negligible.

§ 3. The Hydrogen Positions in Cubic Ice

The measurement of the intensity of the diffraction rings from cubic ice has been extended recently by Honjo and Shimaoka (1957) using a deposit very slowly formed at -150°c on collodion. The specimens were composed of crystals of size about 100 Å, this being presumably deduced from the measured breadth of the rings. The pattern showed no trace of preferred orientation nor of an hexagonal admixture. The rings were

Fig. 6



(*a*) Potential Fourier map of cubic ice projected on (001). The unit of the contour scale is 0·37 v.a.
(*b*) The corresponding Fourier map with the oxygen contributions subtracted.

photographed by means of a sector camera and the intensities were measured both photometrically and visually. By comparing intensities at -190° and at -120°c, a Debye temperature of 200 ± 15°k was found and this was used to correct all the measured intensities. Comparison was then made with calculations of intensity on the cubic equivalent of the Barnes model (Barnes 1929), on Pauling's model (Pauling 1935), and on one in which the hydrogen scattering was neglected.

It was concluded both from the overall agreement and from the appearance of the (222) and (442) reflections (forbidden on the Barnes model) that the Pauling model is the most probable.

Fourier maps were also calculated using the structure amplitudes given by the square root of the observed intensities corrected for the temperature effect. In the calculations it was assumed that a centre of symmetry exists at the centre of the O–O bond. The results are shown in fig. 6 ; the chief features are the contours showing the hydrogen

positions. The O–H distance is found to be 0·97 Å, which is lower than that deduced from neutron diffraction studies (1·02 Å). The difference is not, however, thought to be significant.

§ 4. Spacing Measurements

Measurements of the lattice constant of the cubic form of ordinary ice were carried out by König (1942, 1943). In one set of these experiments evaporated layers of silver were used to calibrate the voltage of the electron beam ; in the other a layer of zinc was deposited on the ice film and the two ring systems were recorded on the same plate. The cube spacing is given as $6{\cdot}36 \pm 0{\cdot}01$ Å at -100°C. It seems probable that König's spacing is in x.u. rather than in ångström units, in which case his value should be increased by 0·2%.

In the work of Blackman and Lisgarten (1957), the standard substances used were thin films of thallium chloride and of rocksalt. The spacings of the standard substances at low temperature were first determined by comparing ring patterns obtained at high and at low temperature. A series of experiments was carried out with both the cubic and hexagonal forms of ordinary ice, attention being paid to the statistical errors involved in the measurements. Less detailed measurements were also made on the patterns from heavy ice. The results are given in table 2.

Table 2. Results on Lattice Constants

Form of ice	Temp. (°C)	Lattice constants
Cubic, normal	−130	$a_0 = 6{\cdot}350 \pm 0{\cdot}008$ Å
Hexagonal, normal	−110	$a = 4{\cdot}493 \pm 0{\cdot}004$ Å $c = 7{\cdot}337 \pm 0{\cdot}006$ Å $c/a = 1{\cdot}632 \pm 0{\cdot}001$
Cubic, heavy	−130	$a_0 = 6{\cdot}351 \pm 0{\cdot}008$ Å
Hexagonal, heavy	−130	$a = 4{\cdot}495 \pm 0{\cdot}004$ Å $c = 7{\cdot}335 \pm 0{\cdot}007$ Å $c/a = 1{\cdot}632 \pm 0{\cdot}001$

There does not appear to be any difference between normal and heavy ice, within the limits of accuracy of these measurements. The accuracy attained does not, however, reach that possible with the best x-ray techniques. The only x-ray data available at present in which a higher accuracy is claimed are those by Megaw (1934) on normal hexagonal ice at 0°C and at −66°C. It is not possible, in the absence of accurate data on expansion coefficients, to extrapolate reliably Megaw's values to the lower temperatures used in the electron diffraction work. The data available suggest that the a and c values obtained by electron diffraction are about 0·4% lower than the x-ray values. What may be more

significant is the difference in the values found for the c/a value. The electron diffraction results give $c/a = 1{\cdot}632 \pm 0{\cdot}001$ for both normal and heavy ice, which is the value for close packing (within experimental error). Megaw's value at $-66°$C is 1·628 and the value at 0°C, 1·629, suggests that this ratio is decreasing with temperature.

Recently Shallcross and Carpenter (1957) have made an x-ray study of polycrystalline mixtures of normal hexagonal and cubic ice at $-190°$C and at $-130°$C. The accuracy of their measurements is, however, about 0·5%, and these do not show any difference with either the electron diffraction or the previous x-ray results. It is, however, of interest to record the spacings found for the cubic modification, which are $a_0 = 6{\cdot}37 \pm 0{\cdot}02$ Å at $-190°$C and $6{\cdot}36 \pm 0{\cdot}03$ Å at $-130°$C.

§ 5. General Comments and Discussion

The properties of deposits formed from water vapour at low temperatures have been the subject of a number of investigations ; in addition to the electron diffraction investigations, there have been a number of x-ray studies and calorimetric studies. The existence of the so-called amorphous form of ice, i.e. the form which gives a diffraction pattern consisting of diffuse rings, was established by Burton and Oliver (1935). The examination of deposits formed at different temperatures showed also a region described as ' semi-crystalline ', the interpretation of which is at present obscure. Vegard and Hillesund (1942) showed that the ' amorphous ' form was produced from the vapour at liquid air temperature, provided the deposit was formed slowly. It is rather a curious fact that only in the recent experiments of Shallcross and Carpenter (1957) has the cubic form been found at all in x-ray work and even in this case the cubic form has not been obtained by itself. It seems that it is necessary to form the deposit sufficiently slowly and, of course, in a particular temperature region.

The same considerations probably explain the calorimetric experiments of Staronka (1939) and of Pryde and Jones (1952). In these, deposits were formed at the temperature of liquid air and heating curves were taken. These showed a change in slope at about $-130°$C, which was interpreted as a change-over from the amorphous to the hexagonal form of ice. This temperature is close to the one found by Blackman and Lisgarten for the transition from amorphous to cubic ice, though appreciably higher than that given by König (1943) and by Honjo *et al.* (1956). The low heat of transformation of between 2 and 12 calories per gram was attributed to the existence of a crystalline fraction, which is certainly a possibility. A rather higher value, namely 16 calories per gram, was in fact obtained in the more recent work of Ghormley (1956), in conditions under which the deposition would be a good deal slower than in the earlier work or in the experiments of de Nordwall and Staveley (1956). The data obtained by various experimenters on the nature of the deposits are summarized in fig. 7.

In none of the calorimetric work is there any indication of the transformation from the cubic to the hexagonal form at about −80°C ; it is, however, unlikely that the heat of transformation would be sufficiently

Fig. 7

EXPERIMENTAL METHOD	TEMPERATURE RANGES − °C (−180 −160 −140 −120 −100 −80 −60)	REFERENCE
X-RAY DIFFRACTION	AMORPHOUS / SEMI-CRYSTALLINE / HEXAGONAL	BURTON & OLIVER 1935
CALORIMETRIC	AMORPHOUS / CRYSTALLINE	STARONKA 1939
X-RAY DIFFRACTION	SMALL CRYSTALS / INTERMEDIATE RANGE NOT INVESTIGATED / HEXAGONAL	VEGARD & HILLESUND 1942
ELECTRON DIFFRACTION	SMALL CRYSTALS / CUBIC / HEXAGONAL	KÖNIG 1942
CALORIMETRIC	VITREOUS / CRYSTALLINE	PRYDE & JONES 1952
ELECTRON DIFFRACTION	CRYSTAL GROWTH POOR / CUBIC / HEXAGONAL	HONJO ET AL. 1956
CALORIMETRIC	AMORPHOUS / CRYSTALLINE	GHORMLEY 1956
CALORIMETRIC	VITREOUS / CRYSTALLINE	DE NORDWALL & STAVELEY 1956
ELECTRON DIFFRACTION	AMORPHOUS OR SMALL CRYSTALS / CUBIC / HEXAGONAL	BLACKMAN & LISGARTEN 1957

Summary of experimental results on deposits formed from water vapour on a base at low temperatures. The description of the deposit is that given by the respective authors.

large to be noticeable in this type of experiment. It would be of considerable interest to see the results of a detailed calorimetric study of a

cubic deposit which was heated slowly through the critical region. This would enable one to decide whether cubic ice represents a structure which is thermodynamically more stable below −80°c than the hexagonal form of ice.

The exact nature of the so-called amorphous form of ice has also been the subject of differing views. While some investigators have assumed that this is a glassy form, König (1942) and Vegard and Hillesund (1942) suggest that it is composed of very small crystallites. This is based on the observation that the centre of gravity of the main diffuse diffraction ring coincides with the centre of gravity of a prominent group of rings in the hexagonal (and cubic) structures, i.e. the density of the various forms would appear to be equal. This argument is not conclusive, as super-cooled water has a negative volume expansion coefficient at −15°c and its density could well become equal to that of ice at −100°c. The arguments based on the calorimetric studies are also inconclusive. The low value of the heat of transformation is probably due in part to the presence of hexagonal or cubic ice. Although Ghormley (1956) obtained a higher value (about 16 cal/g), this is still rather low and is difficult to account for, unless special assumptions are made.

An attempt was made by Blackman and Lisgarten (1957) to see whether there was any evidence of a systematic change in ring breadth in the region of temperature in which a mixture of both amorphous and cubic ice is obtained by deposition. In all cases the pattern consisted of rings which were either very broad or reasonably sharp.

It is doubtful whether any detailed distinction can be drawn on the basis of diffraction studies alone. It would seem that the best way to proceed would be to carry out a careful repetition of the calorimetric studies, in which care is taken to ensure that only the amorphous form is present at the start.

References

Barnes, W. H., 1929, *Proc. roy. Soc.* A, **125,** 670.

Blackman, M., and Lisgarten, N. D., 1957, *Proc. roy. Soc.* A, **239,** 93.

Burton, E. F., and Oliver, W. F., 1935, *Proc. roy. Soc.* A, **153,** 166.

Ghormley, J. A., 1956, *J. chem. Phys.*, **25,** 599.

Honjo, G., Kitamura, N., Shimaoka, K., and Mihama, K., 1956, *J. phys. Soc., Japan,* **11,** 527.

Honjo, G., and Shimaoka, K., 1957 *Acta cryst.*, **10,** 710.

König, H., 1942, *Nachr. Akad. Wiss. Göttingen*, no. 1, 1 ; 1943, *Z. Kristallogr.*, **105,** 279.

Lisgarten, N. D., and Blackman, M., 1956, *Nature, Lond.*, **178,** 39.

Megaw, H. D., 1934, *Nature, Lond.*, **134,** 900.

Mongan, C., 1935, *Dissertation*, E.T.H. (Zürich).

de Nordwall, H. J., and Staveley, L. A. K., 1956, *Trans. Faraday Soc.*, **52,** 1061.

Pauling, L., 1935, *J. Amer. chem. Soc.*, **57,** 2680.

Pryde, J. A., and Jones, G. O., 1952, *Nature, Lond.*, **170,** 685.

Shallcross, F. V., and Carpenter, G. B., 1957, *J. chem. Phys.*, **26,** 782.

Staronka, L., 1939, *Roczn. Chem.*, **19,** 201.

Tschudin, P., 1946, *Helv. phys. acta*, **19,** 91.

Vegard, L., and Hillesund, S., 1942, *Avh. norske VidenskAkad.*, no. 8, 1.

The Infra-Red and Raman Spectra of Ice

By Nathan Ockman
Department of Chemistry, Harvard University

§ 1. Introduction

Ice was one of the first substances to be studied by the methods of infra-red and Raman spectroscopy. It is a little surprising to find that the number of investigations of ice by these techniques have been increasing in recent years despite the fact that the initial infra-red and Raman studies of ice were made some sixty and thirty years ago respectively.

The reason for this sustained interest lies in the fact that the important questions raised by the study of the vibration spectrum of ice have not been completely answered. On one hand, they deal with the interpretation of the spectrum in terms of the crystal structure. On the other hand, they are concerned with the identification of the vibration bands in terms of the internal and intermolecular motions of the water molecules in the lattice. It appears that the study of the vibration spectrum of ice can only limit the number of possible crystal structures. This is unfortunate because the location of the hydrogen atoms by means of x-ray diffraction analysis has proved to be a formidable problem. With regard to the assignments of the vibration bands, a great deal of progress has been made. However, a completely satisfactory set of assignments must await the solution to the difficult lattice-dynamical problem which in turn depends on the determination of the crystal structure.

This paper is divided into five sections. In the first section is presented the results of infra-red investigations of hexagonal ice (H_2O, D_2O and HDO) and cubic ice (H_2O, D_2O and HDO). (The oxygen atoms of ice crystallized at temperatures above about $-80°C$ form an hexagonal lattice. If the crystallization temperature is lower, the lattice has cubic symmetry—see previous article by Blackman and Lisgarten.) The second section contains the results of Raman studies of hexagonal ice (H_2O and D_2O). A review of the interpretation of the spectra in terms of structure models is given in the third section. The fourth section discusses the various assignments which have been suggested for both hexagonal and cubic ice. The final section summarizes the paper.

This paper reviews all the published work on the subject up to and including September 1957.

§ 2. Infra-Red Spectra of Ice

2.1. *Hexagonal, Ordinary* (H_2O) *Ice*

The first transmission studies on polycrystalline ice films appear to have been made by Saunders (1899). He found a broad absorption

region between the visible and 3100 cm^{-1} for ice layers of 0·025 cm and 0·08 cm thickness. Bode (1909) resolved this broad absorption region into two bands located at 5125 cm^{-1} and 6670 cm^{-1}. He also found a band at 2220 cm^{-1} and an indication of one at 1660 cm^{-1} for frozen soap films at about $-45°C$. In this paper, Bode also presented the first reflection spectrum of ice, exhibiting a reflection maximum of 5·25% at 3080 cm^{-1}.

The first polarized transmission spectrum of a single crystal was obtained by Plyler (1924). He found bands at 7740 cm^{-1}, 9440 cm^{-1}, 10 870 cm^{-1} and 12 350 cm^{-1} which were polarized parallel to the optic axis and bands at 7940 cm^{-1}, 9800 cm^{-1}, 11 250 cm^{-1} and 12 650 cm^{-1} which were polarized perpendicular to the optic axis.

The band which was reported by Bode (1909) at 2220 cm^{-1} was found by Tammann (1927) at 2130 cm^{-1}. Cartwright (1935) found a broad absorption band at 160 cm^{-1} in polycrystalline ice at $-10°C$. This was the only band which he found between 50 cm^{-1} and 200 cm^{-1} in the only low frequency (< 300 cm^{-1}) infra-red measurements ever made of ice. Bosschieter and Errera (1937) made the first transmission studies of the region of the hydrogen stretching frequencies. At a temperature of $-16°C$, they found three bands at 3150 cm^{-1}, 3250 cm^{-1} and 3350 cm^{-1}. The central band was the most intense with the other bands appearing as well-defined inflections on the sides of the 3250 cm^{-1} absorption.

Fox and Martin (1940) made a careful re-examination of the polycrystalline ice spectrum. At a temperature of 0°C, bands were located at 1644 cm^{-1}, 2222 cm^{-1} and 3259 cm^{-1}. At $-8°C$, the first two frequencies were unchanged but the very strong 3259 cm^{-1} band shifted to 3256 cm^{-1}. A shoulder which was observed on the high frequency side of the 3259 cm^{-1} band was ascribed to the presence of liquid water-like structure.

White (1953) extended the measurements to a temperature of $-190°C$. He observed bands at 830 cm^{-1}, 1620 cm^{-1}, 2230 cm^{-1}, ~3020 cm^{-1}, ~3140 cm^{-1}, 3220 cm^{-1} and ~3400 cm^{-1}. The crystalline films were formed by condensing water vapour on to plates of CaF_2, NaCl, AgCl, KBr and KRS-5 held at $-78°C$. The plates were cooled to $-190°C$ after the films had reached their desired thickness.

The high frequency region of the spectrum of single crystals was re-examined by Vanderberg (1954) at a temperature of $-15°C$. Bands were observed at 5050 cm^{-1}, 6720 cm^{-1}, 7930 cm^{-1}, 9730 cm^{-1}, 11 100 cm^{-1} and 12 500 cm^{-1}. The absorption was essentially identical for the incident light polarized parallel and perpendicular to the optic axis. These polarization results are in disagreement with those of Plyler (1924). The latter could not possibly have observed appreciable absorption at frequencies greater than 10 000 cm^{-1} for his 0·5 cm thick crystals since Vanderberg required thicknesses greater than 4 cm to be able to observe the absorption bands. In addition, the band shapes observed by Plyler are very unlike that expected of absorption bands. Consequently, one must discard the earlier results.

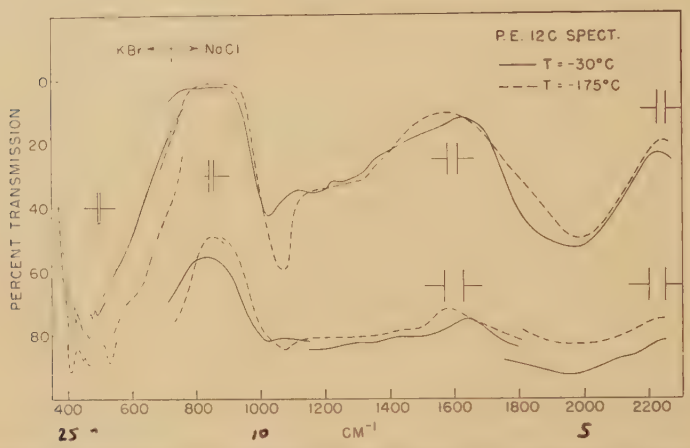
Giguère and Harvey (1956) obtained the spectra of polycrystalline films between 500 cm^{-1} and 5000 cm^{-1}. At $-55°C$ they found bands at 820 cm^{-1}, 1500 cm^{-1}, 1650 cm^{-1}, 2240 cm^{-1}, 3240 cm^{-1}, 4150 cm^{-1} and 5000 cm^{-1}. At $-170°C$, bands appeared at 850 cm^{-1}, 1650 cm^{-1}, 2250 cm^{-1} and 3260 cm^{-1}. The films were condensed on NaCl plates at a temperature lower than $-50°C$ and some were then sealed with salt windows to prevent evaporation losses.

Table 1. Frequencies (cm^{-1}) of the Infra-Red Bands of Hexagonal Ice

Ockman (1957)				Giguère and Harvey (1956)				Vander-berg (1954)	White (1953)
Reflection (H_2O)		Transmission (H_2O)		H_2O	D_2O	H_2O	D_2O	H_2O	H_2O
−24°c	−160°c	−30°c	−175°c	−55°c		−170°c		−15°c	−190°c
—	—	—	395?	—	—	—	—	—	—
—	—	—	430	—	—	—	—	—	—
522	540	540	590	—	—	—	—	—	—
620	680	660?	700?	—	—	—	—	—	—
745	808	820	846	820	610	850	630	—	830
—	—	1120	1150	—	—	—	—	—	—
—	—	1450	1450	1500	—	—	—	—	—
1600	1575	1640	1580	1650	1210	1650	1210	—	1620
—	—	—	1850?	—	—	—	—	—	—
−26°c	−134°c								
—	—	2225	2235	2240	1620	2250	1630	—	2230
—	—	—	—	—	—	—	—	—	3020
3165	3137	—	3140	—	—	—	—	—	3140
3243	3233	3252	3224	3240	2440	3260	2450	—	3220
3400	3370	—	3340	—	—	—	—	—	3400
—	—	3955	3975	—	—	—	—	—	—
—	—	4150	4200	4150	—	—	—	—	—
—	—	4530	4520	—	3295	—	—	—	—
—	—	5005	4960	5000	3720	—	—	5050	—
—	—	5600	5600	—	—	—	—	—	—
—	—	6100	6062	—	—	—	—	—	—
—	—	6500	6400	—	—	—	—	—	—
—	—	6690	6672	—	—	—	—	6720	—
—	—	7775	7685	—	—	—	—	—	—
—	—	7940	7856	—	—	—	—	7930	—
—	—	9025	9000	—	—	—	—	—	—
—	—	9667	9520	—	—	—	—	9730	—
—	—	—	—	—	—	—	—	11100	—
—	—	—	—	—	—	—	—	12500	—

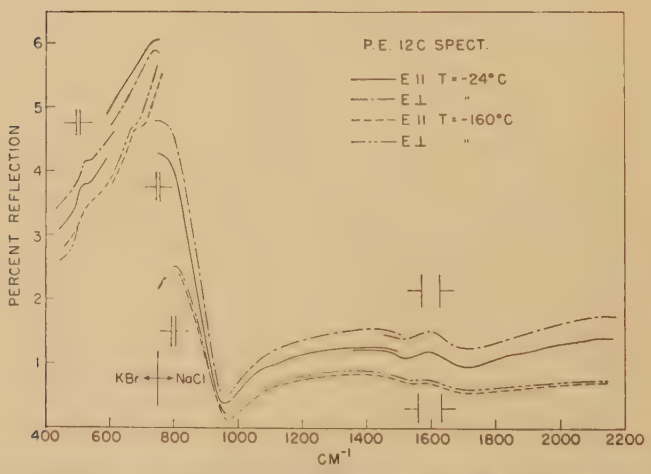
In the most recent infra-red investigation, Ockman (1957) studied the transmission and reflection spectra of single crystals and polycrystalline films. Polarized transmission and reflection spectra of single

Fig. 1



The Infra-red Transmission Spectra of Two Films of Ordinary, Hexagonal Ice (Ockman 1957).

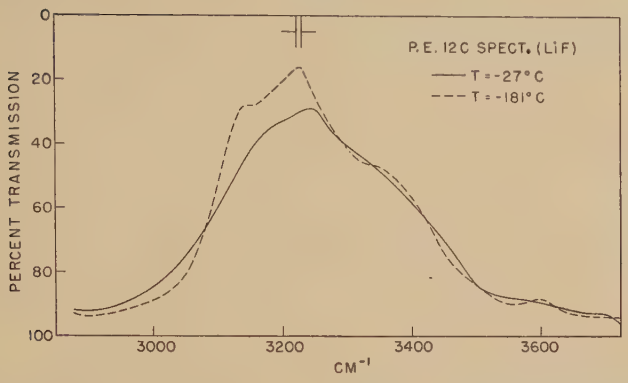
Fig. 2



The Polarized Infra-red Reflection Spectrum of a Crystal of Ordinary, Hexagonal Ice (Ockman 1957).

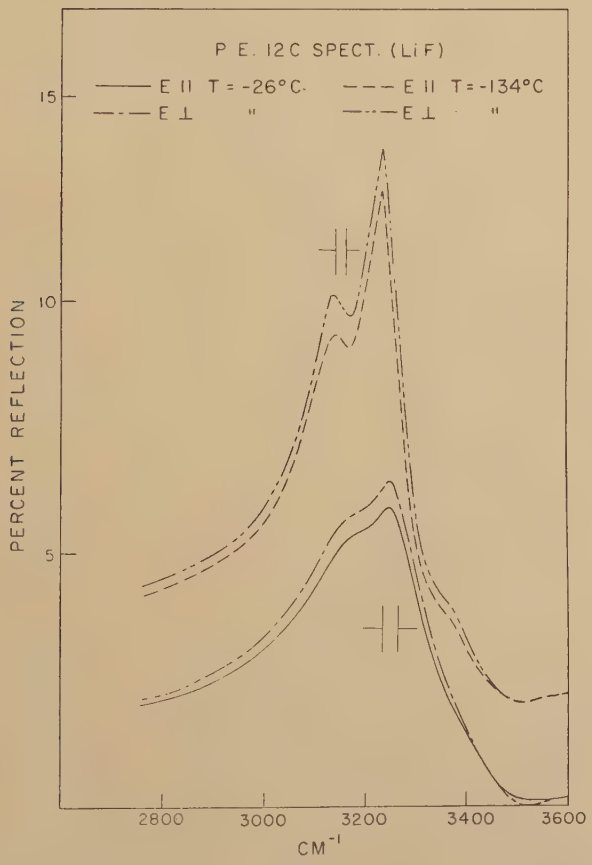
crystals were obtained in the regions 3900 cm^{-1} to 11 250 cm^{-1} and 400 cm^{-1} to 4400 cm^{-1} respectively, at temperatures of $-30°C$ and $-175°C$. The reflection spectrum was studied because of the inability

Fig. 3



The Infra-red Transmission Spectrum of a Film of Ordinary, Hexagonal Ice (Ockman 1957).

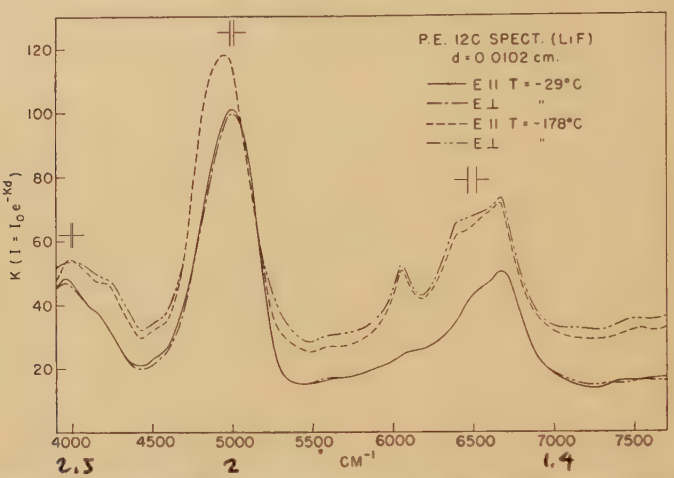
Fig. 4



The Polarized Infra-red Reflection Spectrum of a Crystal of Ordinary, Hexagonal Ice (Ockman 1957).

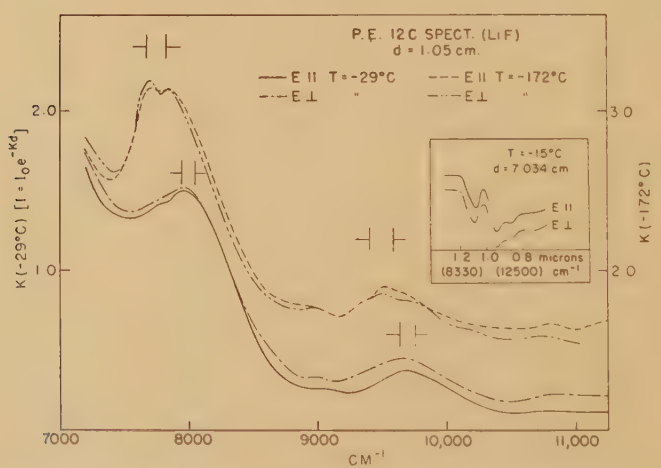
to grow crystals of sufficiently small thickness to obtain the transmission spectrum of the highly absorbing region having frequencies smaller than 4000 cm^{-1}.

Fig. 5



The Polarized Infra-red Transmission Spectrum of a Crystal of Ordinary, Hexagonal Ice (Ockman 1957).

Fig. 6



The Polarized Infra-red Transmission Spectra of Crystals of Ordinary, Hexagonal Ice (Ockman 1957, Inset, Vanderberg 1954).

Unpolarized transmission spectra of very thin films were obtained in the region 370 cm^{-1} to 3700 cm^{-1} at the aforementioned temperatures. In the transmission spectrum of ice, Ockman (1957) observed twenty-five bands ; the seven most intense bands also appearing in the reflection

spectrum. The nineteen bands which appeared in the single crystal spectra showed identical transmissivities and reflectivities for the incident radiation polarized parallel and perpendicular to the projection of the optic axis on the crystal faces.

The band frequencies observed by White (1953), Vanderberg (1954), Giguère and Harvey (1956) and Ockman (1957) are presented in table 1. The differences between the absorption maxima and the corresponding reflection maxima have been qualitatively explained by Ockman (1957) in terms of dielectric theory. The spectra of Ockman and Vanderberg appear in figs. 1–6.

2.2. *Hexagonal, Heavy* (D_2O) *Ice*

A comparison between the spectrum of ordinary ice and that of completely deuterated ice should be useful in distinguishing between those lattice motions arising from molecular translational vibrations from those arising from molecular rotational vibrations. In addition, this type of study would greatly help in the identification of the crystal modes originating in the internal molecular vibrations.

Table 2. Frequencies (cm^{-1}) of a 25% H_2O/D_2O Mixture of Hexagonal Ice (Maisch 1956)

−78°c	−190°c
—	630
—	678
—	820
—	853
—	1210
—	1630
2312	2301
2350	2348
2400–2600	2415
—	2493
3285	3260
—	3410

Cartwright (1935) examined the spectrum of polycrystalline heavy ice between 50 cm^{-1} and 200 cm^{-1} at −10°c. His spectrum was identical to that of ordinary ice, showing a broad band at 160 cm^{-1}. The bands which Giguère and Harvey (1956) found at temperatures of −55°c and −170°c are listed in table 1 next to the corresponding ordinary ice frequencies.

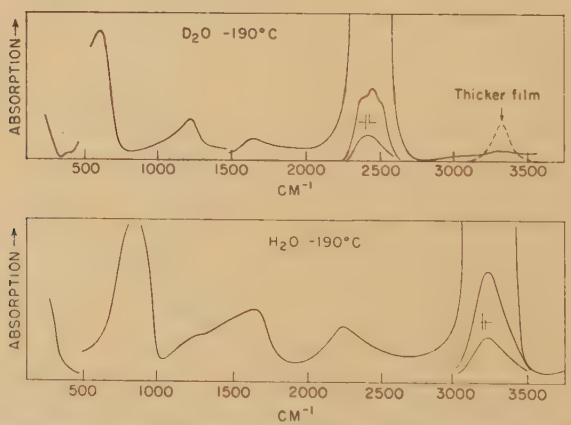
A remark should be made on the usefulness of studying the spectra of crystalline mixtures of H_2O and D_2O. Such spectra will exhibit bands due to H_2O, D_2O and HDO molecules. The frequencies of the

HDO molecule would be helpful in determining the force constants in a normal coordinate treatment of the crystal. Maisch (1956) determined the infra-red frequencies of the mixture, $H_2O/D_2O \simeq 25\%$, at temperatures of $-78°C$ and $-190°C$. His frequencies are given in table 2. It has been shown by Pimentel and Hrostowski (1951) and Hiebert and Hornig (1952) that the study of dilute mixtures can sometimes lead to a determination of the decoupled molecular frequencies. This may allow an evaluation of the intermolecular force constant governing the interaction of nearest-neighbour pairs. Haas (1957) has made such studies on dilute crystalline mixtures of HDO in H_2O. He found the frequency for the $2\nu_2$(HDO) mode, thereby determining its anharmonicity. In addition, he found bands due to HDO pairs from which he was able to evaluate the intermolecular coupling constant.

2.3. *Cubic Ice*

A growing amount of evidence leads to the conclusion that in crystals of ice formed at temperatures lower than $-80°C$, the oxygen lattice has a cubic (diamond-like) symmetry. (Honjo and Shimaoka 1957, Lisgarten and Blackman 1957). White (1953) investigated the infra-red spectra of crystalline films of H_2O, D_2O, and mixtures of the two formed at a temperature of $-190°C$. His H_2O and D_2O spectra are shown in fig. 7.

Fig. 7



The Infra-red Transmission Spectra of Films of Ordinary and Heavy, Cubic Ice (White 1953).

The frequencies of the observed bands are listed in table 3. The major differences between White's spectrum of the hexagonal and cubic forms of ice seem to be the existence of a weak 3020 cm^{-1} band in the former and a reversal in the intensity ratio of the 1620 cm^{-1} and 2230 cm^{-1} bands of hexagonal ice in the latter.

Table 3. Frequencies (cm^{-1}) and Assignments of the Infra-Red Bands of Cubic Ice†

Hexagonal H_2O (for comparison)		H_2O (100%)		H_2O (48%), D_2O (52%)		H_2O (1%), D_2O (99%)	
—	—	520	$2\nu_L$	—	—	385	$2\nu_L(D_2O)$
—	—	—	—	620	$\nu_{L'}(D_2O)$	605	$\nu_{L'}(D_2O)$
830	$\nu_{L'}$	812	$\nu_{L'}$	790	$\nu_{L'}(H_2O)$	—	—
—	—	1220	$2\nu_{L^*}$	1220	$\nu_2(D_2O)$, $2\nu_{L^*}(H_2O)$	1212	$\nu_2(D_2O)$
—	—	—	—	1470	$\nu_2(H_2O)$	—	—
—	—	1620	ν_2	1630	$\nu_2(H_2O)$	1627	$\nu_2+\nu_{L^*}$ (D_2O)
—	—	—	—	1925	$\nu_2(HDO)+\nu_{\bar{L}}$	—	—
2230	$\nu_2+\nu_{L^*}$	2230	$\nu_2+\nu_{L^*}$	—	—	—	—
—	—	—	—	—	—	2380	$\nu_3(D_2O)$
—	—	—	—	2440	$\nu_3(HDO)$	2440	$\nu_1(D_2O)$, $\nu_3(HDO)$
—	—	—	—	—	—	2520	—
3020	—	—	—	—	—	—	—
3140	$2\nu_2$	3170	$2\nu_2$	—	—	—	—
3220	ν_3	3240	ν_3	3290	$\nu_1(HDO)$, $\nu_3(H_2O)$	3320	$\nu_1(HDO)$
3400	ν_1	3380	ν_1	—	—	—	—

† White (1953), T = −190°C

ν_L, $\nu_{L'}$, ν_{L^*}, $\nu_{\bar{L}}$, are rotatory frequencies

§ 3. Raman Spectra of Ice

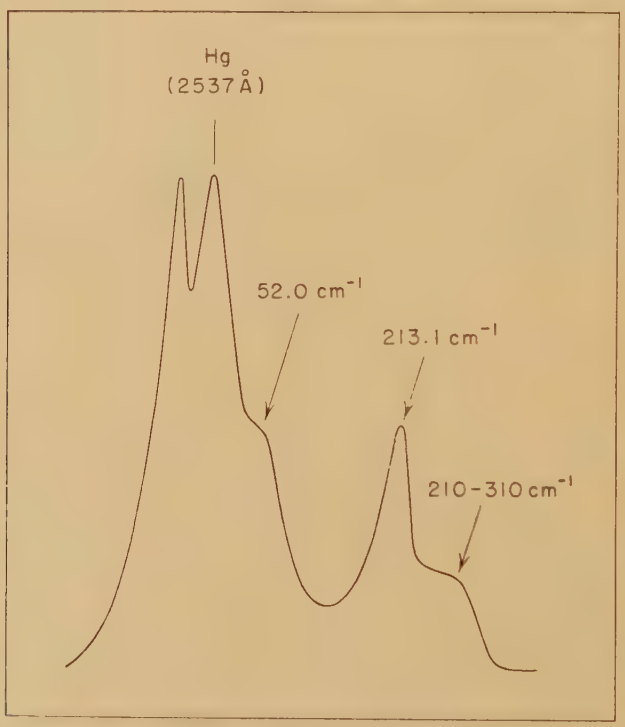
3.1. *Hexagonal, Ordinary* (H_2O) *Ice*

In his announcement of the discovery of the scattering phenomenon now bearing his name, Raman (1928) stated that the scattering spectrum of ice shows sharp lines in approximately the same positions as in liquid water. Rao (1928) made the first measurement of the frequencies of these lines for three different mercury excitation lines and found the Raman band to have an average displacement of 3220 cm^{-1}. Using a higher resolution spectrograph, Ganesan and Venkateswaran (1929) found two medium–strong bands having average values of 3193 cm^{-1} and 3391 cm^{-1} for the 3650 Å and 4046 Å excitations. Weak bands at 3549 cm^{-1} and 5393 cm^{-1} were produced by the 4046 Å and 3650 Å mercury lines, respectively.

Rasetti (1932) reported diffuse bands at 53·5 cm^{-1} and 212·1 cm^{-1} and a strong band extending from 3300 cm^{-1} to 3420 cm^{-1}. Sutherland (1933) found a strong sharp band at 3090 cm^{-1} and a faint one at 3135 cm^{-1} at −183°C. Rao (1934) resolved the 3000 cm^{-1} region, at a temperature of 0°C, into a strong, fairly sharp band at 3196 cm^{-1} and a weaker, broad band at 3321 cm^{-1}. Cabannes and de Riols (1934) found these bands at 3158 cm^{-1} and 3376 cm^{-1}.

Cross *et al.* (1937) found Raman displacements at 210 cm^{-1}, 3156 cm^{-1}, 3270 cm^{-1} and 3390 cm^{-1} at 0°c. Hibben (1937) located the previous bands at 205 cm^{-1}, 3136 cm^{-1} and 3330 cm^{-1}. He found additional weak bands at 601 cm^{-1} and 2225 cm^{-1}. Narayanaswamy (1948), using the 2537 Å excitation line, found the low frequency Raman displacements at 52·0 cm^{-1}, 213·1 cm^{-1} and in the region between 210 cm^{-1} and 310 cm^{-1}. This portion of his microphotometer tracing is shown in fig. 8. He also resolved the hydrogen stretching region into the bands at 3147 cm^{-1}, 3264 cm^{-1} and 3347 cm^{-1}. Gross and Val'kov (1950) reported a series of weak broad bands at 177 cm^{-1}, 193 cm^{-1}, 232 cm^{-1}, 252 cm^{-1}, 272 cm^{-1} and 299 cm^{-1} and a more intense band at 212 cm^{-1}. Their measurements were made at −4°c on single crystals of ice.

Fig. 8



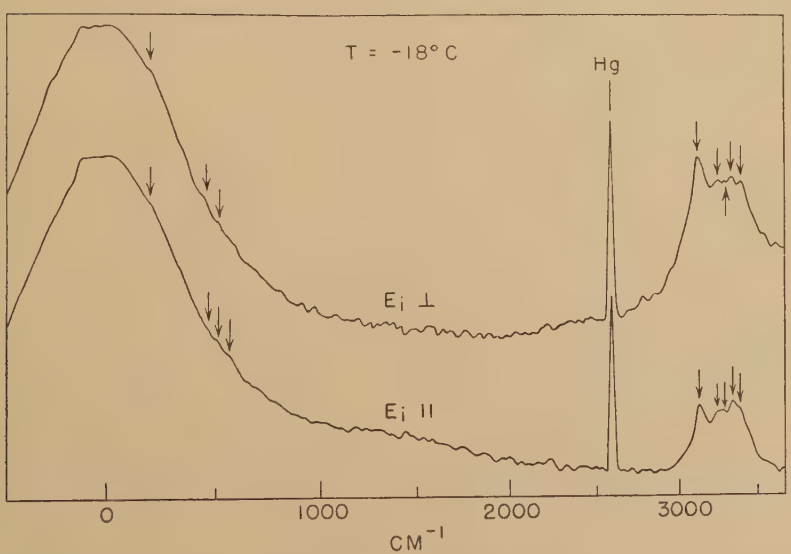
The Low Frequency Raman Spectrum of Ordinary, Hexagonal Ice (Narayanaswamy 1948).

Maisch (1956), using a photoelectric recording spectrometer, made the first polarized Raman investigations of single crystals of ice. His study was limited to the hydrogen stretching region. At a temperature of −5°c, he found the three bands in this region located at 3159 cm^{-1}, 3275 cm^{-1} and 3370 cm^{-1}. In his measurements, Maisch employed

various combinations of orientations of the crystal with polarizations of the incident and scattered radiation. The crystal c-axis (optic axis) was either parallel, perpendicular or oblique to the vertical. The incident radiation was polarized either parallel or perpendicular to the vertical while either the entire scattered radiation or that confined to one of the many possible polarizations in the plane perpendicular to the c-axis was measured. Maisch defined the depolarization ratio, ρ, as the total scattered intensity with the incident polarization vertical divided by the total scattered intensity with incident polarization horizontal. He found the following values for ρ for four different crystal orientations.

Angle between c-axis and vertical (γ)	3159 cm^{-1} band	3370 cm^{-1} band
oblique	0·534	0·82
0°	0·574	0·75
54° 35′	0·703	0·98
90°	0·569	0·78

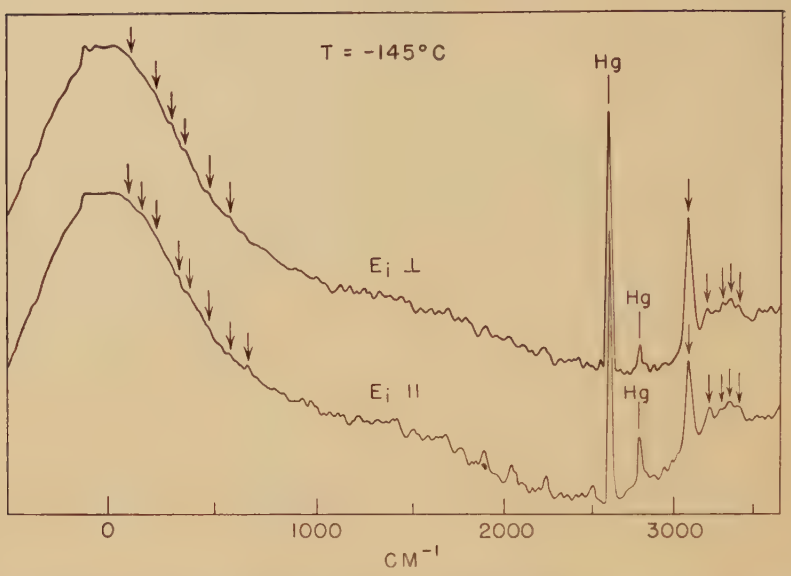
Fig. 9



The Polarized Raman Spectrum of a Crystal of Ordinary, Hexagonal Ice at $T = -18$°c (Ockman 1957).

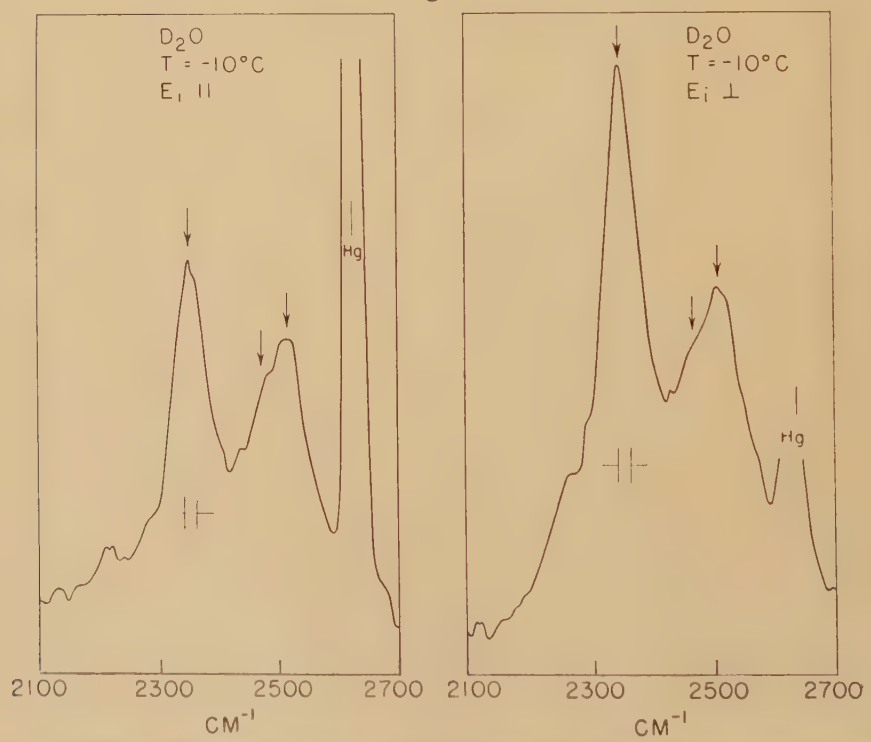
The uncertainties of these values are about 11%. Maisch also found ρ to be constant across each of the bands. This latter result has important bearings on the characterization of the ice structure and will be discussed later.

Fig. 10



The Polarized Raman Spectrum of a Crystal of Ordinary, Hexagonal Ice at $T = -145°$C (Ockman 1957).

Fig. 11



The Polarized Raman Spectrum of a Crystal of Heavy, Hexagonal Ice at $T = -10°$C (Maisch 1956).

Ockman (1957) obtained the polarized Raman spectrum of a single crystal at temperatures of −18°C and −145°C. In these measurements, the crystal *c*-axis was oriented vertically and the incident radiation polarized parallel and perpendicular to the optic axis. The entire

Table 4. Frequencies (cm^{-1}) of the Raman Bands of Hexagonal Ice

Ockman (1957)		Maisch (1956)		White (1953)	Gross and Val'kov		Naray. (1948)
H_2O		H_2O	D_2O	D_2O	H_2O (1950)	D_2O (1951)	H_2O
−18°C	−145°C	−5°C	−10°C	−150°C	−4°C		
—	—	—	—	—	—	—	52·0
—	68	—	—	—	—	—	—
—	83	—	—	—	—	—	—
—	100	—	—	—	—	—	—
122	—	—	—	—	—	—	—
163	152	—	—	—	—	—	—
—	—	—	—	—	177	166	—
—	—	—	—	—	193	—	—
205	219	—	—	210	212	203	213·1
—	—	—	—	—	232	218	—
—	—	—	—	—	252	236	—
—	—	—	—	—	272	256	—
—	292	—	—	—	299	275	—
—	330	—	—	—	—	—	—
—	356	—	—	—	—	—	—
—	373	—	—	—	—	—	—
458	466	—	—	—	—	—	—
516	—	—	—	—	—	—	—
567	566	—	—	—	—	—	—
—	659	—	—	—	—	—	—
3139	3089	3159	2347	2304	—	2330	3147
3259	3215	3275	—	—	—	—	3264
3307	3302	—	—	—	—	2445	—
3353	3345	3370	2514	2477	—	2500	3347
3403	3410	—	—	—	—	—	—
—	—	—	—	2730	—	2690	—

scattered radiation was recorded photographically. His microphotometer tracings are shown in figs. 9 and 10. The frequencies he observed are tabulated in table 4 together with other recent data.

3.2. *Hexagonal, Heavy Ice*

The first Raman investigation of heavy ice crystals were made by Gross and Val'kov (1951). They found bands at 166 cm^{-1}, 203 cm^{-1}, 218 cm^{-1}, 236 cm^{-1}, 256 cm^{-1}, 275 cm^{-1}, 2330 cm^{-1}, 2445 cm^{-1}, 2500 cm^{-1}

and 2690 cm^{-1}. In the low frequency region, the 203 cm^{-1} band was much more intense than the others. In the high frequency region, the 2330 cm^{-1} and 2500 cm^{-1} bands were the strongest.

White (1953) found bands at 210 cm^{-1}, 2304 cm^{-1}, 2477 cm^{-1} and 2730 cm^{-1} at $-150°C$. Maisch (1956) studied the polarized Raman spectrum of single crystals at $-10°C$. He found bands at 2347 cm^{-1} and 2514 cm^{-1} having depolarization ratios of 0·564 and 0·82 respectively. His tracings appear in fig. 11.

The Raman frequencies for heavy ice are given in table 4.

§ 4. Relation of Spectra to Crystal Structure

The first attempt to explain the vibration spectrum of ice in terms of its crystal structure was made by Rao (1931, 1934). Guided by the polymer model for the structures of liquid water and ice proposed by W. Sutherland (1900), Rao postulated that liquid water consists of a mixture of monomers, dimers and trimers of H_2O molecules while ice consists only of a mixture of dimers and trimers. He accordingly assigned the liquid Raman bands at 3217 cm^{-1}, 3433 cm^{-1} and 3582 cm^{-1} to the trimer, dimer, and monomer respectively, and the solid Raman bands at 3196 cm^{-1} and 3321 cm^{-1} to the trimer and dimer. G. B. B. M. Sutherland (1933) explained the Raman spectrum of ice in terms of a dimer structure. He assigned the 3200 cm^{-1} band to the dimer while he attributed the other two bands in this region to a resonance interaction between the dimer frequency and the overtone of the deformation frequency of the water molecules.

These attempts to use the Raman spectrum to prove the polymer structure of ice and *vice versa* turned out to be unsuccessful. The x-ray investigations of liquid water by Stewart (1931) and Morgan and Warren (1937) ruled out the polymer structure for water. The studies of ice by x-ray diffraction (Owston 1953), neutron diffraction (Levy and Peterson 1957), and electron diffraction (Honjo and Shimaoka 1957), reject the polymer structure for ice.

Methods for relating the vibration spectra of molecular crystals to the symmetry properties of their primitive unit cells have been developed by Bhagavantam and Venkatarayudu (1939), Halford (1946), Hornig (1948) and Winston and Halford (1949). The application of these methods to the analysis first of the spectrum of hexagonal ice, and then of cubic ice, will now be discussed.

Miller (1954) made the first attempt to interpret the infra-red spectrum of hexagonal ice in terms of a structure. Using the general formulation of Hornig, Miller solved the normal co-ordinate problem for the intramolecular modes for the Bernal and Fowler unit cell (1933). (This cell contains 12 molecules and belongs to the space group $P6_3cm$.) Neglecting the coupling between stretching and deformation modes, including only nearest-neighbour interactions, and assuming the force constants

determined by White (1953) for cubic ice, Miller calculated the hydrogen stretching frequencies. The lack of agreement with White's spectra led Miller to reject the Bernal and Fowler model. (It should be noted that Miller assumed White's incorrect assignment for ν_1.)

Maisch (1956) also used the coupled oriented gas approximation of Hornig (1948) to analyse the polarized Raman spectrum of hexagonal ice. He developed a theoretical expression for the depolarization ratio, ρ (as defined in § 3·1) of the ν_3 mode as a function of the angle (γ) between the c-axis and the vertical (direction of his scattered beam) for a general structure in which the H_2O molecules have the Pauling (1935) orientations. The Pauling disordered structure (1935) and the Bernal and Fowler ordered structure (1933) are special cases of this general structure. (The calculation was limited to ν_3 because this is the only fundamental mode for which ρ can be calculated without a knowledge of the components of the polarizability tensor.)

First, Maisch showed that ρ should be identical for all structures belonging to his general group. As a consequence, Raman polarization measurements cannot distinguish between the Bernal and Fowler and Pauling models. Secondly, he took into account the effect of librational modes in causing a deviation from the equilibrium values of the mean squares of the orientation parameters. These latter quantities appear in the expression for ρ. Maisch calculated ρ as a function of γ for four cases. (*a*) The H_2O molecules are oriented in their equilibrium positions, (*b*) the H_2O molecules are freely rotating, (*c*) the H_2O molecules have librational frequencies of 475 cm^{-1} and 820 cm^{-1}, (*d*) the librational frequencies are 260 cm^{-1} and 450 cm^{-1} or have the equivalent set of values, 335 cm^{-1}, 335 cm^{-1}. (The frequencies in case (*d*) were determined by fitting the calculated and observed ρ at $\gamma = 0°$). A comparison of the calculated curves with the measured values of ρ for the 3370 cm^{-1} band, given in § 3.2, showed only fair agreement for case (*d*). As will be shown in the next section, Maisch's choice for the ν_3 assignment was incorrect, consequently, it is not surprising that his calculations did not agree too well with the measurements.

From the constancy of ρ over each of the bands in the hydrogen and deuterium stretching regions, Maisch concluded that either the ice structure is disordered or the intermolecular coupling in ice is weak. The strong hydrogen bonding in ice would seem to eliminate the latter conclusion.

Ockman (1957) utilized the methods of Bhagavantam and Venkatarayudu (1939) and Hornig (1948) to analyse the polarized infra-red and Raman spectra of single crystals of hexagonal ice. He first considered the following four ordered structures.

(1) Bernal and Fowler (1933).

(2) Bernal and Fowler Modification I. (12 molecules per unit cell, unit cell symmetry (P1), $\angle HOH$ = tetrahedral.)

(3) Bernal and Fowler Modification II. (12 molecules per unit cell, unit cell symmetry (P1), $\angle HOH = 104{\cdot}5°$.)

(4) Owston Model (1953). (8 molecules per unit cell, unit cell symmetry (Pc), $\angle HOH$ = tetrahedral.)

The normal modes of the crystal arising from the three internal modes of the H_2O molecule were calculated for each of the four structures. This enabled him to obtain a quantity, K_j, proportional to the jth component of the absorption coefficient for a space-fixed co-ordinate system with its Z-axis coinciding with the crystal c-axis. The results of these calculations are:

	ν_1, ν_2		ν_3	
Model (1)	$Kx : Ky : Kz$	1·00:1·00:1·00	$Kx : Ky : Kz$	1·00:1·00:1·00
(2)	,,	,,	,,	,,
(3)	,,	3·92:3·85:4·21	,,	4·06:4·18:3·76
(4)	,,	8·00:2·64:5·34	,,	4·00:6·66:5·32

Another result of the analysis of these four structures was the prediction that the Raman bands due to the intramolecular modes should not be completely polarized for the two polarizer orientations used by Ockman in obtaining his data. Ockman (1957) also calculated the dichroism for the following three disordered models; (*a*) Pauling's Model (1935), (*b*) Modified Pauling Model ($\angle HOH = 104{\cdot}5°$ rather than $109{\cdot}5°$), (*c*) Rundle Model (1953). The first two models predict isotropic infra-red activity while the Rundle model predicts a 10% anisotropy with respect to the c-axis. All three models, give the same Raman effect predictions as for the ordered models.

Ockman felt that his assumption of undistorted H_2O molecules in the crystal, the neglect of ν_1, ν_3 interactions and also those involving nearest neighbours not coupled by symmetry operations, should lead to an uncertainty of 10% in these calculations. It is clear from figs. 2, 4, 5, and 6, that within experimental error (10%), hexagonal ice is isotropic with regard to its infra-red activity. The polarized Raman spectra (figs. 9–11) are in agreement with all seven models. However, Owston's ordered model must be rejected because of its predicted infra-red dichroism.

White (1953) used the method of Hornig (1948) to analyse the spectrum of polycrystalline cubic ice. König (1944) had established that the unit cell of cubic ice belongs to the space group Fd3m and that it contains eight H_2O molecules. White interpreted his spectrum in terms of the Fd3m group and the eight subgroups; I4md, I4, Imm, Fdd, C2, Cm, Cc and P1. The P1 subgroup was rejected because it predicted more coupling components than were seen, the groups Cc, Cm, C2, and Imm were eliminated because they required the existence of two non-identical

H_2O molecules which White felt was unlikely. The site symmetries of the I4 and Fdd groups required the hydrogen atoms to be off the 0–0 directions. White believed this condition to be unreasonable. The Fd3m group was discarded because it required the H_2O molecules to possess a 3-fold symmetry axis. Consequently, the I4md structure (2 molecules per unit cell, site symmetry 2mm) was chosen. However, this structure must be rejected because the recent electron diffraction work of Honjo and Shimaoka (1957) convincingly shows that cubic ice has the Pauling disordered structure.

§ 5. Assignment of Frequencies

The frequency assignments of hexagonal ice will be discussed in the first three subsections and that of cubic ice in the last. For both types of ice, the selection rules for all of the structures considered in the previous section predict that all of the intramolecular crystal modes and most of the intermolecular modes will be active in the infra-red and Raman spectra.

5.1. *Low Frequency Region* (0–1500 cm^{-1})

The assignments of the bands in this region for both ordinary and heavy hexagonal ice are given in table 5. In the absence of a complete theoretical treatment of the lattice-dynamical problem, one can only hope to distinguish between translatory and rotatory vibrations by a comparison of the H_2O and D_2O spectra. If the observed frequency ratio, H_2O/D_2O, of bands arising from a particular vibration is about $(20/18)^{1/2}$, the vibration has a translatory nature. If the ratio is about $(2)^{1/2}$, the mode has a rotatory nature. This kind of analysis is the basis for most of the assignments in table 5. It should be said here that this division of lattice modes is only an approximation although it is also a consequence of the theory of Bhagavantum and Venkatarayudu (1939).

The assignments of Gross and Val'kov (1950) refer to the translatory vibrations of the centre of gravity of an O–H group relative to the adjacent hydrogen-bonded oxygen atom. The band at 294 cm^{-1} (H_2O) is assigned to the (0–1) vibrational transition, that at 272 cm^{-1} to the (1–2) transition, etc. The frequencies of this diatomic oscillator model are not degenerate but instead decrease in value with an increase of the vibrational quantum number of the initial state because of the large anharmonicity. The average anharmonicity of the series gives a dissociation energy of 7·1 kcal/mole for the hydrogen bond. Before the treatment of Gross and Val'kov can be taken seriously, a comparison should be made between the observed intensity ratios of the bands and those calculated from the Boltzman factors.

In the assignments of Ockman (1957), (ν_T)? refer to those based on the assumption that all frequencies smaller than 300 cm^{-1} are translatory.

The assignments (ν_T)?? refer to those based on the observation of a greater temperature dependence of the rotatory vibrations.

Table 5. Assignments of Hexagonal Ice Bands Having Frequencies Smaller than 1500 cm^{-1}

$\nu(H_2O)$	$\nu(D_2O)$	Ockman (1957)	Giguère and Harvey (1956)	Gross and Val'kov (1950)
53 cm^{-1}	—	(ν_T)?	—	—
97	—	(ν_T)?	—	—
122	—	(ν_T)?	—	—
160(IR)	160(IR)	ν_T†	—	—
177	—	(ν_T)?	—	$(\nu_T)_H$
193	—	(ν_T)?	—	$(\nu_T)_H$
212	203	ν_T‡	—	—
232	218	ν_T	—	$(\nu_T)_H$
252	236	ν_T	—	$(\nu_T)_H$
272	256	ν_T	—	$(\nu_T)_H$
294	275	ν_T	—	$(\nu_T)_H$
457	—	(ν_T)??	—	—
516	—	—	—	—
540(IR)	—	$(\nu_{R'})$??	—	—
600	—	—	—	—
660(IR)	—	$(\nu_{R''})$??	—	—
800(IR)	590(IR)	ν_R	ν_R§	—
1120(IR)	—	$\nu_R+\nu_T$	—	—
1450(IR)	—	$2\nu_R$	$2\nu_R$§	—

† previously assigned by Cartwright (1935).
‡ previously assigned by Cross, Leighton and Burnham (1937).
§ previously assigned by White (1953).
(IR) infra-red frequencies, others from Raman scattering.

5.2. *Fundamental Region* (1500 cm^{-1}–3800 cm^{-1})

In molecular crystals the intramolecular forces are much larger than those between molecules. As a result, one expects to find a readily recognizable correlation between the active internal modes in the crystal and the corresponding modes in the liquid and vapour. Consequently, it has been the practice to assign the bands observed in the crystalline state to the corresponding internal modes of the isolated molecules. On the basis of a very clear-cut correlation, the 1640 cm^{-1} ice band has been assigned to ν_2.

In the water vapour spectra of this region, ν_1 is assigned to the most intense Raman band and ν_3 to the most intense infra-red band. If one makes an intensity correlation between the vapour and crystalline states, then the very strong bands (H_2O) at 3143 cm^{-1} (Raman) and 3252 cm^{-1} (infra-red) should be assigned to ν_1 and ν_3 respectively. A confirmation

of the assignment of ν_1 to the bands at 3143 cm^{-1} (H_2O) and 2347 cm^{-1} (D_2O) is found in the depolarization ratio measurements of Maisch (1956) giving values of about 0·56 for both of the bands. The ν_1 and ν_3 bands

Table 6. Assignments of Hexagonal Ice Bands Having Frequencies Larger than 1500 cm^{-1}

$\nu(H_2O)$	$\nu(D_2O)$	Ockman (1957)	Maisch (1956)	Giguère and Harvey (1956)	White (1953)	Fox and Martin (1940)
1640 cm^{-1}	1210 cm^{-1}	ν_2	—	ν_2	ν_2	ν_2
2225	1620	$\nu_2+\nu_{R'}$, $\nu_2+\nu_{R''}$	—	$\nu_2+\nu_R$	$\nu_2+\nu_{R^*}$	$\nu_2+\nu_R$
3020	—	—	—	—	—	—
3143(R)	2347(R)	ν_1	ν_1	—	$\nu_1(D_2O)$, $2\nu_2(H_2O)$	—
3180	—	$2\nu_2$	—	—		—
3252	2440	ν_3	$2\nu_2$	ν_3	ν_3	ν_3
3307(R)	—	$\nu_1+\nu_T b$, $\nu_3+\nu_T c$	—	—	—	—
3352(R)	2514(R)	$\nu_3+\nu_T e$	ν_3	—	—	—
3402(R)	—	$\nu_3+\nu_T b$	—	—	ν_1	—
		Ockman (1957)				
—	2690	$\nu_3+\nu_T$, $\nu_3+\nu_T e+\nu_T$				
3955	—	$\nu_1+\nu_R$, $\nu_3+\nu_R$				
4150	—	$\nu_1+\nu_R+\nu_T$, $\nu_3+\nu_R+\nu_T$, $3\nu_2$				
4530	3295	$\nu_1+\nu_R+\nu_{R'}$, $\nu_3+\nu_R+\nu_{R'}$, $\nu_1+2\nu_R$, $\nu_1+\nu_R+\nu_{R''}$, $\nu_1+\nu_2$, $3\nu_2$				
5005	3720	$\nu_2+\nu_3$				
5600	—	$\nu_1+\nu_2+\nu_{R'}$, $\nu_2+\nu_3+\nu_R$				
6100	—	$\nu_2+\nu_3+\nu_R+\nu_T$, $\nu_2+\nu_3+2\nu_{R'}$, $\nu_2+\nu_3+2\nu_{R''}$, $2\nu_1$, $\nu_1+2\nu_2$, $2\nu_2+\nu_3$, $2\nu_3$				
6500	—	$\nu_2+\nu_3+2\nu_R$, $\nu_1+2\nu_2+\nu_T$, $2\nu_2+\nu_3+\nu_T$, $2\nu_2+\nu_3$, $2\nu_3$, $2\nu_1$, $\nu_1+2\nu_2$				
6690	—	$\nu_1+\nu_3$				
7775	—	$\nu_1+\nu_3+2\nu_R$, $\nu_1+\nu_3+\nu_R+\nu_{R'}$, $\nu_1+\nu_3+\nu_R+\nu_{R''}$, $\nu_1+\nu_3+2\nu_{R''}$, $3\nu_2+\nu_3$, $\nu_2+2\nu_3$, $2\nu_1+\nu_2$, $\nu_1+3\nu_2$				
7940	—	$\nu_1+\nu_2+\nu_3$				
9025	—	$\nu_1+\nu_2+\nu_3+\nu_R$, $3\nu_2+\nu_3+\nu_R$, $\nu_1+3\nu_2+\nu_R$, $\nu_2+2\nu_3+\nu_R$				
9667	—	$2\nu_1+\nu_3$				
11100	—	$2\nu_1+\nu_2+\nu_3$				
12500	—	$3\nu_1+\nu_3$				

(R) Raman data, others from infra-red: *see* tables 1 and 4.
ν_T, $\nu_T a$, etc. denote translatory modes.
ν_R, $\nu_{R'}$, etc. denote rotatory modes.

assigned in this manner also exhibit the correct temperature behaviour associated with hydrogen-bonded systems.

The other bands in this region can be attributed to $2\nu_2$ and to combinations of ν_1 and ν_3 with translatory modes. The present lack of knowledge

of the crystal anharmonicities makes a satisfactory assignment impossible The possibilities given in table 6 by Ockman (1957) utilize the observed lattice frequencies.

5.3. *High Frequency Region* (3800 cm^{-1}–13 000 cm^{-1})

Ockman (1957) assigned the strong bands at 5005 cm^{-1}, 6690 cm^{-1}, 7940 cm^{-1} and 9667 cm^{-1} to the intramolecular combination bands given in table 6, by a correlation with the most intense liquid and vapour bands in this region. Similarly, the 11 100 cm^{-1} and 12 500 cm^{-1} bands can be assigned to $2\nu_1+\nu_2+\nu_3$ and $3\nu_1+\nu_3$ respectively. The other bands cannot be given definite assignments because of the lack of knowledge of the anharmonicities associated with both the molecular and intermolecular vibrations. All of the possibilities conceived by Ockman (1957) are presented in table 6 as a matter of interest. This list includes bands unobserved in the vapour spectrum because of the possibility of intensity enhancements by the crystal field. The intensity increase at low temperature of the 6100 cm^{-1} and 7775 cm^{-1} bands indicates a possible resonance between some of these choices and nearby intense bands.

5.4. *Cubic Ice*

White's assignments (1953) for cubic ice (H_2O), cubic heavy ice and a crystalline mixture of the two are presented in table 3. Since the strong arguments presented by Ockman lead to the assignment of the hexagonal band at 3140 cm^{-1} to ν_1, the cubic band at 3170 cm^{-1} should also be assigned to ν_1.

White attempted to justify his assignments for ν_1, ν_2 and ν_3 for crystalline H_2O, D_2O and HDO, by a normal co-ordinate treatment based on a complete four constant harmonic potential. (In this treatment, the effect of the intermolecular force field is incorporated into the internal force constants.) The calculated frequencies deviated on the average by 0·79% from the observed values. The Redlich Teller product rule also gave the best agreement for White's assignments.

Miller (1954) solved the normal vibration problem for the I4md unit cell chosen by White (1953). He considered only the interaction of nearest neighbours. Using the frequencies and assignments of White, Miller was able to calculate the internal force constants k_d, k_α, k_{dd} and $k_{d\alpha}$ and the two intermolecular constants $k_{dd'}$ and $k_{\alpha\alpha'}$. His calculated frequencies show an average deviation of 0·56% from the observed values.

The justification of an incorrect assignment by the calculations of White and Miller should introduce a note of caution in the consideration of future calculations of this type. The assumption of the harmonic approximation and the neglect of other than nearest-neighbour interactions for strongly hydrogen-bonded crystals like ice do not seem justifiable.

6. Summary

This paper has reviewed all of the available work on the infra-red and Raman spectroscopy of hexagonal and cubic ice. It has been shown by the studies of Maisch (1956) and Ockman (1957) that it is not possible to obtain a unique solution to the structure problem of ice by measuring its polarized vibration spectrum. However, Maisch's observation of the constancy of the depolarization ratio across each of the bands in the hydrogen stretching region is a strong argument for a disordered structure.

Satisfactory assignments have only been made for the three bands originating in the fundamental modes of the water molecule and for the six strong bands which can be correlated with the overtone and combination modes of the liquid and vapour spectra. An explicit characterization of the low frequency bands in terms of lattice motions must await a solution to the lattice-dynamical problem as well as a careful study of the low frequency, polarized spectra of single crystals.

The solution to the dynamical problem of the ice lattice should make possible a determination of the crystal anharmonicities. This would then enable one to assign the overtone and combination bands.

Note added in proof.—The following two references came to the attention of the author after the manuscript had been submitted.

(1) Reding, F. P., 1951, *Thesis*, Brown University.

Reding studied the infra-red absorption spectra of polycrystalline films of hexagonal, ordinary ice and heavy ice. For H_2O, his frequencies and assignments are; 520 cm^{-1} ($-190°C$, torsion), 812 cm^{-1} ($-190°C$, torsion), 1220 cm^{-1} ($-190°C$, torsion overtone), 1620 cm^{-1} ($-78°C$, $-190°C$, ν_2), 2230 cm^{-1} ($-78°C$, $-190°C$, ν_2+ torsion), 3240 cm^{-1}($-78°C$, $-190°C$, hydrogen stretching), 4050 cm^{-1} ($-78°C$, $-190°C$, stretching + torsion), 4940 cm^{-1} ($-78°C$, stretching + ν_2), 6100 cm^{-1}($-78°C$, ?) and 6580 cm^{-1} (stretching overtone). For D_2O; 605 cm^{-1} ($-190°C$, torsion), 1212 cm^{-1} ($-190°C$, ν_2), 1627 cm^{-1} ($-190°C$, ν_2 + torsion), 2436 cm^{-1} ($-190°C$, deuterium stretching). Reding also assigned the Raman bands observed by Cross *et al.* (1937) at 3150 cm^{-1}, 3270 cm^{-1} and 3390 cm^{-1} to ν_1, ν_3 and ν_1 + translatory respectively.

(2) Val'kov, V. I., and Maslenkova, G. I., 1956, *Optika Spekt.*, 1, 881.

Val'kov and Maslenkova investigated the unpolarized Raman spectrum of a single crystal of ordinary ice at $-196°C$. They observed low frequency bands at 230 cm^{-1}, 291 cm^{-1} and 310 cm^{-1} with their spectrum indicating additional bands in this region. For the high frequency spectrum, their frequencies and assignments are; 3088 cm^{-1} (ν_1), 3210 cm^{-1} (ν_3), 3321 cm^{-1} ($\nu_1 + 230$ cm^{-1}) and 3400 cm^{-1}($\nu_1 + 310$ cm^{-1}). Their spectrum also indicated a weak band between 3321 cm^{-1} and 3400 cm^{-1} while the 3400 cm^{-1} band appeared to have structure.

References

Bernal, J. D., and Fowler, R. H., 1933, *J. chem. Phys.*, **1**, 515.
Bhagavantam, S., and Venkatarayudu, T., 1939, *Proc. Indian Acad. Sci.* A, **9**, 224.
Bode, G., 1909, *Ann. d. Phys.*, **30**, 326.
Bosschieter, G., and Errera, J., 1937, *C. R. Acad. Sci. Paris*, **205**, 560.
Cabannes, J., and de Riols, J., 1934, *C. R. Acad. Sci. Paris*, **198**, 30.
Cartwright, C. H., 1935, *Nature, Lond.*, **136**, 181.
Cross, P. C., Leighton, P. A., and Burnham, J., 1937, *J. Amer. chem. Soc.*, **59**, 1134.
Fox, J. J., and Martin, A. E., 1940, *Proc. roy. Soc.* A, **174**, 234.
Ganesan, A. S., and Venkateswaran, S., 1929, *Indian J. Phys.*, **4**, 195.
Giguère, P. A., and Harvey, K. B., 1956, *Canad. J. Chem.*, **34**, 798.
Gross, E. F., and Val'kov, V. I., 1950, *Doklady Akad. Nauk, SSSR*, **74**, 453; 1951, *Ibid*, **81**, 761.
Haas, C., 1957, private communication from Professor D. F. Hornig, Princeton University.
Halford, R. S., 1946, *J. chem. Phys.*, **14**, 8.
Hibben, J. H., 1937, *J. chem. Phys.*, **5**, 166.
Hiebert, G. L., and Hornig, D. F., 1952, *J. chem. Phys.*, **20**, 918.
Honjo, G., and Shimaoka, K., 1957, *Acta. cryst.*, **10**, 710.
Hornig, D. F., 1948, *J. chem. Phys.*, **16**, 1063.
König, H., 1944, *Z. Kristallogr.*, **105**, 279.
Levy, H. A., and Peterson, S. W., 1957, *Acta. cryst.*, **10**, 70.
Lisgarten, N. D., and Blackman, M., 1957, *Proc. roy. Soc.* A, **239**, 93.
Maisch, W., 1956, *Thesis*, Brown University.
Miller, R. L., 1954, *Thesis*, Brown University.
Morgan, J., and Warren, B. E., 1937, *J. chem. Phys.*, **6**, 666.
Narayanaswamy, P. K., 1948, *Proc. Indian Acad. Sci.* A, **27**, 311.
Ockman, N., 1957, *Thesis*, University of Michigan.
Owston, P. G., 1953, *J. chim. Phys.*, **50**, C13.
Pauling, L., 1935, *J. Amer. chem. Soc.*, **57**, 2680.
Pimentel, G. C., and Hrostowski, H. J., 1951, *J. chem. Phys.*, **19**, 661.
Plyler, E. K., 1924, *J. Opt. Soc. Amer.*, **9**, 545.
Raman, C. V., 1928, *Indian J. Phys.*, **2**, 387.
Rao, I. R., 1928, *Indian J. Phys.*, **3**, 131; 1931, *Proc. roy. Soc.* A, **130**, 489; 1934, *Ibid*, **145**, 489.
Rasetti, F., 1932, *Nuovo Cim.*, **9**, 72.
Rundle, R. E., 1953, *J. Chem. Phys.*, **22**, 344.
Saunders, F. A., 1899, *Johns Hopkins University*, Circular No. 140.
Stewart, G. W., 1931, *Phys. Rev.*, **37**, 9.
Sutherland, G. B. B. M., 1933, *Proc. roy. Soc.* A, **141**, 535.
Sutherland, W., 1900, *Phil. Mag.*, **50**, 460.
Tammann, G., 1927, *Naturwissenschaften*, **15**, 632.
Vanderberg, R. M., 1954, *Thesis*, University of California at Los Angeles,
White, H. F., 1952, *Thesis*, Brown University.
Winston, H., and Halford, R. S., 1949, *J. chem. Phys.*, **17**, 607.

The Supercooling and Nucleation of Water

By B. J. Mason
Warren Research Fellow of The Royal Society, Imperial College, London

§ 1. Introduction

Interest in the supercooling and freezing of water, matters which have been extensively studied since the early publications of Fahrenheit in 1724, has greatly increased during the last ten years, mainly because of their essential importance in the physics of clouds and precipitation.

Although large quantities of water such as lakes and ponds do not usually supercool by more than a few hundredths of a degree, the tiny droplets composing atmospheric clouds commonly exist in the supercooled state down to temperatures as low as $-20°$C; on occasion, water-droplet clouds have been observed at $-35°$C; and droplets of very pure water, only a few microns in diameter, may be supercooled to $-40°$C in the laboratory. In cloud physics one is concerned with the temperatures at which airborne drops, varying in diameter from a few microns, to about 5 mm for the largest raindrops, will freeze, and how the attainable degree of supercooling may depend upon the drop size, the rate of cooling and the purity of the water. In the absence of sufficiently detailed and careful experiments and of anything approaching a satisfactory theory, it was not possible, until very recently, to gain some real insight into these problems.

Although there was some indication in the extensive literature that the attainable degree of supercooling tends to increase with decreasing volume of the water sample, there was so much scatter in the results, with serious discrepancies between those of different workers, that no clear-cut relationships could be deduced. It appears that the earlier work may have failed to provide the required information for three main reasons. First, the water samples used by different investigators varied greatly in their origin and purity; secondly, they were usually contained in glass tubes or supported as drops on variously-treated metal surfaces so that nucleation may often have been induced by the solid boundaries; thirdly, in any one investigation, the volume of the sample was not usually varied sufficiently to establish clearly how this might be related to the attainable supercooling, particularly as there was usually a considerable spread in the freezing temperatures recorded for specimens of the same volume.

For these reasons, the whole subject has recently been examined afresh, and it is with the results of this later work, both experimental and theoretical, that this review is mainly concerned.

The great majority of the experiments have been concerned with the study of *heterogeneous* nucleation in that the water used almost certainly

contained foreign particles which initiated crystallization. The fact that the freezing temperature of the same water sample is not generally reproducible to within 0·5°c, or more, suggests that, to some extent, freezing is a random process, and that a given sample has only a statistical probability of freezing at a particular temperature. This is brought out even more clearly by the fact that, if a water sample is subdivided into a large number of equal volumes, the freezing temperatures of the latter show a simple probability distribution. This statistical character of the nucleation events, which has not always been clearly recognized, has the important implication that, in order to obtain significant and characteristic relationships, it is necessary to determine the freezing points of large numbers of samples.

§ 2. The Supercooling of Water Containing Foreign Particles; Heterogeneous Nucleation

The results of some recent experiments in which the freezing points of large numbers of samples of widely different volumes have been determined, and which undoubtedly show a marked volume dependence, will now be summarized.

Vonnegut (1948) placed 64 drops each weighing about 3 mg on a polished chromium-plated surface covered with a thin film of polystyrene. The plate was then held at a fixed temperature below 0°c, and the number of unfrozen drops was counted at successive intervals of time. The proportion of frozen to unfrozen drops, interpreted as the probability of freezing, increased more rapidly with time when the plate was held at a lower temperature. This result was interpreted by Vonnegut as indicating that the nucleation was time-dependent but, it would seem, only to the extent that there was a higher probability, at a lower temperature, of a drop becoming infected with an effective airborne freezing nucleus during the course of the experiment.

Heverly (1949) studied the freezing of drops of water and dilute aqueous solutions which were supported either on a small thermocouple junction or on waxed paper in a cryostat. The drop diameters varied from 50 μ to 1·1 mm and the cooling rates from 1 to 20°c/min. The freezing points of the drops fell roughly on the same diameter–temperature curve irrespective of the origin and contamination of the water. The freezing points of drops of 400 μ to 1·1 mm diameter were roughly constant at -16°c, but there was a rapid fall of freezing point with decreasing diameter below 400 μ. The freezing points appeared to be independent of the cooling rate.

The results of an investigation by Hosler (1954), in which 490 droplets of distilled water were frozen on a platinum surface, show a variation of mean-freezing temperatures from -19°c for a group of 200 μ-diameter droplets, to -30°c for 25 μ-droplets, with an occasional droplet of the latter size being supercooled to -34°c. Hosler also describes some experiments on the supercooling of water in Pyrex tubes of diameters ranging

from 0·25 mm to 3 mm. Using ordinary laboratory-distilled water in tubes cleaned by prolonged washing with chromic acid and flushed with distilled water, he reported that the freezing points of the samples were independent of their length, volume or surface area but appeared to depend only on the diameter of the containing tube. This challenge to the generally accepted view that the attainable degree of supercooling is dependent upon the *volume* of the sample seems to have been met by the much more careful experiments of Mossop (1955). He showed that Hosler's results were almost certainly a consequence of a thin film of water on the inner surface of a tube becoming nucleated by particles lodged on the walls, and that if the walls were coated with a hydrophobic film, volume-dependent freezing points were obtained.

Rau (1953 a, b) has studied the freezing of large numbers of drops, varying in diameter from 300 μ to 1 cm, on a highly polished metal surface in the presence of room air. Plots showing the relative frequencies with which drops of the same size froze at different temperatures showed distinct maxima at about $-12°$C and $-20°$C, the former being more prominent for the larger drops and the latter dominant for the smaller droplets. Very few drops froze at temperatures above $-4°$C and the maximum supercooling attained in the presence of nuclei was $-33°$C. Rau suggests that his observed bimodal distribution of freezing temperatures truly represents the activity–temperature relationship for airborne freezing nuclei. However, such a bimodal distribution was not observed by Bigg (1953) or by Langham and Mason (1958) for the freezing temperatures of drops suspended at the interface of two liquids. It is possible that Rau's curves really represented the superposition of two probability distributions, the high-temperature peak being associated with the original nucleus population of the water, and the second with the activity of nucleation sites on the supporting surface. Such an interpretation would be consistent with Rau's findings that the amplitude of the $-12°$C peak increased relative to that of the $-20°$C peak for larger drops, and that there was a reverse trend if the water was progressively purified.

An interesting investigation on the nucleating effects of both atmospheric contamination and the containing walls on the supercooling of water in glass tubes is described by Wylie (1953). Vapour, produced from triply-distilled water and carried in a stream of particle-free oxygen, was condensed in glass tubes which had been flushed with chromic acid and steam and heated to softening point to drive off nuclei from the walls. Despite these precautions, the experiments showed clearly that freezing was governed by the glass surface. Successive freezings of the same sample occurred at temperatures which lay in a narrow range governed by a probability distribution curve. Freezing was often observed to occur repeatedly at a particular nucleation site on the glass wall, and these sites were able to survive the heating of the glass to softening point. Volumes of about 2 cm^3 usually froze at temperatures between $-13°$C and $-20°$C but, on two occasions, supercooling was prolonged to $-30 \pm 1°$C

The results of experiments with open tubes were much less reproducible, and showed that contamination by airborne dust sometimes caused the samples to freeze at temperatures as high as $-5°$C.

A considerable improvement in the technique of investigating the supercooling of water was made in this laboratory by Bigg (1953), who eliminated the influence of solid supporting surfaces by suspending water drops at the interface of two liquids having different densities, where they were also protected from infection by airborne particles. He also investigated a wide range of drop diameters—from about 20 μ to 2 cm—and thus volumes differing by a factor of 10^9. The use of five pairs of supporting liquids, the members of a pair being practically immiscible with water and each other, established that the observed freezing temperatures of the drops were a property of the water and not of the surrounding media.

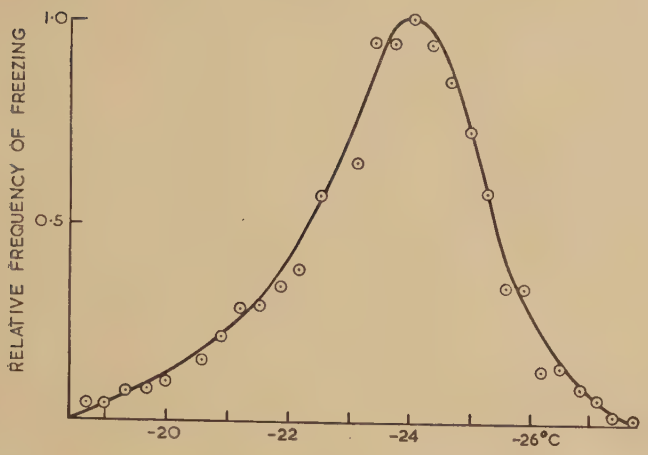
Bigg determined the freezing temperatures of large numbers of drops of various sizes, cooled at a constant rate, and divided them into groups according to drop diameter, each group containing not less than 100 individual observations. A curve showing a typical distribution of freezing temperatures of drops in a particular size group is shown in fig. 1 which contains observations on 1127 drops of distilled water of 1 mm diameter. One significant feature of this curve, and of several similar curves obtained for other drop sizes, is that the scatter of the freezing points about the median value is much less than obtained with droplets supported on a solid surface which itself may provide a number of nucleation sites. The median freezing temperature for each size group, i.e. the temperature below which half the drops froze, is plotted against the drop diameter, on a logarithmic scale, in fig. 2. Bigg thus discovered a linear relationship between the logarithm of the drop diameter (or volume) and the depth of supercooling $T_s = (273 - T)°$C, the line in fig. 2 being represented by the relationship

$$\log V = A - BT_s, \qquad \ldots\ldots \quad (1)$$

where A and B are constants for the particular sample of water used.

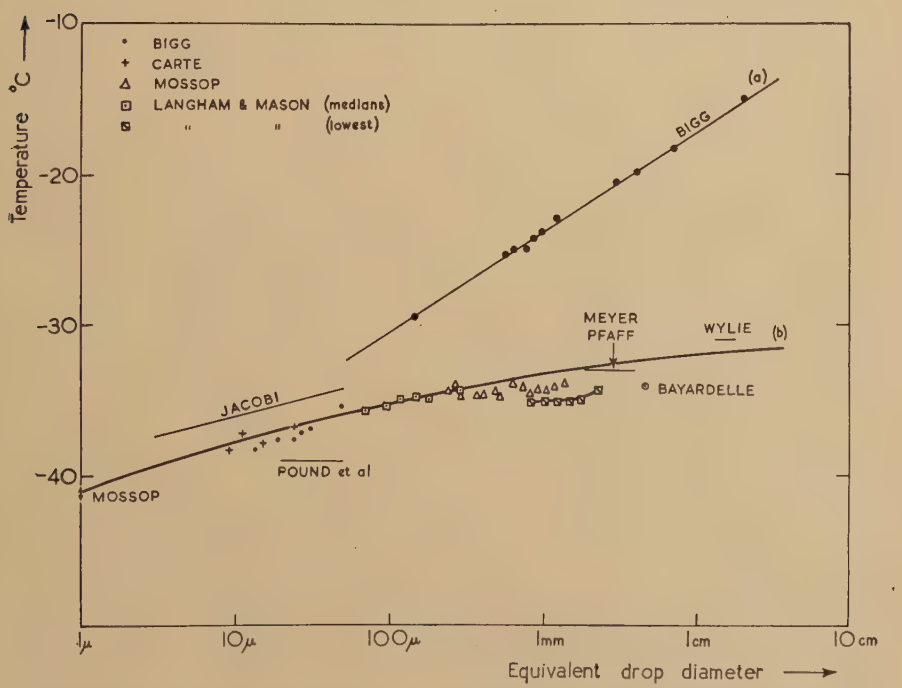
Bigg's work has recently been checked by Langham and Mason (1958) using a slightly improved version of his apparatus in which the drops were suspended between carbon tetrachloride and liquid paraffin (or a silicone fluid) in a shallow metal dish and cooled at the rate of 0·3°c/min. The results obtained with water varying in purity from that of rain water to that produced by multiple distillation showed the same general trend as those of Bigg; plots of the median-freezing temperatures of groups of drops against the logarithm of their diameters produced straight lines almost parallel to that of Bigg, but lying below or above it, depending upon whether the water used was more, or less pure than that investigated by him. Further confirmation of the general validity of relation (1) was found by Mason (1956) in re-analysing the results of some earlier work by Dorsch and Hacker (1950) in which 5000 water droplets, with diameters between 8·75 μ and 1 mm, were cooled at rates varying from 6° to 15°c/min on a metal plate. Although the observed freezing temperatures of a group

Fig. 1



The distribution of freezing temperatures of 1127 water drops of 1 mm diameter (after Bigg).

Fig. 2



(*a*) Bigg's relationship between the median freezing temperatures and the diameters of water drops containing foreign nuclei (heterogeneous nucleation). (*b*) Median freezing temperatures for groups of droplets of very pure water having diameters $<0{\cdot}5$ mm, and the *lowest* freezing temperatures recorded for drops of diameter $>0{\cdot}5$ mm. These experimental data all lie close to the curve calculated from the theory of homogeneous nucleation.

of drops of a particular size had a considerably greater spread than in Bigg's experiments, a plot of median temperatures versus drop diameter produced a line exactly parallel to his, but displaced by 7°c towards higher temperatures.

Bigg also investigated how the supercooling of water drops was affected by the rate at which they were cooled. With a cooling rate of 0·05°c/min, he found the median freezing temperature of 164 drops of 1 mm diameter to be 2° higher than the corresponding value for a cooling rate of 0·5°c/min. A smaller effect has been reported by Carte (1956). For drops of about 20 μ diameter, a ten-fold variation in cooling rate produced a shift of only 0·5°c in the freezing temperatures but in the same sense as found by Bigg, and an effect of similar magnitude was found by Mossop (1955) for much larger volumes. It is not unlikely, however, that spurious shifts in temperature were introduced in these experiments, at high rates of cooling, by a lag in the thermometers, and a rather more careful investigation is required to establish the reality of the effect.

Although Bigg removed the grosser particles from his water samples by double distillation, his drops almost certainly contained large numbers of small particles which can be removed only by taking extreme measures (see § 4). It therefore seems reasonable to consider his log $V-T_s$ relationship as representing nucleation by foreign particles (heterogeneous nucleation). This is also suggested by the fact that other workers, who have taken greater precautions to purify their water, have occasionally been able to supercool specimens to temperatures well below those indicated by Bigg's line (see § 4 and fig. 2).

Langham and Mason (1958) suggest that Bigg's relationship between droplet volume and depth of supercooling may be explained on the assumption that his water was contaminated by particles which were originally airborne and whose efficiency as freezing nuclei might be expected to vary with temperature in much the same way as for atmospheric aerosol.

The numbers of ice crystals appearing in a supercooled cloud, produced by condensation on atmospheric aerosols in cloud chambers, have been determined by several different workers; the results have been summarized by Mason (1957). In the temperature range -10°c to -35°c (above which natural ice nuclei are very rare, and below which the effects of homogeneous nucleation become apparent), the numbers of particles which initiate the freezing of supercooled droplets increases roughly logarithmically with decreasing temperature. Langham and Mason assume that the bulk water used in the supercooling experiments contained a representative sample of what were originally atmospheric particles, so that the activity of the contained freezing nuclei may also be represented by

$$n = n_0 \exp(aT_s), \qquad (2)$$

where n is the concentration of nuclei which become effective at temperatures between 0°c and $-T_s$°c, and n_0 and a are constants. For drops of

volume V being cooled to a temperature $-T_s$°C, and containing a randomly-distributed population of nuclei, the probability P of a drop containing at least one effective nucleus on reaching this latter temperature is given by

$$P = 1 - \exp(-Vn), \qquad (3)$$

or

$$\ln(1-P) = -Vn = -Vn_0 \exp(aT_s). \qquad (3\,a)$$

Now Bigg's empirical relationship (fig. 2 (*a*)) shows the value of T_s for which drops of different volumes have a 50% probability of freezing, i.e. $P = 0{\cdot}5$, and for these, eqn. (3 *a*) becomes

$$Vn_0 \exp(aT_s) = \text{const.} \qquad (4)$$

or

$$\ln V = \ln C - aT_s, \qquad (4)$$

which is Bigg's relationship. The value of the constant a fixes the shape of the freezing-nucleus distribution, while the value of C depends upon the absolute concentration of nuclei, i.e. upon the purity of the water.

§ 3. The Properties of Freezing Nuclei

One may imagine the freezing of a water sample to be initiated as follows. As the temperature is lowered, the molecular arrangement in the supercooled liquid becomes progressively more and more ice-like as revealed by x-ray diffraction patterns (Dorsch and Boyd 1951). In the absence of foreign surfaces, nucleation of the ice phase may occur only by the chance orientation of local groups of water molecules into an ice-like configuration. A suitable solid particle, however, may cause water molecules to become ' locked ' into the ice lattice under the influence of its surface force field. The molecular aggregate will not only be bound to the surface of the particle, but will have only one exposed surface; on both counts it will be less vulnerable to thermal bombardment than will a spontaneously formed aggregate, and will therefore have a higher probability of attaining the critical size at which it may nucleate the ice phase. Whether or not a stable ice nucleus is formed must be largely determined by the configuration of the surface force field of the substrate, since this will affect the ability of the water molecules lying within its sphere of influence to form an ice lattice.

The ice nucleating ability of a wide variety of both natural and artificial substances has been tested, usually by dispersing them as fine dusts, smokes or sprays into a cloud of supercooled water droplets, and determining the highest temperature at which about 1 in 10^4 of the particles produced an ice crystal.

The threshold temperatures, thus determined, of the most efficient nucleators so far discovered, are shown in table 1, which is based upon the experiments of Mason and Hallett (1956, 1957) and Mason and Maybank

(1958). The five most effective substances, which induce crystallization at temperatures at least as high as -7 °c, occur naturally in only negligibly small quantities. The most active of abundant naturally occurring minerals is kaolinite, but a number of silicate minerals, especially of the clay and mica groups, have threshold temperatures higher than -15 °c.

All the substances listed in table 1, except kaolinite, are, like ice, hexagonal crystals in which the a lattice spacing, which is important for epitaxy on the basal faces, differs from that of ice by less than 16%. They all have the further important property of being almost insoluble in water. There is, however, no direct correlation between the degree of misfit of

Table 1. Crystal Structures of the Most Efficient Ice Nucleating Substances

Substance	Crystal symmetry	Lattice parameters (Å)			Degree of misfit† %	Threshold temp. for nucleation (°c)
		a	c	b		
Silver iodide	Hex.	4·58	7·49	—	1·3	−4
Lead iodide	Hex.	4·54	6·86	—	0·4	−6
Cupric sulphide	Hex.	3·80	16·43	—	15·9	−6
Vaterite	Hex.	4·12	8·56	—	8·9	−7
β-Tridymite	Hex.	5·03	8·22	—	11·3	−7
Kaolinite	Triclinic	5·16	8·94	7·38	—	−9
Specular hematite	Hex.	5·03	13·75	—	11·3	−10
Ice	Hex.	4·52	7·37	—	—	—

† Defined as $100\,(a-a_{\text{ice}})/a_{\text{ice}}$.

ice relative to the nucleating substrate, as indicated by the percentage difference of the a spacings in table 1, and the threshold temperature of nucleation. An interesting example is provided by montmorillonite, a clay mineral, which has a and b spacings identical with those of kaolinite, but a variable c spacing depending upon the water content of the crystal, and which fails to initiate ice-crystal formation even at temperatures as low as -25 °c. This all suggests that, while similarity of crystal symmetry and lattice spacing for ice and the substrate are, no doubt, important factors in determining the efficiency of an ice-forming nucleus, consideration of these geometrical factors alone seems insufficient. The author has observed that the nucleation of ice on single crystals of lead iodide tends to occur only at specially favoured sites, such as dislocations, and that it is extremely difficult to form ice-crystals on apparently perfect single crystals as substrates. In other words, it is the configuration of

the surface force field of the substrate and its interaction with the polar water molecules which is fundamentally important, and the detailed study of this has scarcely begun.

§ 4. The Homogeneous Nucleation of Supercooled Water

A number of experimenters have reported on the possibility of supercooling small droplets (radius $< 5\ \mu$) to about $-40°$C before freezing occurs. Cwilong (1947 a) and Fournier d'Albe (1949), by expanding atmospheric air in small cloud chambers, found that while at temperatures above $-40°$C a few ice crystals appeared among a much larger number of water droplets, below $-41°$C the fog was composed almost entirely of ice crystals. Mossop (1955), in a rather more careful study of the freezing of tiny droplets ($d \simeq 1\ \mu$), also found that the number of ice crystals increased rapidly as the temperature fell below $-40°$C, and all the droplets were estimated to have frozen after being maintained at $-41{\cdot}2 \pm 0{\cdot}4°$C for 0·6 sec. Very similar results have been reported by Mason (1956) from observations on droplets formed on small ions in the clean air of a diffusion cloud chamber as they fall at the rate of about 0·25 cm sec^{-1} through a vertical temperature gradient.

As solid particles are excluded from these tiny droplets formed in clean air, nucleation of the ice phase can occur only by small groups of water molecules becoming locked by chance into an ice-like configuration; such molecular aggregates will continually arise and disappear through thermal fluctuations. The lower the temperature, the greater their size and frequency of formation until, eventually, they attain a critical size above which they survive and continue to grow, forming nuclei for the ice phase. An expression for the rate of formation of such nuclei has been derived by Mason (1952, 1957) viz:

$$\log I = 32{\cdot}84 + \log T - \frac{U}{2{\cdot}303\ kT} - \frac{1{\cdot}11 \times 10^{17}\sigma^3_{SL}}{L_f^2 T\{\ln(T_0/T)\}^2} \quad . \quad . \quad (5)$$

where I is the rate of production of nuclei per cm^3 per sec, U the activation energy for self-diffusion of a molecule in the liquid, k Boltzmann's constant, σ_{SL} the specific surface free energy of the crystal–liquid interface, L_f the latent heat of fusion, T the absolute temperature and T_0 ($= 273°$K), the thermodynamic freezing point. Because the parameter σ_{SL} cannot be calculated with confidence, and because a 10% error would lead to an error of 10^6 in the calculated value of I, it does not appear profitable to make a close comparison between the nucleation rate calculated from eqn. (5) and that which may be deduced from experimental observations of freezing droplets. However Mason, using Mossop's experimental data on 1 μ droplets to calculate, from eqn. (5), a value for $\sigma_{SL} = 17{\cdot}2$ erg cm^{-2} at $-41°$C, used this to compute the temperature coefficient of nucleation, dI/dT, which is not very sensitive to the adopted value of σ_{SL}, and having

then found quite good agreement between the computed value of $dI/dT \simeq 10$ and that deduced from observation at temperatures close to $-40°$C, provided some check of the theory.

Having evaluated σ_{SL} as just described, eqn. (5) can be used to predict the temperatures at which water drops will crystallize spontaneously, in terms of their volume and the time. Thus the lower curve of fig. 2, calculated on the basis of Mossop's data that 1 μ-diameter droplets freeze after being held at $-41°$C for 0·6 sec, indicates the temperatures at which larger drops would freeze when cooled for a similar period. This curve, representing homogeneous nucleation, differs markedly from that of Bigg's line which represents heterogeneous nucleation.

Also in fig. 2 are plotted the observations of a number of different workers who have been able to supercool small droplets (10–30 μ diameter) down to temperatures approaching $-40°$C, and also a few exceptional cases, recorded in the literature, of much larger volumes being supercooled to unusually low temperatures. The essential information on these observations is summarized in table 2.

The close grouping of these experimental observations about the theoretical curve (the shape and position of which is not materially affected by changing the time factor by an order of magnitude) strongly suggests that, in those cases listed in table 2, the nucleation of the water samples was spontaneous and that freezing nuclei were not involved. It is not possible to make a more exact comparison between the experimental data and the theory because the cooling rates employed are not always stated in the original papers, but they were unlikely to have differed by more than tenfold from those used by Bigg and Mossop, in which case, the corresponding temperature corrections would always be less than one degree.

This analysis encouraged Langham and Mason (1958) to try and produce, in appreciable quantity, water entirely free from foreign particles and to study systematically the homogeneous nucleation of large numbers of drops varying in diameter from about 10 μ to 1 mm. Purification of water to this degree proved difficult but, using a multiple distillation technique in which extreme precautions were taken to exclude room air, to remove particles from the inner walls of the all-Pyrex still, and to prevent ebullition, they produced drops of up to 2 mm diameter which could be regularly supercooled to temperatures very close to limits indicated by the theory of homogeneous nucleation.

In fig. 2 are plotted, for drops of diameter less than 0·5 mm, the median freezing temperatures of uniform size groups each containing about 100 drops. The distribution of freezing temperatures for one hundred 90 μ-diameter drops is shown in fig. 3. The freezing temperatures of drops larger than 0·5 mm diameter showed a wider spread and only about 10% of them could be supercooled to within one degree of the curve in fig. 2; the remainder may have been nucleated by tiny particles which could not be removed from the supporting liquids.

Table 2. Summary of Experimental Data on the Supercooling of Water Samples to Very Low Temperatures—Probably to the Threshold of Homogeneous Nucleation

Author	Method of preparation of water	Equivalent drop diameters	Median freez. temp.	Lowest freez. temp.	Remarks
Meyer and Pfaff (1935)	Multiple distillation and filtration through sintered glass and collodion filters. Test sample contained in quartz tube.	Between 1·8 and 3·8 mm (estimated)	—	−33°C	Only a very few samples were supercooled to this temperature.
Wylie (1953)	Water condensed from a moist, nucleus-free stream of oxygen into fairly large glass tubes.	Between 1·4 and 1·7 cm (estimated)	—	−30 ± 1°C	Only one sample supercooled to this low temperature on two occasions.
Bigg (1953)	Doubly-distilled water dispersed as small droplets at the interface of two immiscible liquids.	15 μ to 50 μ	−37·6°C to −36·2°C	—	Six groups covered this diameter range with more than 100 droplets in each.
Pound *et al.* (1953)	Water condensed as small droplets to form an emulsion in silicone oil	20–50 μ	−39°C	−42°C	No differentiation with respect to droplet size reported.
Mossop (1955)	Water condensed into glass, silica and silicone-treated glass capillaries	0·25 mm to 1·05 mm	—	−33·8°C to −34·7°C	15 samples altogether supercooled to these low temperatures.
	Tiny droplets produced by condensation in an expansion chamber	1 μ	—	−41·2 ± 0·4°C	—
Jacobi (1955)	Droplets condensed on collodion films supported by highly-polished metal surfaces.	3 μ to 50 μ	—	−37·4°C to −34·2°C	—
Bayardelle (1954)	Drops of doubly-distilled water suspended between mercury and a silicone liquid	4·6 mm	—	−34·1°C	—
Carte (1956)	Droplets condensed on a metal surface and covered with silicone oil.	9 μ to 30 μ	−38·2°C to −37·3°C	−39°C to −37·8°C	Results of repeated freezings of 3 individual drops of 9, 15, 30 μ-diam., and of a single freezing of 100 droplets of 10 μ-diam.

It will be seen that the median freezing temperatures for drops of $90\ \mu < d < 500\ \mu$ lie very close to the curve for homogeneous nucleation and that, in this respect, they fit in very well with the results of Bigg, Carte, and others for even smaller droplets. The *lowest* freezing temperatures for the millimetre-size drops agree very well with those obtained by Mossop for water samples contained in glass tubes. Altogether the agreement between the theoretical curve and the experimental data of the several different workers, each of whom investigated only a restricted range of drop sizes, but together covered a volume range of more than 10^{12}, is rather impressive.

Fig. 3



The distribution of freezing temperatures of 100, 90 μ-diameter droplets of very pure water.

There is therefore a substantial body of experimental evidence to suggest that Bigg's result, expressed by eqn. (1) and the line in fig. 2, represents the relationship between the volume of a water drop and the depth of supercooling for *heterogeneous* nucleation, and that the curve in fig. 2, which is based on eqn. (5), represents the corresponding relationship for *homogeneous* nucleation.

§ 5. Evidence for the Supercooling of Water Below −40°c

Although it has been established, by several different workers, that micron-size droplets of very pure water freeze within less than a second after being supercooled to −41°c, and that this temperature is generally

accepted as the lower limit for spontaneous nucleation, it should be mentioned that evidence has been offered to suggest that water may exist in the liquid state at considerably lower temperatures.

One such claim was made by Rau (1944), who stated that when all foreign nuclei were removed (or rendered impotent!), it was possible to supercool drops supported on a metal plate to $-72°$C and to maintain them at that temperature for several hours. Below $-72°$C, the drops froze to produce crystals in the form of either octahedra, tetrahedra or cubes in contradistinction to the hexagonal crystals formed at higher temperatures. The crystals melted on being warmed above $-72°$C. Rau suggested that at $-72°$C spontaneous freezing occurred without the aid of nuclei, the result being a new crystalline ice structure. Attempts to repeat these observations have been made by Cwilong (1947 b) and by Brewer and Palmer (1951), who reported that they could not reproduce Rau's results unless they deliberately contaminated their water drops with fairly high concentrations of organic vapours such as acetone or alcohol, and criticized Rau's experimental arrangement on the grounds that alcohol contamination could have arisen from his cooling system. In a private communication, Rau says that he has repeated his experiments, eliminating any possibllity of contamination of his water drops by alcohol, and that he has been able to reproduce his earlier results. Unfortunately, he gives so little information on his experimental arrangement, the methods he uses to remove impurities and to determine the physical state of his condensate (visual inspection is not good enough), that it is very difficult to assess his work, which will require independent confirmation before it is accepted. The fact that his crystals *melted* at $-72°$C makes it very difficult to believe that they could have been pure ice in any form. Evidence suggesting a phase change at about $-62°$C was obtained by Sander and Damköhler (1943) who measured the critical supersaturation for the precipitation from water vapour in air cooled, by rapid expansion in a cloud chamber, down to temperatures of $-75°$C. Until a terminal temperature of $-62°$C was reached, the precipitate appeared to be spherical particles and were reported as droplets. Below $-62°$C, the precipitate appeared to consist of angular ice crystals. These authors suggested that either the crystals were formed by direct nucleation of ice from the vapour or that $-62°$C represented the crystallization temperature of what, at higher temperatures, had been liquid droplets.

This work has been repeated rather more carefully by Pound, Madonna and Scuilli (1955) using clean nitrogen as the carrier gas. Their results are very similar to those of Sander and Damköhler, the appearance of spherical particles rapidly giving way to a cloud of glittering ice crystals at temperatures below $-65°$C. Pound *et al.* suggest, though, that the non-glittering particles appearing at temperatures between $-41°$C and $-65°$C need not necessarily be liquid droplets but frozen spheres which have not developed crystalline faces. A similar suggestion was made earlier by Mason (1952) to account for the appearance of iridescence in mother-of-pearl clouds which occur in the stratosphere at heights of about

23 km and temperatures of $-80°$C. The sudden appearance of crystals at temperatures below about $-65°$C may be the result of direct sublimation from the vapour without the intervention of the liquid phase, but there appears to be no acceptable evidence for liquid water being supercooled appreciably below $-40°$C.

References

Bayardelle, M., 1954, *C.R. Acad. Sci.*, **239,** 988.

Bigg, E. K., 1953, *Proc. phys. Soc. Lond.* B, **66,** 688.

Brewer, A. W., and Palmer, H. P., 1951, *Proc. phys. Soc. Lond.* B, **64,** 765.

Carte, A. E., 1956, *Proc. phys. Soc. Lond.* B, **69,** 1028.

Cwilong, B. M., 1947 a, *Proc. roy. Soc.* A, **190,** 137; 1947 b, *J. Glaciology*, **2,** 53.

Dorsch, R. G., and Boyd, B., 1951, *U.S., N.A.C.A., Washington, Tech. Note* No. 2532.

Dorsch, R. G., and Hacker, P. T., 1950, *U.S., N.A.C.A., Washington, Tech. Note*, No. 2142.

Fournier d'Albe, E. M., 1949, *Quart. J. R. met. Soc.*, **75,** 1.

Heverly, J. R., 1949, *Trans. Amer. geophys. Un.*, **30,** 205.

Hosler, C. L., 1954, *Proc. Toronto Met. Conf.* 1953, (R. Met. Soc.), p. 253.

Jacobi, W., 1955, *J. Met.*, **12,** 408.

Langham, E. J., and Mason, B. J., 1958, *Proc. roy. Soc.* (in the press).

Mason, B. J., 1952, *Quart. J. R. met. Soc.*, **78,** 22; 1956, *Science Progress* No. 175, p. 479; 1957, *The Physics of Clouds* (Oxford: Clarendon Press), p. 128.

Mason, B. J., and Hallett, J., 1956, *Nature, Lond.*, **177,** 681; 1957, *Ibid.*, **179,** 357.

Mason, B. J., and Maybank, J., 1958, *Quart. J. R. met. Soc.* (in the press).

Meyer, J., and Pfaff, W., 1935, *Z. anorg. Chem.*, **224,** 305.

Mossop, S. C., 1955, *Proc. phys. Soc. Lond.* B, **68,** 193.

Pound, G. M., Madonna, L. A., and Peake, S. L., 1953, *J. Colloid. Sci.*, **8,** 187.

Pound, G. M., Madonna, L. A., and Scuilli, C. M., 1955, *Proc. Conf. on Interfacial Phenomena and Nucleation, Geophys. Res. Pap.* No. 37 Air Force Cambridge Research Center.

Rau, W., 1944, *Schr. dtsch. Akad. Luftf., Berlin*, **8,** 65; 1953 a, *Geofis. pur. appl.*, **26,** 75; 1953 b, *Z. Naturf.*, **8 a,** 197.

Sander, A., and Damköhler, G., 1943, *Naturwissenschaften*, **31,** 460.

Vonnegut, B., 1948, *G. E. Res. Lab., Project Cirrus, Occas. Rep.* No. 6.

Wylie, R. G., 1953, *Proc. phys. Soc. Lond.* B, **66,** 241.

The Growth of Ice Crystals from the Vapour and the Melt

By B. J. Mason
Warren Research Fellow of the Royal Society, Imperial College, London

Part I.—Crystal Growth from the Vapour

§ 1. Introduction

Research on the formation of ice crystals from the vapour has been largely concerned with the growth of snow crystals in both the atmosphere and the laboratory. The importance of such studies in cloud physics stems from the fact that the higher atmospheric clouds are composed almost entirely of ice and that most of the rain falling in temperate latitudes, at least, results from the growth, aggregation and melting of snow crystals. Also, the remarkable variety of shape and pattern exhibited by snow crystals poses some very interesting and perplexing problems in crystal physics.

The collection, photography, and classification of snow crystals has long been an attractive pastime, the books by Bentley and Humphreys (1931) and by Nakaya (1954) being particularly famous for their thousands of beautiful photo-micrographs. Also, valuable data has been obtained on the masses, dimensions, and terminal velocities of the different crystal forms. But it is only in recent years that any real progress has been made in relating the shape, structure and growth rate of the crystals to the environmental conditions in which they are formed. These studies, which have revealed the growth mechanisms of ice crystals to be very complicated, with many puzzling features which are apparently peculiar to ice, will now be reviewed.

§ 2. The Occurrence of Ice Crystals in Natural Clouds

Although extensive observations have been made of snow crystals reaching the ground, and attempts have been made to correlate the relative frequencies of the various crystal forms with the temperature at the place of observation, very little in the way of consistent results has emerged. This is not, perhaps, surprising, since only the conditions prevailing during the growth of the crystal are likely to be of major importance in determining its shape, and it is only in recent years that crystals have been collected from different types of cloud having widely different conditions of temperature, water-vapour concentration, and supersaturation relative to ice. The most comprehensive collection of ice crystals from natural clouds has been obtained by Weickmann (1947) at different heights in the troposphere up to cirrus levels, the temperature of the sampling region being measured. His observations, summarized in table 1, are not as detailed as one could wish, but the sampling of crystals from aircraft presents considerable difficulties, particularly at

high speeds, when it becomes difficult to avoid the shattering of the crystals during their collection.

Weickmann found that, at temperatures below $-25°C$, the dominant crystal form was the hexagonal prismatic column which develops by preferential growth along the principal (c) axis, i.e. normal to the basal plane. These crystals are typically $\frac{1}{2}$ mm in length, the ratio of length to breadth varying from one to five, and appear as single crystals, as basal twins (fig. 1, Pl. 18), and in clusters originating from a central frozen droplet (fig. 2, Pl. 18). If grown under conditions of high supersaturation, the crystals usually contain pronounced funnel-shaped cavities, while in clouds only slightly supersaturated with respect to ice, occasional prismatic columns with a single pyramidal end (fig. 3, Pl. 19) are found.

Table 1. Weickmann's Observations of Predominant Crystal Forms in Different Cloud Types

Level of observation	Temperature range	Cloud types	Crystal forms
Lower troposphere	0°c to −15°c	Nimbostratus Stratocumulus Stratus	Thin hexagonal plates. Star-shaped crystals showing dendritic structures.
Middle troposphere	−15°c to −30°c	Altostratus Altocumulus	Thick hexagonal plates. Prismatic columns—single prisms and twins.
Upper troposphere	< −30°c	Isolated cirrus	Clusters of prismatic columns containing cavities. Some single hollow prisms.
		Cirrostratus	Individual complete prisms.

In proceeding from high- through medium- to low-level clouds, and therefore to higher temperatures, Weickmann reported that there was a gradual transition from prisms, through thick plates to thin hexagonal plates, the latter resulting from preferential growth of the prism faces. The thin hexagonal plates (fig. 4, Pl. 19), which occur at temperatures usually above $-20°C$, are generally less than $500\,\mu$ in diameter and less than $50\,\mu$ in thickness.

At temperatures around $-15°C$ the striking star-shaped crystals are dominant. They usually possess six arms, which may grow rapidly

and develop side-branches to assume the fine dendritic structure illustrated in fig. 6, Pl. 20, and attain diameters of several millimetres. Although the development of all six arms is often superficially very similar, the crystals rarely show exact hexagonal symmetry in their detailed fine structure. These stellar crystals often develop from a hexagonal plate, which at a certain stage of its development, begins to sprout at the corners, but some photographs suggests that the crystal may originate from a frozen droplet which has developed crystal faces.

Needle-shaped crystals, such as are illustrated in fig. 7, Pl. 21, are not represented in Weickmann's classification, but are often observed at the ground when the temperature is only slightly below 0°c, and there are other observations to show that these originate from clouds with temperatures between about −3°c and −8°c. The needles, which often occur in clusters, are a skeletal form of hollow prism. They arise as the result of rapid growth along the principal axis; not only are the basal faces incomplete, but growth may occur on only some of the edges of the basal plane or, in extreme cases, only from one or more corners.

Crystals which are a combination of two or more of the basic types (prism, plate, star) are not uncommon—the prismatic column with end plates and the combination of plate and star crystal, which are shown in figs. 8, Pl. 21 and 6, Pl. 20, are good examples. These metamorphic forms reflect the changes in environmental conditions (temperature, supersaturation, etc.) through which a crystal passes on its journey towards the ground.

§ 3. Studies of Ice-Crystal Growth in the Laboratory

The existence of at least three basic forms of natural snow crystals, and of an almost infinite number of variations on each of these main themes, suggests that their growth and development are complicated matters which may best be studied in the laboratory where the whole life history of a crystal can be observed under controlled conditions.

The growth of ice crystals in supercooled water clouds, the latter being produced in room-size cold chambers whose temperature could be controlled, has been studied by Aufm Kampe *et al.* (1951), and by Mason (1953). The clouds were produced by the introduction of steam into the chamber. Within a few seconds, the fog cooled to the temperature of the chamber and was then seeded with dry ice or silver iodide if insufficient natural ice nuclei were present. Mason projected a small pellet of dry ice to produce a horizontal seeded track near the top of the chamber, and caught the crystals on plastic coated slides near the floor after they had fallen through about 3 metres of supercooled cloud. The plastic replicas of the crystals were subsequently studied and photographed under the microscope.

The observed changes of crystal habit with temperature were very similar in both sets of experiments and are summarized in table 2.

The classification of these laboratory-produced crystals according to temperature bears a marked similarity to that of natural snow crystals

(table 1), showing that it is possible to simulate quite well the early stages of growth of snow crystals in the laboratory and, at the same time, determine the transition temperatures for the different crystal forms more precisely than can be done in the atmosphere. The most striking feature of table 2 is the remarkable sequence of habit—plates → prisms → plates (and stars) → prisms—which occurs as the temperature is lowered from 0°C to −25°C.

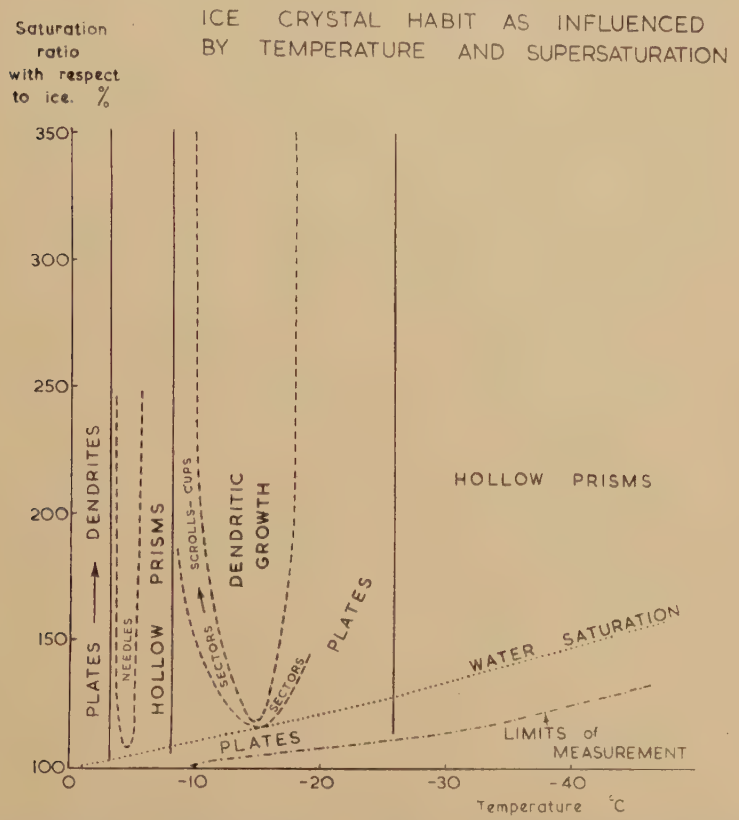
Table 2. Changes of Crystal Habit with Temperature in Artificially-produced Water Clouds (after Aufm Kampe *et al.* and Mason)

Temperature range	Crystal habit
0°C to −5°C	Simple, clear hexagonal plates with no surface markings ; some trigonal shapes.
−4°C to −9°C	Prisms, some showing marked cavities and similarity to needles.
−10°C to −25°C	Hexagonal plates showing ribs, surface markings, and tendency to sprout at corners. Sector stars. Dendritic stars, most prominent around −15°C.
−25°C to −40°C	Single prisms, twins, and hollow prisms. Aggregates of prisms and irregular crystals, (Aufm Kamp *et al.*).

A series of experiments to study the growth of individual ice crystals in different environmental conditions has been described by Nakaya (1951, 1954). The crystals were grown on a fine rabbit hair stretched on a frame and suspended in an air stream whose temperature and water-vapour content could be varied. The crystal development was followed over a period of 30 min or so by time-lapse photography. The apparatus consisted of two concentric glass cylinders, the warm water vapour from an electrically heated reservoir being convected upwards inside the inner tube, cooled on its way up, and returned through the annular space. The whole apparatus was placed in a thermostat and located in a cold chamber maintained at about −30° C. The degree of supersaturation in the experimental space was varied by altering the temperature T_w of the water in the reservoir. The temperature T_a of the air in the immediate neighbourhood of the growing crystal was a function of both T_w and the temperature T_t of the thermostat. For a given value of T_w, the air temperature was regulated by adjusting T_t. Crystals were produced at various combinations of T_a and T_w, with a view to studying the relationship between the crystal form and the external conditions. Unfortunately,

the conditions in Nakaya's apparatus were not steady nor well defined because the strong convection gave rise to large fluctuations in both temperature and supersaturation. The *average* temperature of the air in the neighbourhood of the crystal was measured with an alcohol-in-glass thermometer, but only rather crude relative estimates of the supersaturation were possible.

Fig. 9



The growth habits of ice crystals in relation to the temperature and supersaturation (relative to ice) of the environment as observed by Mason and Hallett in a diffusion cloud chamber.

Nevertheless, it emerged that T_a and T_w were the two main parameters controlling the growth forms of the crystals, and Nakaya's classification of habit in relation to the air temperature T_a is in broad agreement with the data of table 2 and fig. 9. Nakaya was of the opinion that the temperature rather than the supersaturation of the environment was the main factor controlling the crystal shape, except in the case of dendritic growth which occurred only at relatively high supersaturations and at air temperatures between $-14°$C and $-17°$C. However, Marshall

and Langleben (1954) interpreted Nakaya's results as showing that the habit is principally determined by the excess of the ambient vapour density over that which would be in equilibrium with the surface of the ice crystal, that is, by a quantity closely related to the supersaturation, and proportional to the flux of vapour directed towards the crystal. A similar suggestion was made earlier by Weickmann (1950). Marshall and Langleben hypothesize that resistance to growth will be greatest at the crystal corners and greater on the prism faces than on the basal faces, so that growth of the corners and the prism faces will occur only when the excess vapour density $\Delta\rho$ becomes sufficiently large to overcome these inhibitions. Thus, prismatic columns would be expected to develop at relatively low values of $\Delta\rho$, plates only when $\Delta\rho$ is relatively large, and the corners (dendritic growth) only when $\Delta\rho$ achieves very high values.

Strong experimental evidence against such an interpretation was obtained by Shaw and Mason (1955) who studied the growth of individual ice crystals growing on a metal surface under conditions such that the temperature and supersaturation of the surrounding air could be controlled *independently*. The crystals were viewed through a metallurgical microscope and photographed at one-minute intervals. The growth rates of individual crystal faces were determined from measurements made on the negative with a micrometer eyepiece.

In order to determine whether the various crystal forms appearing in natural and laboratory-produced clouds could be produced at the same temperatures on the metal plate, the plate temperature was held constant at various temperatures between -5°C and -40°C, and crystals were grown under conditions of saturation relative to liquid water. The crystal habit was found to vary as follows:

-5°C to -9°C	Prisms
-9°C to -25°C	Plates
below -25°C	Prisms,

in a manner very similar to that observed in the cloud experiments. Stars were absent, but a new crystal form appeared quite often on the plate at temperatures between -4°C and -8°C and also below -22°C. This took the form of a prism terminated at one end only by a pyramid. The appearance of such hemimorphic forms, which have been found only very occasionally in natural clouds (usually cirrostratus), but not at all in small-scale laboratory clouds, is of considerable interest in connection with the possibility of ice possessing a polar lattice.

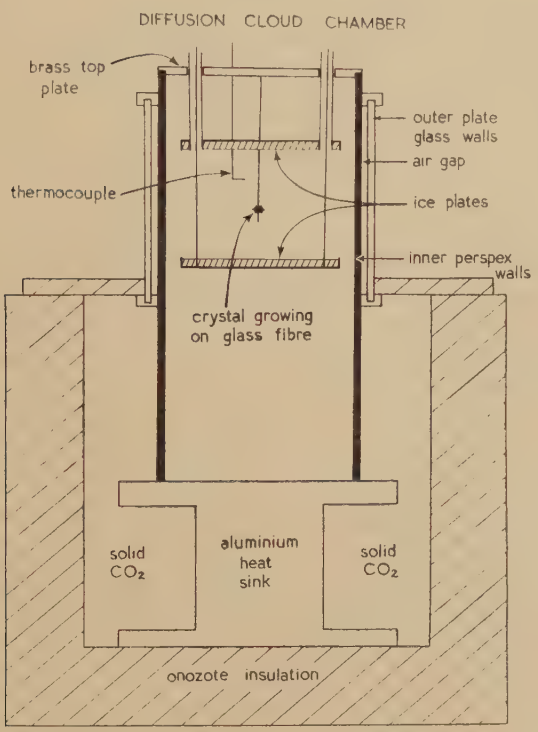
When maintained at a constant temperature and supersaturation, the crystals grew towards a limiting habit defined by

$$\Gamma = \left|\frac{c}{a}\right|_{\lim} = \sqrt{\left(\frac{dc^2}{dt}\right) \Big/ \left(\frac{da^2}{dt}\right)},$$

where c and a are respectively the principal and secondary crystal axes. Shaw and Mason established that this habit, and therefore whether a

crystal developed as a prism or a plate, was determined very largely by the temperature, the supersaturation, though varied over wide limits, having no systematic effect. It was also established that a minimum critical value of the supersaturation was required to start growth on any crystal face, but this varied in an apparently random manner from face to face and from crystal to crystal; there was no systematic difference between the critical supersaturations required for growth on the basal and prism faces as required by the hypotheses of Marshall and Langleben.

Fig. 10



The diffusion cloud chamber used by Mason and Hallett for growing ice crystals at various temperatures and supersaturations.

It must be admitted, however, that conditions for crystal growth on the metal surface may not have fairly simulated those occurring in the free air. To meet this point and to study the whole problem in more detail, a new series of experiments have recently been carried out by Mason and Hallett (1958).

The crystals are grown on a thin glass or nylon fibre running vertically through the centre of a water-vapour diffusion chamber which is 50 cm high $\times$ 30 cm diameter, constructed of Perspex, and rests upon a solid aluminium block maintained at about $-60°$C by dry ice. The apparatus is shown diagrammatically in fig. 10. Cooled from below, with its top

maintained either at or above room temperature, the chamber encloses a thermally stratified, convectively stable atmosphere in which steady-state conditions are readily achieved. Water vapour, evaporated from an extended source, diffuses downwards through the chamber towards the low-temperature sink, the supersaturation régime being largely determined by the temperatures of the source and sink, the vertical separation of which can be varied. In such a chamber containing room air, condensation of water vapour upon the aerosol particles produces a dense cloud of tiny water droplets which freeze spontaneously on falling beneath the $-40°$C level. In the presence of a persistent droplet cloud, the air may be regarded as saturated relative to liquid water, the supersaturation relative to ice at any level being determined solely by the temperature at that level. The variation of temperature with height is measured with a thermocouple, the separation of the 0°C and $-40°$C levels being about 10 cm.

If the chamber is sealed and left for some hours, the condensation nuclei are progressively removed by sedimentation, leaving clean, highly supersaturated air in which condensation tracks produced by cosmic rays may be seen.

In order to simulate conditions in natural clouds, where ice crystals may grow at humidities below water saturation and therefore at supersaturations of only a few per cent relative to ice, the chamber was modified so that the crystals are grown on a fibre suspended centrally between two plane parallel sheets of ice. The vertical profiles of both temperature and supersaturation between the ice plates, the upper of which serves as the vapour source, is determined by their positions in the chamber, which are adjustable ; additional control is provided by electrical heating of the top plate. A thermocouple passing through a small hole in this plate measures the temperature profile between the plates and this, together with the solution of the diffusion equation for the profile of water-vapour concentration, allows the supersaturation at each level to be calculated.

With these facilities, Mason and Hallett were able to grow crystals over the temperature range 0°C to $-50°$C and under supersaturations ranging from a few per cent to about 300%. The results of many experiments are summarized in fig. 9. Consistently, the crystal habit varied along the length of the fibre in the following manner :

0°C to $-3°$C	Thin hexagonal plates
$-3°$C to $-5°$C	Needles
$-5°$C to $-8°$C	Hollow prisms
$-8°$C to $-12°$C	Hexagonal plates
$-12°$C to $-16°$C	Dendritic crystals
$-16°$C to $-25°$C	Plates
$-25°$C to $-50°$C	Hollow prisms.

This scheme is very similar to that of table 2, but the simultaneous growth of all the crystal forms on the same fibre brought to light the sharpness of the boundaries between one habit and another. For example, the transition between the plates and needles at $-3°$C, and that between hollow prisms and plates at $-8°$C, occurred within temperature intervals of less than one degree. A photograph showing the variation of crystal habit along the length of the fibre is reproduced in fig. 11, Pl. 22.

Figure 9 is similar, in many respects, to the diagram published by Nakaya (1954), but it covers much wider ranges of temperature and supersaturation. It differs from his in that it shows the existence of plates between 0°C and $-3°$C, of hollow prisms rather than needles between $-5°$C and $-8°$C, and does not show prisms to occur between $-10°$C and $-15°$C at low supersaturations.

Crystals having an almost identical variation of habit with temperature have recently been grown from the vapour of heavy water (99·75% pure) but with the transition temperatures all shifted upwards by nearly 4°, in conformity with the difference between the melting points of H_2O and D_2O—Mason and Hallett (unpublished).

These experiments appear conclusive in showing that very large variations of supersaturation do not change the basic crystal habit as between prism and plate-like growth although, of course, the growth rates are profoundly affected. On the other hand, the supersaturation appears to govern the development of various secondary features such as the needle-like extensions of hollow prisms, the growth of spikes and sectors at the corners of hexagonal plates, and the fern-like development of the star-shaped crystals, all of which occur only if the supersaturation exceeds values which, in these experiments, correspond roughly to saturation relative to liquid water.

The effect of suddenly changing the temperature and supersaturation on the growth form of a particular crystal could be observed simply by raising or lowering the fibre in the chamber. Whenever a crystal was thus transferred into a new environment, the continued growth assumed a new habit characteristic of the new conditions. Thus when needles grown at temperatures between $-3°$C and $-5°$C were suddenly moved up in the chamber, to about $-2°$C, plates developed on their ends (fig. 12, Pl. 23), and when similar needles were lowered to about $-14°$C, they gave way to star-shaped crystals. Figure 13, Pl. 23 shows a quadruple transition; needles, grown at $-4°$C, were transferred to $-13°$C where plates developed on their ends, then to $-8°$C where the plates developed into hexagonal cup-shaped crystals and finally, back to $-4°$C where needles grew from the corners of the cups. These are only some examples of metamorphosis which were observed when crystals were suddenly transferred to a new environment; in fact, combination forms of all the basic crystal types shown in fig. 9 were readily produced in this way. Such radical changes in crystal shape could not be produced by

varying the supersaturation at constant temperature but, in some cases, were produced by only a degree or two change in temperature at constant supersaturation.

At the present time there is no convincing explanation for the observed variations of ice-crystal habit with temperature. The author believes that they are associated mainly with changes in the surface structure and properties of the crystal, but present theories of crystal growth contain few, if any, parameters which are likely to be strongly face-dependent and, at the same tine, sensitive to temperature changes of only a few degrees. The detailed mechanism of ice-crystal growth is clearly a matter for much further experiment.

§ 4. The Growth Rates of Ice Crystals

The rate at which the mass of an ice crystal will increase when suspended in an atmosphere of given supersaturation and temperature will be governed by the rate of diffusion of water vapour to and of latent heat away from the crystal surface. If it is assumed that the crystal is at rest relative to the air and that the diffusion field has achieved a steady state the governing equations are :

$$\frac{dm}{dt} = 4\pi CD\{\rho - \rho(s)\} \quad . \quad . \quad . \quad . \quad . \quad . \quad . \quad (1)$$

and

$$L_s\frac{dm}{dt} = 4\pi CK(T_s - T), \quad . \quad . \quad . \quad . \quad . \quad . \quad (2)$$

where dm/dt is the rate of increase of mass, C is a shape factor for the crystal equivalent to its electrostatic capacity, D the coefficient of diffusion of water vapour in air, K the thermal conductivity of air, $\rho(s)$, ρ are respectively the vapour densities in the immediate vicinity of the crystal surface and at infinity, T_s, T the temperatures of the crystal surface and of the undisturbed environment, and L_s the latent heat of sublimation. Combining these equations with the Clausius–Clapeyron equation, $(1/p_e)dp_e/dT = L_sM/RT^2$, where p_e is the equilibrium vapour pressure of water vapour at temperature T, M the molecular weight of water, and R the universal gas constant, Mason (1953) obtains the equation

$$\frac{dm}{dt} = 4\pi C\sigma \Big/ \left\{\frac{L_s^2M}{KRT^2} + \frac{RT}{DMp_e}\right\}, \quad . \quad . \quad . \quad . \quad . \quad (3)$$

where $\sigma = p/p_e - 1$ is the supersaturation of the environment relative to a plane ice surface. At constant air pressure, the term in the curly brackets is a function of temperature only.

Equation (3) can be applied to calculate the growth rate of ice crystals whose shapes approximate to those of conductors of known electrostatic capacity. To a first approximation, one may follow Houghton (1950)

and treat the thin hexagonal plate as a circular disc, and a hexagonal prismatic column as a prolate spheroid of large eccentricity. The following substitutions then apply:

Crystal shape:	Sphere	Circular disc	Prolate spheroid
Capacity C:	r	$2r/\pi$	$2ae/\ln\{(1+e)/(1-e)\}$

where the eccentricity $e=(1-b^2/a^2)^{1/2}$ and a and b are the major and minor semi-axes respectively.

Experiments designed to measure the rate of mass increase of crystals growing in a supercooled water cloud have been described by Reynolds (1952) and by Mason (1953). In both cases a supercooled cloud was produced in a large cold chamber and seeded with dry ice, the crystals being collected near the floor at successive time intervals, measured under the microscope and the masses calculated from their linear dimensions. Mason made measurements on simple, regular, hexagonal plates grown at $-2{\cdot}5$°C, and on prisms grown at -5°C, for growth periods of up to 3 min during which time the crystals achieved maximum linear dimensions of order $100\,\mu$. The experimentally-determined values of dm/dt agreed with those predicted by eqn. (3) to within about 10%, which was as good as could have been expected in view of the experimental conditions and the difficulty of making very accurate measurements on such small crystals. Reynolds used much the same procedure, but made his measurements on plane dendritic stellar-crystals grown at -18°C, the masses of which are more difficult to determine from their dimensions because of their irregular outline and non-uniform thickness. Because of this, and also the fact that the temperature and supersaturation in his chamber varied considerably during the course of the experiment, Reynolds obtained rather poorer agreement between his measurements and the theory.

Although eqn. (3) may predict quite well the rate of *mass* increase of stationary ice crystals and of small crystals falling only very slowly through a supersaturated environment, it cannot predict how the mass will be distributed, and hence the detailed shapes of the crystals. Measurements on the growth rates of individual faces were made by Shaw and Mason for crystals growing on their metal plate. Under conditions of constant temperature and supersaturation, the square of the linear dimensions of a crystal increased linearly with time, this relationship being in accord with theory for a crystal growing slowly in a steady-state diffusion field. However, the growth rates of both prism and basal faces were often different in different crystals, while crystallographically similar faces of the same crystal sometimes grew at different rates. Furthermore, the growth rate of a particular face sometimes changed abruptly, even though the external conditions remained constant. These results indicate that the growth of crystal faces is not determined solely by the flux of material to, and heat away from the crystal, but is

partly influenced by certain individual characteristics of the faces themselves which control the rate at which the material can be built into the crystal structure. Such behaviour is to be expected on the basis of modern views of crystal growth as described, for example, by Burton *et al.* (1951) in which the growth rate of crystal face is influenced, to some extent, by the density and configuration of dislocations.

§ 5. Influence of the Fall Motion of the Crystal : Transition from Polyhedral to Dendritic Growth

When an ice crystal in the atmosphere grows to such a size that it attains an appreciable fall speed, its growth becomes complicated by the fact that it can no longer be considered stationary with respect to the air and the diffusion field. The crystal will always be moving into new surroundings and the diffusion field will be limited to a boundary layer around the crystal in which the vapour concentration and temperature gradients will be larger than those directed towards a stationary crystal. For a spherical crystal of radius r, Mason (1953) shows the concentration gradient at the crystal surface at time t after being introduced into a new environment to be

$$\frac{\partial \rho}{\partial r} = (\rho - \rho(s))\left[\frac{1}{r} + \frac{1}{(\pi D t)^{1/2}}\right], \qquad (4)$$

where the symbols have the same meaning as in eqn. (1). The second term in the square brackets is a measure of the enhancement of the concentration gradient at the crystal surface relative to the steady-state value, and the effect will be marked if $(\pi D t)^{1/2} \ll r$. It implies that the mass growth rate of the falling crystal will be increased by a factor $[1 + (vr/2\pi D)^{1/2}] = (1 + 0{\cdot}22 Re^{1/2})$, where Re is the Reynolds number. $(\pi D t)^{1/2}$ has the dimensions of a length and may be defined as the thickness of the diffusion boundary layer.

Let us now consider a hexagonal plate crystal falling with its c axis vertical. Since the strongest concentration and temperature gradients will be directed towards the corners, which protrude farther into the field, vapour molecules will arrive and condense preferentially there, the effect being more marked when the boundary layer is thin compared with the crystal radius. For a plate of thickness x falling with velocity v, the time t for which any given parcel of air will remain in contact with it before being replaced, will be $t \simeq x/v$, when the criterion for the transition from polyhedral to dendritic growth becomes $vr^2 \gg Dx$. Thus for crystals of thickness $20\,\mu$, pronounced dendritic growth, leading to well-developed stellar crystals, will not set in until the crystal radius well exceeds $100\,\mu$, which is in accord with observation. Once the crystal corners start to sprout, the diffusion field will organize itself to become convergent towards the growing tips so that dendritic growth will tend to continue while the supply of vapour lasts.

Although this explanation, which regards the fall motion of a natural snow crystal as being an important factor in determining the onset of

dendritic growth, seems plausible, it can hardly account for the appearance of dendrites, at considerably higher supersaturations, among the stationary crystals growing in Mason and Hallett's diffusion chamber, and also for the fact that they appear only in the temperature range $-12°C$ to $-16°C$. But again the above treatment considers only the conditions in the diffusion field and, as we have seen, such factors as surface structure and surface diffusion of molecules may also be of major importance in determining the crystal habit. Again these appear to be issues for experiment rather than for theoretical argument at the present time.

§ 6. The Influence of Aerosols and Foreign Vapours on Ice Crystal Habit

It has been reported by Nakaya (1955) that the growth forms of ice crystals may be modified by the presence of atmospheric aerosols. For example, he states that when the air is filtered to remove the suspended particles, the plate and dendritic crystals which normally occur in the temperature range $-10°C$ to $-20°C$ are replaced by hollow prisms. Hallett and Mason (1958) have been unable to confirm this result. Crystals growing in their diffusion chamber show exactly the same variation of habit with respect to temperature irrespective of whether they grow in the presence of a water cloud, formed by condensation on atmospheric aerosol particles, or in very clean air from which all the particles have been removed by sedimentation.

However, they find that the presence of traces of organic vapours may profoundly influence the growth habit of ice crystals. For example, needle-like crystals appeared at all temperatures between $0°C$ and $-40°C$ when a small trace of camphor vapour was introduced into the chamber. Even more remarkable changes followed the introduction of iso-butyl alcohol. In the temperature range $-12°C$ to $-16°C$, when the partial pressure of alcohol exceeded about 10^{-3} mb, the normal dendritic growth was suppressed and replaced by plate-like crystals. A further rather small increase in alcohol concentration caused these to be replaced by either hollow prisms or needles which persisted until the concentration was raised beyond 0·1 mb above which there was a further transition to plates, and finally, at higher concentrations still a reversion to a rather malformed type of dendritic growth.

An earlier observation by Vonnegut (1948) that a cloud of tiny hexagonal plate-like crystals growing at $-20°C$ was transformed into prismatic columns by the addition of butyl alcohol at about 10^{-2} mb partial pressure is confirmed by Hallett and Mason, with a reversion to plates if the concentration exceeds about 0·2 mb. Similar transitions are also observed in the temperature range $-8°C$ to $-12°C$.

The mechanism by which such sharp changes in crystal habit are produced by either small changes of temperature or by the adsorption of small quantities of certain organic vapour is far from clear. However, it appears that the habit changes, which reflect changes in the relative growth rates of the basal and prism faces of the crystals, are due primarily

to changes in surface properties which are likely to be profoundly affected by the adsorption of foreign polar molecules, perhaps by the poisoning of dislocation sites.

§ 7. The Epitaxy of Ice on Foreign Substrates

In table 1, p. 228, of the previous article are listed a number of substances with crystal lattices geometrically similar to that of ice and which provide highly efficient nuclei for ice-crystal formation. An obvious first step in investigating the mechanism of nucleation is to study the growth of ice on single crystals of these nucleating agents and to determine whether the ice deposit is strongly orientated by the underlying substrate. The problem has recently been examined from two points of view.

In the first method, the ice crystals are grown in an apparatus almost identical to that of Shaw and Mason (1955) in which single crystals of the substrate are placed on the end of the chilled copper rod. By visual examination through an optical microscope, Jaffray and Montmory (1957 a, b) and Mason (unpublished) have observed, at about $-10°$C, the orientation of hexagonal plate-like ice crystals on the basal faces of single crystals of both lead and silver iodide (see fig. 14, Pl. 24). Jaffray and Montmory also report that the oriented growth of ice crystals occurs on cleaved muscovite mica and upon thin films of silver deposited on a mica base, but these observations are, as yet, unconfirmed†

The second method of investigation—electron diffraction—has been employed at Imperial College, London, by Lisgarten (1957). Unfortunately, in this case, the experiments can be conducted only below $-90°$C because it is impossible to maintain thin deposits of ice at higher temperatures under the vacuum conditions which are necessary to operate the electron-diffraction camera. Because of the difficulty of growing sufficiently large and perfect single crystals of silver iodide from solution for the purpose, the substrate was prepared in the following way. Silver was evaporated *in vacuo* on to a cleaved mica surface and the silver was attacked chemically by suspending it in an atmosphere in equilibrium with a very dilute solution of iodine, to produce flat monocrystalline surface layers of silver iodide. The crystals had to be exposed in the dark to prevent photolytic decomposition of the silver iodide by daylight. The deposit was normally a mixture of the hexagonal and cubic forms of silver iodide, but frequently the cubic form ($a = 6{\cdot}47$ Å) predominated.

At temperatures between $-90°$C and $-110°$C, thin deposits of hexagonal ice (thin enough to allow the diffraction patterns from the underlying basal faces of hexagonal silver iodide to be seen) were found to be strongly oriented with the lattice dimension of the ice being 2–3% less then that of the silver iodide. At temperatures of $-110°$C the a dimension for hexagonal silver iodide is 4·59 Å and the corresponding dimension for hexagonal ice is 4·49 Å, the difference again being about $2\frac{1}{2}$%. It is

† Mason and Bryant (unpublished) find that ice is randomly oriented on *clean* silver but that, after exposure to the atmosphere for a few days, patches of impurity (probably Ag_2S) appear on which ice crystals become oriented.

very interesting that orientation of ice on silver iodide occurs even at these low temperatures when the incident molecules have greatly reduced mobility. At temperatures below $-130°$C cubic ice is formed (Blackman and Lisgarten 1957) and this appeared in randomly-oriented polycrystalline aggregates showing no preferred orientation relative to the underlying silver iodide.

Part II.—Crystal Growth from the Melt

§ 8. The Growth of Large Single Crystals

Ice formed on the surface of still water, as in ponds, has been found by many observers, from Brewster onwards, to have its optical (c) axis vertical, i.e. parallel to the temperature gradient, but the lateral faces are usually ill-defined and do not normally correspond to single crystallographic planes. Thus, although the direction of the optical axis can readily be determined by rotating the crystal between crossed polaroids, it is not easy to identify other crystallographic directions. One method of doing this is to make use of ' Tyndall's figures ' in the manner described by Adams and Lewis (1934) and, in considerable detail, by Nakaya (1956). These figures are produced by the absorption of radiant heat by motes or other defects embedded in the ice, which then become hot spots and cause local internal melting. The six-sided liquid Tyndall ' figures or flowers ', closely resembling snow crystals in shape, lie in parallel planes perpendicular to the optic (c) axis. When these liquid figures are refrozen, the resulting ice rarely fills the space completely but leaves a group of small cavities containing only water vapour which are bounded by natural faces. The lines joining opposite corners of these ' vapour figures ' define the directions of the secondary a crystal axes and correspond to the $[11\bar{2}0]$ crystallographic directions, the sides of the cavities being $(10\bar{1}0)$ faces.

To produce large single crystals of ice in the laboratory, Adams and Lewis adopted a method used earlier by Nacken (1915). A columnar fragment of ice, to be used as a seed, was tested and provided with two opposite plane-parallel faces of the desired orientation. One of the faces was frozen to the outside of the bottom of a metal can containing a freezing mixture at $-10°$C, and the opposite face was allowed to dip just below the surface of distilled, de-aerated water in a beaker held at constant temperature close to 0°C. Crystallization proceeded from the seed into the water along an ellipsoidal front at the rate of a few mm/hr. Crystals of linear dimensions about 10 cm were readily produced.

Large crystals may also be produced by slow cooling of the surface of calm water, in much the same way as occurs in ponds. Under these conditions, freezing proceeds from the surface with both temperature and density increasing with depth so that convection is avoided.

This technique was used by Jona and Scherrer (1952). The water was contained in a thermally-insulated metal cylinder on which were wound three electrical heating coils. The whole apparatus was placed

in a cold room with air temperature $-20°C$ and the water temperature brought to 1–2°c and so maintained for several hours. A vertical temperature gradient was then established in the water by decreasing the current in the upper coil. Crystallization of pure water proceeded from the water surface, the impurities moving downward ahead of the advancing ice. In this way, cylindrical single crystals of 5–6 cm length and 9 cm diameter, and clear as glass, were produced. Jona and Scherrer recommend the use of a metal rather than a glass container and of tap rather than distilled water if large single crystals are required, since appreciable supercooling, which lead to rapid poly-crystallization, is thereby avoided.

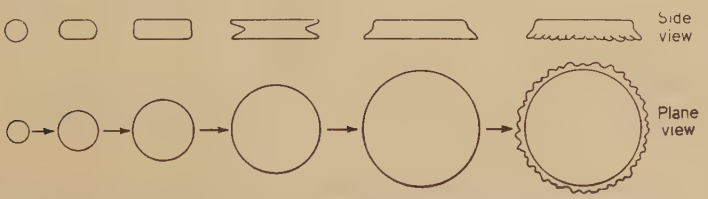
A third method, used originally by Kyropoulos (1926) for the growth of large salt crystals, has been adapted by Jona and Scherrer for ice. On the lower surface of a metal disc, fixed to a micrometer screw, is attached a small single ice crystal with its c axis vertical. This seed crystal is brought into contact with the surface of water maintained at 8°c in a thermally-insulated metal vessel, the whole apparatus being in a cold room held at $-20°C$. After a minute or two, the temperature of the water is lowered by reducing the current in a surrounding coil and simultaneously the seed crystal is slowly withdrawn by rotating the micrometer screw : contact with the water surface always being maintained. With the water temperature held at 2–3°c, the growth velocity is only about $\frac{1}{2}$ mm/hr. Single crystals, 6 cm in diameter and 10 cm long were produced but only if the seed crystal was oriented with its optic axis in the direction of growth.

§ 9. Ice-Crystal Formation on the Surface of Slightly Supercooled Water

When water supercooled by not more than a degree or so is seeded (for example, by tiny ice crystals), crystals form on the surface initially in the form of thin circular discs which may later become notched at the edge and ultimately develop into 6-sided star-shaped crystals. The optic axis of the disc is perpendicular to the surface and, as Arakawa (1955) has shown by producing similarly oriented hexagonal etch pits over the basal plane, these discs are single crystals possessing hexagonal symmetry. In cold climates these crystals, initiated perhaps by frost or snow crystals and multiplied by fragmentation, may form in large concentrations in lakes and rivers supercooled by only a few hundredths of a degree. These collect on underwater obstacles to form huge masses of what is known as frazil ice having a cinder-like texture. The formation of frazil ice has been described by Barnes (1926), Altberg (1936) and Schaefer (1950), among others, but only recently have more detailed studies of the growth of ice crystals in supercooled water been made in the laboratory, mainly in Japan, by Kumai and Itagaki (1953), Arakawa and Higuchi (1952), and Arakawa (1954).

The Japanese workers have taken time-lapse pictures of crystals growing on the still surface of water contained in shallow dishes placed in constant temperature enclosures in a cold room. Usually the water surface was seeded with minute ice crystals formed in the overlying air by suddenly chilling it with a rod cooled to about $-50°$C. Within a few seconds the hexagonal seed crystals lose their angular shape, become rounded in outline and then grow into circular discs. The subsequent development and growth rates of the crystals are functions of both the temperature of the water and the size of the crystals. Thus in water supercooled by not more than a few tenths of a degree, the crystals normally grow as circular discs up to diameters of 2–3 mm, but thereafter may develop notches round the edge, and later still, become six-sided stellar dendritic crystals (see fig. 15). But in water supercooled by a degree or more, dendritic growth may set in much earlier, the crystal growing as a disc in only the very early stages.

Fig. 15



Stages in the development of ice crystals growing on the surface of slightly supercooled water ($T \simeq -0{\cdot}1°$C). (After Arakawa 1954.)

Arakawa (1954) found that, in water at $-0{\cdot}1°$C, circular discs, semi-circular discs (which appeared to be half submerged circular discs), and needles which usually grew out from the edge of the dish, were formed initially, but at later stages, the discs became serrated at the edges and grew into stellar crystals. In water at $-0{\cdot}9°$C, discs grew only in regions where the crystals were densely packed but the more isolated crystals were rapidly growing feathered needles or dendritic stars. In water supercooled below $-0{\cdot}9°$C, no discs at all were seen, only feathered needles and dendritic stars.

Table 3. Growth Rates of Circular Disc Crystals in Supercooled Water.

Authors	Water temp.	dr/dt (expt)	dr/dt (eqn. (6))
Kumai and Itagaki	$-0{\cdot}05°$C	$0{\cdot}5$–$1{\cdot}3 \times 10^{-3}$ cm/sec	$0{\cdot}125$–$0{\cdot}5 \times 10^{-3}$
Arakawa and Higuchi	$-0{\cdot}1°$C	$1{\cdot}0$–$2{\cdot}5 \times 10^{-3}$ cm/sec	$0{\cdot}25$–$1{\cdot}0 \times 10^{-3}$

The growth rates of the crystals varied with the temperature of the water and the crystal concentration, but the values obtained for the

largest in a batch of circular discs were fairly consistent, and were as shown in table 3. Assuming the crystal to be stationary, the mass growth rate, dm/dt will be given by

$$L_f(dm/dt) = 4\pi CK(T_s - T), \qquad (5)$$

where L_f is the latent heat of fusion, $C = 2r/\pi$ the electrostatic capacity of a thin circular disc, K the thermal conductivity of water, and T_s, T the surface temperature of the crystal and the temperature of the bulk water respectively. If we assume that the thickness, x, of the crystal remains sensibly constant during growth, for which there is some observational evidence, then eqn. (5) becomes

$$\frac{dr}{dt} = \frac{4K(T_s - T)}{\pi\rho L_f x} = 2{\cdot}5 \times 10^{-3}\frac{(T_s - T)}{x}, \qquad (6)$$

where ρ is the crystal density. If x varies between 25 μ and 100 μ (Schaefer 1950), then $dr/dt = 10^{-2} - 2{\cdot}5 \times 10^{-3}\Delta T$, where ΔT is the degree of supercooling of the liquid, since $T_s = 0$°C. It will be seen from table 3 that the observed growth rates, which were proportional to ΔT, are in fair agreement with those predicted by eqn. (6), but are sometimes rather larger, perhaps, because, as indicated in the photographs, some crystals drifted slowly across the water surface. However, more careful measurements over a wider range of temperatures are required.

In a recent paper, Hillig and Turnbull (1956) state that recent measurements of the linear velocity of crystallization of water, as measured by the velocity of the ice-water interface in a capillary tube, are described by

$$v = (0{\cdot}158 \pm 0{\cdot}009)\Delta T^{1{\cdot}69 \pm 0{\cdot}03} \text{ cm/sec},$$

for values of ΔT, the degree of supercooling, ranging from 10^{-2} to 10°K. They also say that in these experiments, v, being independent of the diameters and thermal conductivities of the capillaries in which the ice grew, evidently was not controlled by dissipation of the latent heat of fusion as we have just assumed for the growth of crystals on the free surface of water. They suggest instead that the growth occurs by a screw dislocation mechanism by which only a fraction of the total sites on the crystal surface are available for molecular attachment at a given degree of supercooling, and on this basis, derive the following equation

$$v = \frac{3ML_f^2\rho D}{4\pi RT^3\sigma_{SL}}(\Delta T)^2 = 1{\cdot}3 \times 10^{-2}(\Delta T)^2, \qquad (7)$$

where M, ρ are respectively the molecular weight, and density of ice, D a diffusion coefficient for transport across the water-ice interface and σ_{SL} the interfacial surface energy. Equation (7) accounts fairly well for the observed dependence of v on ΔT, but predicts growth rates about one order of magnitude less than those which are observed.

The rate of advance of the ice-water interface in the capillary-tube experiments, representing the rate of growth of skeletal dendritic crystals

(sometimes in a spiral or helical path along the tube according to Wylie 1953), is not necessarily to be compared with that of a disc crystal growing on a free surface of water. The growth rate of the dendrites, from which the latent heat will be conducted very efficiently, may well be surface-limited (although partly controlled by the conduction of heat through the liquid and the glass walls), while that of the disc crystals is almost entirely limited by the rate of heat dissipation through the liquid.

References

Adams, J. M., and Lewis, W., 1934, *Rev. sci. Instrum.*, **5**, 400.

Altberg, W. J., 1936, *Ass. Inst. Hydrologie Scientifique Bull.*, **23**, 373.

Arakawa, K., 1954, *J. Fac. Sci. Hokkaido Univ.*, (2), **4**, 311 ; 1955, *Ibid.*, (2), **4**, 355.

Arakawa, K., and Higuchi, K., 1952, *J. Fac. Sci. Hokkaido Univ.*, (2), **4**, 201.

Aufm Kampe, H. J., Weickmann, H., and Kelly, J. J., 1951, *J. Met.*, **8**, 168.

Barnes, H. T., 1926, *Ice Engineering* (Montreal: Renouf Publishing Co.).

Bentley, W. A., and Humphreys, W. J., 1931, *Snow Crystals* (London: McGraw Hill).

Blackman, M., and Lisgarten, N. D., 1957, *Proc. roy. Soc.* A, **239**, 93.

Burton, W. K., Cabrera, N., and Frank, F. C., 1951, *Phil. Trans. roy. Soc.* A, **243**, 299.

Hallett, J., and Mason, B. J., 1958, *Nature, Lond.* **181**, 467.

Hillig, W. B., and Turnbull, D., 1956, *J. chem. Phys.*, **24**, 914.

Houghton, H. G., 1950, *J. Met.*, **7**, 363.

Jaffray, J., and Montmory, R., 1957 a, *C. R. Acad. Sci., Paris*, **244**, 859 ; 1957 b, *Ibid.*, **245**, 2221.

Jona, F., and Scherrer, P., 1952, *Helv. phys. acta*, **25**, 33.

Kumai, M., and Itagaki, K., 1953, *J. Fac. Sci. Hokkaido Univ.* (2), **4**, 235.

Kyropoulos, S., 1926, *Z. anorg. Chemie.*, **154**, 308.

Lisgarten, N. D., 1957, *Thesis*, London University.

Marshall, J. S., and Langleben, M. P., 1954, *J. Met.*, **11**, 104.

Mason, B. J., 1953, *Quart. J. roy. Met. Soc.*, **79**, 104.

Mason, B. J., and Hallett, J., 1958, *Proc. roy. Soc.* (in the press).

Nacken, L., 1915, *Neues Jb. Miner.*, 158.

Nakaya, U., 1951, *Compendium of Meteorology*, (Boston: Amer. Met. Soc.) p. 207; 1954, *Snow Crystals* (Havard: University Press); 1955, *J. Fac. Sci. Hokkaido Univ.*, (2), **4**, 341; 1956, Snow, Ice, Permafrost Res. Estab. (U.S. Army) Research Paper No. 13.

Reynolds, S. E., 1952, *J. Met.*, **9**, 36.

Schaefer, V. J., 1950, *Trans. Amer. geophy. Un.*, **31**, 885.

Shaw, D., and Mason, B. J., 1955, *Phil, Mag.*, **46**, 249.

Vonnegut, B., 1948, *G. E. Res. Lab. Project Cirrus*, Occas. Rep. No. 5.

Weickmann, H., 1947, *Die Eisphase in der Atmosphäre, Reports and Translations*, **716**, (Völkenrode) (London: Ministry of Supply); 1950, *Die Umschau*, **50**, 116.

Wylie, R. G., 1953, *Proc. phys. Soc. Lond.* B, **66**, 241.

The Mechanical Properties of Ice
I. The Plastic Properties of Ice

By J. W. Glen
Physics Department, University of Birmingham

§ 1. Plastic Deformation of Ice Single Crystals

1.1. *Geometry of the Deformation*

Single crystals of ice have long been known to deform plastically by glide on the basal plane (0001). McConnel (1891) deduced this from the difference in behaviour shown by bars whose optic axes were differently oriented. It is still not certain, however, whether this glide occurs preferentially in any particular directions in the basal plane. Two methods have been used to look for such directions, in the first the direction of the shearing force is altered, and an attempt is made to find a difference in magnitude either of the force required to produce a given strain or of the rate of strain produced by a given force. Mügge (1895), Tammann and Salge (1928) and Steinemann (1954a) have all used this method and have all reported negative results, that is to say within their experimental error the force required to produce a given effect appeared to be independent of the orientation of that force in the basal plane. The only hint from these experiments of any anisotropy of this kind is given in Steinemann's results. He applied a constant stress and measured the resulting flow rate, and although when the stress was 0·75 Kg/cm^2 there was no measurable anisotropy, at 1·5 Kg/cm^2 the flow was somewhat faster in the [11$\bar{2}$0] direction than in the [10$\bar{1}$0] direction. Steinemann considers the difference to be within experimental error, but for all his four orientations the flow rates show a consistent trend, so that the experiment can be considered as slight evidence in favour of [11$\bar{2}$0] as the glide direction.

The second method for finding the glide direction consists of observing the orientation of single crystals before and after they have been extended in uniaxial tension. If one glide system operates throughout a tensile test, then a cylindrical specimen will deform into a tape having its plane as the slip plane and its length as the slip direction. Such a test can therefore be used both to determine the glide elements and also to see whether other glide systems come into operation, as the resolved shear stress in the first system will gradually become less and less. Glen and Perutz (1954) made tests of this sort and found that their specimens did become tape-shaped with (0001) tending towards the plane of the tape. Even at very large strains this tendency continued, so that most other possible glide planes for ice did not appear to be capable of

acting. The evidence on glide direction was less conclusive. Four of their specimens behaved exactly as would be expected if there was no preferred glide direction in the basal plane, while, their fifth specimen behaved exactly as it should if slip occurred only in a $[11\bar{2}0]$ direction. Clearly further tests are needed to settle this point.

The only evidence in favour of slip planes other than the (0001) plane is indirect. The preferred orientations found in certain glaciers have led some investigators, for example Rigsby (1951), to postulate that they are caused by slip on other planes. The texture Rigsby found in the Emmons Glacier led him to suggest slip along $(11\bar{2}2)$ and $(10\bar{1}2)$ planes. It is difficult to see how his polar diagrams with four major peaks of [0001] directions could be produced by basal slip, but his interpretation depends on the assumption that shear has occurred parallel to glacier bands, and that the structure is not a result of recrystallization. Either of these assumptions could be false, and the experiments of Glen and Perutz show that these planes could only be slip planes if the slip direction was the direction common to the plane and (0001). Steinemann (1954 a) performed bending tests to see if other slip systems could be operating, and found no measurable deformation, but in his tests also the resolved shear stress in the direction common to Rigsby's shear planes and the basal plane was zero. Thus there is no direct experimental disproof of certain of Rigsby's slip systems, but in the absence of direct experimental proof, they must be regarded as no more than possibilities.

The nature of the slip process in ice would appear to be very similar to that in metals. Nakaya (1956) has observed that slip takes place in localized glide planes, similar to those observed in metals but further apart. The large glacier crystals used by Nakaya were very well annealed, and the separation he found of about 0·06 mm may not be typical. These localized regions are almost certainly not single crystallographic planes, but regions in which the slip, is concentrated. Nakaya could identify these planes in a bent crystal using shadow photography, and so they would appear to leave some kind of disturbance in their path which affects the optical properties. Nakaya associated these slip planes with the regions in which melt figures are formed when light is focused within the crystal.

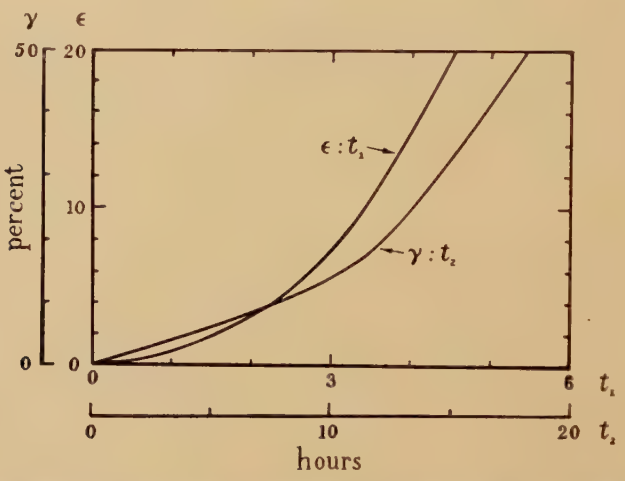
After deformation, ice crystals show x-ray asterism (Glen and Perutz 1954, Steinemann 1954 a), and this asterism is sometimes broken up into small spots suggesting that ice polygonizes (Glen and Perutz 1954). This polygonization can be seen directly by observing a bent ice crystal in polarized light (Nakaya 1956), as the polygon boundaries appear as dark lines perpendicular to the slip planes.

1.2. *The Creep Curve of Ice Single Crystals*

The relation between stress, strain and time for ice single crystals has been investigated by several experimenters. It is found that the crystals creep under all loads for which they deform plastically, and the relation most studied is that between strain and time at constant load.

Tests of this kind have been made by Glen and Perutz (1954) in tension, Steinemann (1954 a) and Rigsby (1957) in shear, and Griggs and Coles (1954) in compression. Because the specimen tends to form a neck, the tension experiments are not of much value in themselves, and it is not entirely surprising that they show a continuously increasing creep rate. What is surprising is that the tests in shear and compression also gave a creep rate that increased with time (see fig. 1) and this was found by all the experimenters mentioned. Ice appears to deform more easily as time proceeds, quite unlike reported results for metals. Recrystallization was not observed to be associated with the acceleration, and changes of stress

Fig. 1



Typical creep curves of ice single crystals. The curve of $\epsilon : t_1$ is for compression test at -10°c with a stress of 4·55 Kg/cm² (after Griggs and Coles 1954). The curve of $\gamma : t_2$ is for a shear test at $-2{\cdot}3$°c with a stress of 0·65 Kg/cm² (after Steinemann 1954 a). Note the different scales in the two cases.

cannot be responsible in Griggs and Coles tests, for the basal plane was at 45° to the compression axis. Griggs and Coles made tests at various temperatures, and found that their creep curves can best be fitted by an equation of the form

$$\epsilon = a[(\sigma - bT^2)t]^2$$

where ϵ is the compressive strain, σ the stress, T the temperature below the melting point and t the time. If ϵ is expressed in per cent, σ in Kg/cm², T in °c and t in hours, the values of the constants are $a = 0{\cdot}62$, $b = 0{\cdot}02$.

Steinemann continued his tests longer than Griggs and Coles (20 hours compared with 6 hours), and found that his creep curves appeared to settle down to a steady rate of flow rather than continue to increase

parabolically, and he has related this steady rate by plotting his shear strain rate $\dot{\gamma}$ against shear stress τ logarithmically. He finds that a relation of the form

$$\dot{\gamma} = k\tau^n$$

with n a constant of about 1·5, gives a good approximation to his data. He has also plotted the creep rate at earlier stages of the creep curve in the same manner, and again finds relations of this form but with values of n between 2·3 and 3·9. He also investigated the effect of changing the direction of glide and of resting the crystal for times up to several hundred hours in the middle of a test ; neither of these procedures restored the original hard part of the creep curve, so the softening seems to be permanent.

1.3. *Effect of Uniaxial Compression and Hydrostatic Pressure on the Deformation of Ice Crystals*

Tammann and Salge (1928) investigated the effect of applying a uniaxial compression perpendicular to the slip plane on the shear stress needed to produce gliding. They found that a lower stress was needed when such a compression was present, and that at a compressive stress whose magnitude depends on temperature, the shear stress needed to give deformation fell to zero. This effect is surprising, since similar effects do not seem to occur in metal crystals. The compressive stresses used were of the same order of magnitude as the shear stresses, and so this result means that a direct comparison between tension and compression tests on the one hand and shear tests on the other cannot be made by the usual assumption that only the resolved shear stress on the glide plane is of significance for the deformation of single crystals.

Hydrostatic pressure does not have a serious effect on the creep properties, however. Rigsby (1957) found that pressures up to 306 atmospheres produced no noticeable change in the creep curve of an ice crystal, provided the temperature was changed so that the temperature difference between the crystal temperature and the melting point was kept constant. Without this adjustment the pressure produced an acceleration in the creep curves, and this shows that at Rigsby's temperature (3·1°C below the melting point) the creep was to some extent determined by this proximity and not simply by thermal activation appropriate to the absolute temperature.

1.4. *Hardness of Ice Crystals*

Butkovich (1954 a) has made hardness tests on ice single crystals using both a Brinell indentation method and a scratch microhardness test. He found that both hardness numbers increased rapidly as temperature decreased, and also found that the hardness was, as might be expected, different for different orientations of the crystal plane tested. He

found that at temperatures below $-10°$C penetrations parallel to the optic axis or scratches on planes containing the optic axis gave higher hardnesses, but that the difference varied linearly with temperature, and for Brinell tests became zero for $-10°$C and reversed in sign above $-10°$C. This interesting result can hardly be explained at the present stage of our knowledge of the plastic properties of ice.

§ 2. Plastic Deformation of Polycrystalline Ice

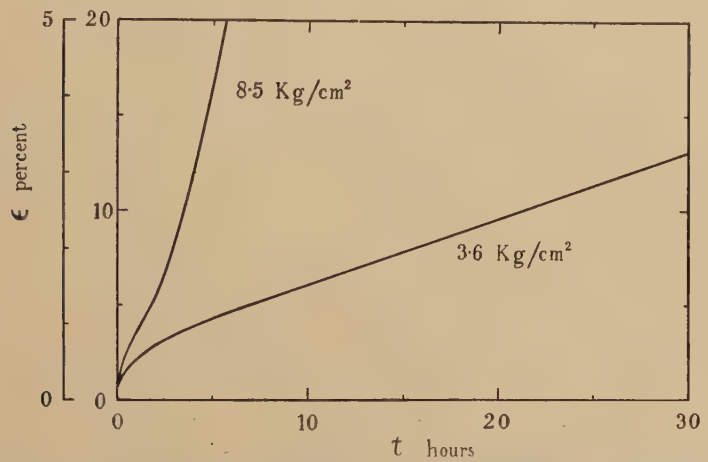
2.1. *The Creep Curve of Polycrystalline Ice*

As ice single crystals are so markedly anisotropic in their plastic properties, having only one well established slip plane, the behaviour of a polycrystalline aggregate can be expected to be very dependent on the relative orientation of its grains. It so happens that one of the commonest methods of forming ice (freezing of a free water surface) tends to produce ice crystals all of whose basal planes are parallel, and such an aggregate will have properties markedly different from one with more random orientations. The ice of glaciers, for example, frequently has quite a strong preferred orientation (see Rigsby 1951 for example), but never to the extent of that found in lake ice. It is thus most important to know how specimens used in tests were formed in order to be able to compare different tests. Early tests in the last century showed that ice was capable of plastic deformation in bending (Reusch 1864) or tension (Pfaff 1875, Main 1887), and that such deformation still occurred down to $-25°$C (Koch 1885), but in most of these cases the exact nature of the specimens used is not clear. The first tests for which the method of preparation was clearly stated, and for which polarized light was used to study the grain structure, were those of McConnel and Kidd (1888). They made specimens in moulds, and also cut them from lake ice, glacier ice and an icicle. They tested all these types in tension, and some in compression. They found that the rate of strain varied with the orientation of the grains, temperature and stress, and that it was not proportional to stress. However as they had no method of temperature control they were unable to study these relations in any detail.

Most of the experiments on the flow of ice for many years after those of McConnel and Kidd were performed in bending, torsion or other systems in which the stress is not constant, and the results were interpreted using theories applicable to materials with a constant coefficient of viscosity, although the results themselves showed this assumption to be untrue ; thus not much progress was made until comparatively recently in the study of the relations connecting stress and strain in polycrystalline ice. During the Second World War work in connection with a proposed iceberg aircraft carrier (Perutz 1948) led to the study of the plastic properties of a frozen mixture of water and wood pulp, and it was found that this material behaved somewhat like a metal at a high temperature ; this suggested that tests on ice more similar to those used

for metals might be rewarding, and so Glen (1955) made a series of compression tests on randomly oriented ice cylinders under controlled temperature conditions. He found that the behaviour of ice under a constant load was indeed similar to that of certain metals (see fig. 2). The creep curve had an initial transient stage in which the rate of strain decreased, and this was followed by a stage in which the ice deformed at a constant rate. As with metals these two components of strain were proportional to the cube root of time and to the time respectively. At higher stresses (above about 4 Kg/cm^2) the creep rate reaccelerated again after its initial fall (see fig. 2), and this tertiary creep is also sometimes observed in metals, where it is associated with recrystallization. Glen therefore

Fig. 2



Typical creep curves of polycrystalline ice in compression. The curve corresponding to a stress of 8·5 Kg/cm^2 uses the right-hand strain scale, that for 3·6 Kg/cm^2 uses the left-hand strain scale. Both tests were performed at −0·02°C.

studied thin sections taken from his specimens, and found that the specimens strained under high stresses showed a smaller grain size than those which had had a smaller stress. He also found that if the stress had been above about 5 Kg/cm^2 the ice actually recrystallized again in thin section, which shows that very large stresses had been trapped in the deformed specimens.

It thus seems likely that recrystallization had been occurring in these ice specimens during creep, and that this is responsible for the shape of the creep curve. However, since single crystals of ice are harder when first formed and soften during creep, recrystallization cannot by itself produce a softer material. The explanation of the creep curve of polycrystalline ice therefore seems to be that the initial decelerating creep is due to the interference between grains of different orientations, and that the reacceleration is caused by recrystallization which produces

grains more favourably oriented for glide than previously. Steinemann (1954 b) made observations of the preferred orientations produced, and found that the orientation on recrystallization did favour grains with their basal planes at 45° to the compression axis, i.e. parallel to planes of maximum shear. He also made tests on the compression of thin discs of ice, for which he was able to follow the variation of grain size with time during and after the test. He found that the recrystallization process can be explained in terms of nucleation and growth, and also that the grain shapes are different for specimens recrystallized under stress ; very complex intergrowing grains are formed, which must make intergranular slip very difficult. This shows that the plastic deformation of polycrystalline ice must be thought of as due to a combination of intra-granular slip and recrystallization.

2.2. *Relation between Creep Rate and Stress*

Both Glen (1955) and Steinemann (1954 b) analysed their results by plotting the logarithm of the minimum observed strain rate $\dot{\epsilon}$ against the logarithm of the stress σ. Glen found that his points lay very close to a straight line, and so suggested the law

$$\dot{\epsilon} = k\sigma^n$$

would be suitable. The value of n was $3{\cdot}17 \pm 0{\cdot}2$ for his tests at both $-0{\cdot}02$°C and $-1{\cdot}5$°C. For the higher temperature Glen also analysed his results to discover what would have been the minimum rate without the effect of the $t^{1/3}$ or transient term. Again he found good agreement with the power law, but now n had the value 4·2. Over the stress range 1 to 10 Kg/cm^2 this flow law would appear to be a good approximation.

Steinemann also found that his results fitted a law of this form, but suggests that his data show a deviation at low stresses. This can be expressed by saying that his value of n varied from about 1·85 at 1 Kg/cm^2 to 4·16 at 15 Kg/cm^2. Naturally it is at the lowest stresses that the tests take the longest time to reach their minimum rate, and Glen's results for minimum creep rates also show such a variation, but his analysed rates do not, and it is therefore likely that the low value of n in these tests at low stresses is caused solely by the experimental fact that the time of the test was limited. The evidence from glacier measurements which was at that time thought to suggest a similar variation has now been reinterpreted (Nye 1957), and is more in agreement with the high value of n.

2.3. *Relation between Creep Rate and Temperature*

Most of Glen's tests were performed at $-0{\cdot}02°$ or $-1{\cdot}5$°C, but he did do some at $-6{\cdot}7°$ and $-12{\cdot}8$°C. In this range the strain rate for a given stress fell off by a factor of about 6. Glen attempted to deduce an activation energy from his data, and obtained a value of 31·8 Kcal/mole but it is important to realize that this depends on the assumption that the creep varies with temperature according to Boltzmann's equation.

The temperature range used was not large enough to check this equation, and particularly if Steinemann's data (all his tests were conducted at $-4{\cdot}8°$C) are considered as immediately comparable with Glen's, there is some evidence that Boltzmann's equation is not followed. Indeed the results on single crystals reported above suggest that it may be the difference in temperature from the melting point that should be used in any temperature analysis on creep curves at these temperatures. This might help to explain the discrepancy between Glen's activation energy and the value of 14 Kcal/mole found by Landauer (1955) from the variation in creep rate of snow in the temperature range from $-5°$ to $-20°$C, for although the details of creep in ice and snow will be very different, the fundamental processes of plastic deformation and hence the activation energy should be the same, unless of course fracture is primarily responsible for the creep of snow.

2.3. *Effect of Uniaxial Compression and Hydrostatic Pressure on the Deformation of Polycrystalline Ice*

Steinemann (private communication†) has studied the effect of superimposing a uniaxial compressive stress parallel to the axis of torsion on the shear strain rate of a ring-shaped specimen. In this case an effect is to be expected, since the compressive stress will increase the maximum shear stress acting in the specimen, and hence will increase the shear strain rate. However this experiment provides a test of the hypothesis that the components of shear strain rate are proportional to those of the stress deviator, the constant of proportionality being determined by the octahedral shear stress alone. Unfortunately the results are not in agreement with this theory, and so the validity of this hypothesis, which is often used in calculations concerning glaciers, must be regarded as suspect, however further experiments on this subject would be desirable.

Steinemann has also studied the effect of hydrostatic pressures up to 80 atmospheres on the rate of shear strain of his ring-shaped specimens. He finds no definite effect, which, taken in conjunction with Rigsby's experiments for single crystals, is evidence that hydrostatic pressure has no direct effect on the plastic properties of ice. The explanation of the failure of the octahedral shear stress hypothesis must therefore be sought not in effects of pressure, but in the effects of the third invariant of the stress tensor, or in a failure of the law of proportionality of components.

2.4. *Elastic After-Effect of Ice*

Koch (1885) noticed that when a load was removed from ice, it not only recovered strain instantaneously, but also continued to recover at a rate which fell off with time. Glen (1955) also observed this effect,

† To be published as *Dissertation*, Eidg. Technische Hochschule, Zürich, and in *Beiträge zur Geologie der Schweiz*, Geotechnische Serie, Hydrologie.

not only when the load was completely removed, but also in some cases if the load was simply reduced ; thus after reduction of the compressive stress the ice would continue extending for several hours before continuing to compress under the action of the remaining stress. Under other conditions, however, Glen found that an opposite effect was produced, in that after a reduction of stress the strain rate was initially higher than that appropriate to the new stress and reduced towards its equilibrium value. Glen attributed this effect to recrystallization, as it occurred only in a specimen initially under a high stress. Brill (1957) has also studied the elastic after-effect in the course of a series of experiments on the visco-elastic behaviour of ice. Unfortunately his experiments were performed in bending, so that his stress was not constant, which makes his data difficult to analyse, but they do show the existence of the after-effect very clearly, and also establish that the after-effect occurs also in single crystals, and so cannot be due to grain boundary effects.

2.5. *Hardness of Polycrystalline Ice*

King (1952) used a diamond pyramid indenter to measure the hardness of polycrystalline ice. He found that the hardness was dependent on time and temperature, and his results, if analysed using the usual methods for comparing such tests with tensile tests, provide evidence for the approximate validity of the power law relation between stress and strain rate up to stresses as high as 100 Kg/cm^2, far beyond the range of the tests of Glen and Steinemann.

§ 3. Evidence on the Plastic Properties of Ice from Measurements on Glaciers

Measurements on glaciers can provide some test of the laws suggested for the mechanical properties of polycrystalline ice under conditions very different from those available in the laboratory. On the other hand, there are uncertainties of interpretation of glacier observations which are not present in the laboratory tests. For example measurements of the rate of flow of glaciers could be used to deduce the flow law of ice if the detailed shape of the glacier bed and the boundary conditions of flow on it were known. These conditions are seldom fulfilled, and all that can be done from the majority of such measurements is to show, as Perutz (1953) has done, that the glacier data are not inconsistent with the laboratory law.

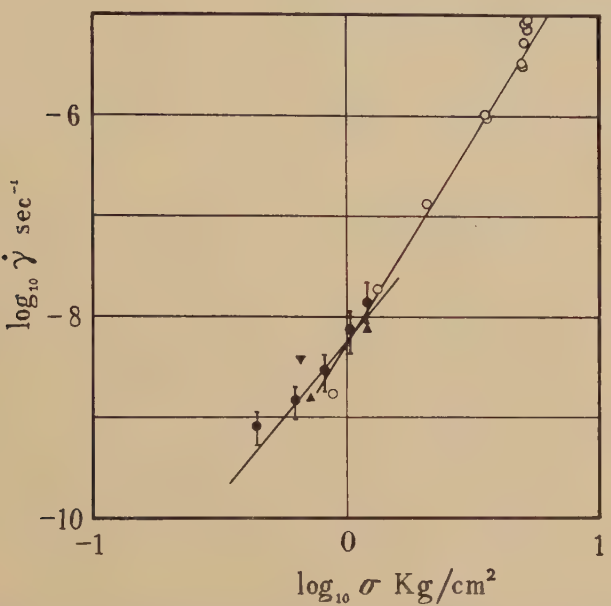
In two cases more useful results can be obtained. The closure of a tunnel dug into a glacier has been shown by Nye (1953) to be capable of direct interpretation in terms of the flow law of ice provided there are no large stresses present due to the glacier flow. Three tunnels have been measured which fulfil this condition, these were in the Z'Mutt Glacier (Haefeli and Kasser 1951), Vesl Skautbreen (McCall 1952) and the ice cap on the Jungfraujoch (Haefeli and Brentani 1955). Nye

(1953) analysed the results from the first two of these tunnels and showed that they corresponded to a relation between octahedral shear stress τ and octahedral shear strain rate $\dot{\gamma}$ of the form

$$\dot{\gamma} = k\tau^n$$

where the value of n obtained was 3·07. This is in good agreement with the laboratory results found by Glen (see fig. 3), and indeed the

Fig. 3



Plot of logarithm of octahedral creep strain rate against logarithm of octahedral shear stress for laboratory and glacier tests. ○—points derived from Glen's (1955) analysed steady creep rate in compression tests. ●—points derived by Nye (1953) from tunnel closure measurements by McCall (1952). ▲—points derived by Nye from tunnel closure measurements by Haefeli and Kasser (1961). ▼—point derived from the vertical closure rate of the tunnel in the Jungfraujoch (data given by Haefeli and Brentani 1955). The lines drawn are those derived by Glen and Nye from the laboratory and glacier data respectively.

two curves can be said not to differ within experimental error in the region where they overlap. The third tunnel, that of Haefeli and Brentani, differs somewhat in that it was beneath cold ice (−2 to −3°C) which was not fully consolidated. The tunnel did not remain circular, but compressed vertically. However if this rate of vertical compression is used in Nye's theory, then a point is obtained which is again very close to the line deduced from the other tunnels.

Two tunnels have been measured which close much more rapidly than is to be predicted on Nye's theory ; these were in the Arolla Glacier

(Haefeli 1951) and in Austerdalsbreen (Glen 1956). In both cases, however, the tunnels were at the foot of an ice fall, a point where large longitudinal stresses due to the glacier flow are to be expected.

The other case where glacier measurements have been used to give detailed comparison with the flow law of ice is the measurement by Gerrard *et al.* (1952) of the deformation of a pipe sunk through the Jungfraufirn. Using data on the surface strains, Nye (1957) has shown that here too the data are in complete agreement with the laboratory flow law.

These successes of the laboratory flow law are the more interesting because they involve its extrapolation to lower stresses than those used in its discovery ; the tunnels extend the range down to strain rates of 5×10^{-10} sec^{-1}, and this, together with the hardness results, show that the law has some validity over a range of strain rates of 10^6.

§ 4. Fracture Strength of Ice

The fracture strength of ice depends markedly on the method of formation of the specimen and the details of the test ; it also depends on the size and shape of the specimen. A very large number of experiments have been reported, and only two of the most recent will be discussed here. Jellinek (1957) has made a detailed study of the size and shape effects, which shows that they are quite large. For example a large specimen with a volume of about 6 cm^3 and an area of 3 cm^2 had an ultimate tensile strength of about 16 Kg/cm^2, but a disc shaped specimen of volume 2×10^{-2} cm^3 and area 0·78 cm^2 had an ultimate tensile strength of 70 Kg/cm^2. Jellinek has analysed his results in full, and his paper gives a good idea of the tensile strength to be expected of polycrystalline ice of random orientation. He did not find a marked temperature dependence.

Butkovich (1954 b) did find quite a marked temperature variation in compression and torsion however, and as he worked with more normally shaped specimens, his results are probably more typical in this respect. In all cases the strength rose as the temperature fell, but the ratio of strength at low temperature to that near the melting point was much greater for clear lake ice, probably with a strong preferred orientation, than for ice formed from snow. Some typical results are shown in the following table.

Crushing Strength of Ice in Kg/cm^2

	Load	0°c	−50°c
Clear lake ice	Parallel to axes	20·2	82·4
Clear lake ice	Perpendicular to axes	12·5	70·3
Snow ice	—	18·3	40·6

This difference is somewhat surprising, and may indicate that the mechanism of fracture is different in the different cases.

Acknowledgment

I am indebted to Dr. S. Steinemann for sending me details of his unpublished work.

References

Brill, R., 1957, *Structure of Ice*, U.S. Army, Corps of Engineers, Snow, Ice and Permafrost Research Establishment, SIPRE Report 33, 67p.

Butkovitch, T. R., 1954 a, *Hardness of single ice crystals*, Snow, Ice and Permafrost Research Establishment, Research Paper 9, 12p.; 1954 b, *Ultimate strength of ice*, Ibid., Research Paper 11, 12p.

Gerrard, J. A. F., Perutz, M. F., and Roch, A., 1952, *Proc. roy. Soc.* A, **213,** 546.

Glen, J. W., 1955, *Proc. roy. Soc.* A, **228,** 519 ; 1956, *J. Glaciol.*, **2,** 735.

Glen, J. W., and Perutz, M. F., 1954, *J. Glaciol.*, **2,** 397.

Griggs, D. T., and Coles, N. E., 1954, *Creep of single crystals of ice*, Snow, Ice and Permafrost Research Establishment, SIPRE Report 11, 24p.

Haefeli, R., 1951, *J. Glaciol.*, **1,** 496.

Haefeli, R., and Brentani, F., 1955, *J. Glaciol.*, **2,** 571.

Haefeli, R., and Kasser, P., 1951, Geschwindigkeitsverhaeltnisse und Verformungen in einem Eisstollen des Z'Muttgletschers. *U.G.G.I., Association Internationale d'Hydrologie Scientifique, Assemblée Générale de Bruxelles*, Tome 1, p. 222–36.

Jellinek, H. H. G., 1957, *Tensile strength properties of ice adhering to stainless steel*, Snow, Ice and Permafrost Research Establishment, Research Report 23, 22p.

King, R. F., 1952, *Dissertation*, Cambridge. Some results quoted in Glen (1955).

Koch, K. R., 1885, *Ann. Phys. Chem.*, N.F., **25,** 438.

Landauer, J. K., 1955, *J. appl. Phys.*, **26,** 1493.

Main, J. F., 1887, *Proc. roy. Soc.*, **42,** 496.

McCall, J. G., 1952, *J. Glaciol.*, **2,** 122.

McConnel, J. C., 1891, *Proc. roy. Soc.*, **49,** 323.

McConnel, J. C., and Kidd, D. A., 1888, *Proc. roy. Soc.*, **44,** 331.

Mügge, O., 1895, *Neues Jb. Min. Geol. Paläont.*, **2,** 133.

Nakaya, U., 1956, *Properties of single crystals of ice, revealed by internal melting*, Snow, Ice and Permafrost Research Establishment, Research Paper 13, 80p.

Nye, J. F., 1953, *Proc. roy. Soc.* A, **219,** 477; 1957, *Ibid.*, **239,** 113.

Perutz, M. F., 1948, *J. Glaciol.*, **1,** 95; 1953, *Proc. roy. Instn G. B.*, **35,** 571, (see also 1953, *Nature, Lond.*, **172,** 929).

Pfaff, F., 1875, *Ann. Phys. Chem.*, VI **5,** 169.

Reusch, E., 1864, *Ann. Phys. Chem.*, V **1,** 573.

Rigsby, G. P., 1951, *J. Geol.*, **59,** 590; 1957, *Effect of hydrostatic pressure on velocity of shear deformation of single crystals of ice*, Snow, Ice and Permafrost Research Establishment, Research Report 32, 7p.

Steinemann, S., 1954 a, *J. Glaciol.*, **2,** 404; 1954 b, Flow and recrystallisation of ice. *U.G.G.I., Association Internationale d'Hydrologie Scientifique, Assemblée Générale de Rome*, Tome 4, [Pub. 1956], p. 449-62.

Tammann, G., and Salge, N., 1928, *Neues Jb. Min. Geol. Paläont., Beil. Bd.* **57,** A, 117.

The Mechanical Properties of Ice. II. The Elastic Constants and Mechanical Relaxation of Single Crystal Ice

By R. W. B. Stephens
Physics Department, Imperial College, London

According to Voigt (1928) the elastic behaviour of crystals is defined by the following relations :

$$\sigma_i = \sum_{n=1}^{n=6} C_{ik}\epsilon_k \quad . \quad . \quad . \quad . \quad . \quad . \quad . \quad . \quad (1)$$

$$\epsilon_i = \sum_{n=1}^{n=6} S_{ik}\sigma_k \quad . \quad . \quad . \quad . \quad . \quad . \quad . \quad . \quad (2)$$

where σ is the stress, ϵ the strain, C_{ik} the elastic moduli and S_{ik} the elastic coefficients. The elastic moduli and coefficients are related by the expression

$$\sum_{n=1}^{n=6} C_{ik}S_{ik} = \begin{cases} 1 \text{ for } i=j \\ 0 \text{ for } i\neq j \end{cases} . \quad . \quad . \quad . \quad . \quad . \quad . \quad . \quad (3)$$

As ice is hexagonal there are five independent elastic constants (C_{ik} or S_{ik}) but their determination by static methods are rendered inaccurate due to inception of plastic flow and elastic after-effect for even very small loading. Although dynamical measurements have been employed by a number of experimenters only one has made a direct determination of the complete set of elastic moduli and another of the full set of elastic coefficients. By using relation (3) the moduli may be deduced from the experimental values of the coefficients and *vice-versa*, but in following this procedure considerable loss of accuracy in the values of the calculated constant is incurred.

A theoretical determination of the elastic constants of ice has been made by Angela H. A. Penny (1948) who used a simplified model of the ice crystal which was equivalent to that proposed previously by Barnes (1935). In this model the hydrogen atoms are assumed to lie centrally between two oxygen atoms, which is in contrast with the proposals made by Pauling (1935), Bernal and Fowler (1933) and Huggins (1936), who suggested, in order to explain certain observed physical phenomena in ice, that the hydrogen atoms are unequally spaced along the line joining two oxygen atoms. Further necessary simplifying assumptions made by Penny were that only first neighbour atoms are considered to act on one another and that there exists a regularity of structure arising from the fact that any four neighbouring oxygen atoms lie at the vertices of an almost regular tetrahedron. These simplifications reduce the number of atomic constants to two, and Penny obtains six expressions

giving the five independent elastic constants of ice (C_{11}, C_{12}, C_{13}, C_{33} and C_{44}) in terms of the atomic constants. The redundant information in the six equations yields the relation $C_{66}=\frac{1}{2}(C_{11}-C_{12})$ which is in accord with general lattice theory. Furthermore since five elastic constants are given in terms of two atomic constants it follows that there must be three other relations between the elastic constants and these are :

$$C_{11}+C_{12}=C_{33}+C_{13}\ ;\ (C_{33}-C_{13})^2=2C_{44}(C_{33}-5C_{13}+4C_{12})\ ;$$
$$12(C_{13})^2+5C_{13}C_{33}-(C_{33})^2+2C_{44}(5C_{13}+2C_{33})$$
$$=C_{12}(15C_{13}+C_{33}+14C_{44}).$$

As no single crystal measurements were at the time available, Penny used an elastic theory applicable to a mixture of randomly oriented crystals which is due to Voigt. This theory enabled the atomic constants to be derived from the experimental values of Young's modulus and Poisson's ratio for polycrystalline ice, found by Northwood (1947), using a dynamic method. The values obtained in units of 10^{10} dyne cm^{-2} were

$$C_{11}=15{\cdot}2,\ C_{12}=8{\cdot}0,\ C_{13}=7{\cdot}0,\ C_{33}=16{\cdot}2,\ C_{44}=3{\cdot}2.$$

The direct experimental determination of the full set of elastic moduli for a single ice crystal was carried out by Jona and Scherrer (1952) using the Schaefer–Bergmann method, which is dependent on the excitation of elastic wave motion in the crystal by means of attached vibrating quartz crystals. The standing-wave systems which are produced will create effectively a three-dimensional grating, and the transmission of light through the crystal will give rise to Laue-type diffraction patterns. From these the velocities of shear and longitudinal elastic waves (and hence the corresponding elastic moduli) in the different crystallographic directions may be found. In their experiments Jona and Scherrer froze glass plates on to the crystal faces through which light, from a high pressure mercury vapour lamp, was transmitted. Exposure times of $\frac{1}{2}$ to 2 min. were necessary for photographing the patterns but this was broken up into a number of equivalent shorter exposure times so as to minimize the heating-up of the specimen by the ultrasonic radiation. Jona and Scherrer's observations were only made at one temperature (-16°C) and over a very limited frequency range 1·5 to 1·8 Mc/s (see table 1).

Bass *et al.* (1957) have also made a complete set of measurements, and by finding the resonant frequencies of single crystal plates and bars they were able to make a direct determination of the elastic coefficients (S_{ik}) ; the particular modes employed are given in table 2. These measurements extended over a temperature range between 0°C and -25°C, a particular temperature being controllable to $\frac{1}{4}$°C, and over a frequency range 5 to 50 kc/s. In the table of numerical values of the coefficients (table 3, which is derived from the curves of Bass *et al.*), the larger inaccuracy in the values of S_{12} and S_{13} arises from the fact that they are only obtainable

Table 1. Elastic Constants and Moduli at $-16°$c

Elastic Moduli $C_{ik} \times 10^{10}$ dyne/cm^2					Elastic Constants $S_{ik} \times 10^{-12}$ cm^2/dyne				
	Penny Theoretical values	Jona and Scherrer. Schaeffer Bergmann method	Bass *et al.* Resonant bars and plates	Green and Mackinnon Ultrasonic pulse method		Penny Theoretical values	Jona and Scherrer. Schaeffer Bergmann method	Bass *et al.* Resonant bars and plates	Green and Mackinnon Ultrasonic pulse method
C_{11}	15·2	13·85 ± 0·08	13·3 ± 0·8	13·33 ± 1·98	S_{11}	9·9	10·4 ± 0·3	10·13 ± 0·05	10·02 ± 1·9
C_{12}	8·0	7·07 ± 0·12	6·3 ± 0·8	6·03 ± 0·72	S_{12}	−4·0	−4·3 ± 0·3	−4·16 ± 0·15	−3·67 ± 0·79
C_{13}	7·0	5·81 ± 0·16	4·6 ± 0·9	5·08 ± 0·72	S_{13}	−2·5	−2·4 ± 0·1	−1·93 ± 0·21	−2·26 ± 0·94
C_{33}	16·2	14·99 ± 0·08	14·2 ± 0·7	14·28 ± 0·54	S_{33}	8·4	8·5 ± 0·4	8·28 ± 0·04	8·61 ± 1·06
C_{44}	3·2	3·19 ± 0·03	3·06 ± 0·015	3·26 ± 0·08	S_{44}	31·3	31·4 ± 0·3	32·65 ± 0·15	30·7 ± 0·8

Table 3. Elastic Constants of Ice as a Function of Temperature in Units of 10^{-12} cm^2/dyne

Constant	$-2°$c	$-5°$c	$-10°$c	$-15°$c	$-20°$c	$-25°$c	Probable error
S_{11}	10·38	10·35	10·24	10·13	10·08	9·98	0·05
S_{33}	—	8·43	8·37	8·30	8·24	8·20	0·04
S_{44}	—	33·2	33·0	32·8	32·5	32·2	0·02
S_{12}	−4·3	−4·27	−4·22	−4·18	−4·13	−4·0	0·1
S_{13}	—	−1·9	−1·9	−1·9	−1·9	−1·9	0·2

After Bass *et al.* (1957).

Table 2

Coefficient	Specimen	Orientation	Mode	Eigenfrequency
S_{11}	rod	axis $\perp$ c-axis	longitudinal	$\nu_n = \frac{h}{2L}\sqrt{\frac{1}{\rho . S_{11}}}\left\{1+\alpha\left(\frac{d}{\lambda}\right)^2\right\}$
S_{33}	rod	axis $\parallel$ c-axis	longitudinal	$\nu_n = \frac{h}{2L}\sqrt{\frac{1}{\rho . S_{33}}}\left\{1+\beta\left(\frac{d}{\lambda}\right)^2\right\}$
S_{13}	rod	axis 48° to c-axis	longitudinal	$\nu_n = \frac{h}{2L}\sqrt{\frac{1}{\rho S'_{11}}}\left\{1+\gamma\left(\frac{d}{\lambda}\right)^2\right\}$ S'_{11} = function $(S_{13}, S_{11}, S_{33}, S_{44})$
S_{44}	rod	axis $\parallel$ to c-axis	torsional	$\nu_n = \frac{h}{2L}\sqrt{\frac{1}{\rho S_{44}}}$
S_{12}	plate 	$\perp$ to c-axis	radial	$\nu_{moR} = \frac{X_{mo}}{\pi . d}\sqrt{\frac{1}{\rho}\left(C_{11}-\frac{C_{13}^2}{C_{33}}\right)}\left\{1+\delta\left(\frac{h}{\lambda}\right)^2\right\}$
			distortional	$\nu_{mn} = \frac{X_{mm}}{\pi . d .}\sqrt{\frac{1}{\rho}\left(C_{11}-\frac{C_{13}^2}{C_{33}}\right)}$ $= \frac{y_{mn}}{\pi . d .}\sqrt{\frac{1}{2\rho(S_{11}-S_{12})}}$ y_{mn} is a known function of X_{mn}/x_{mo}

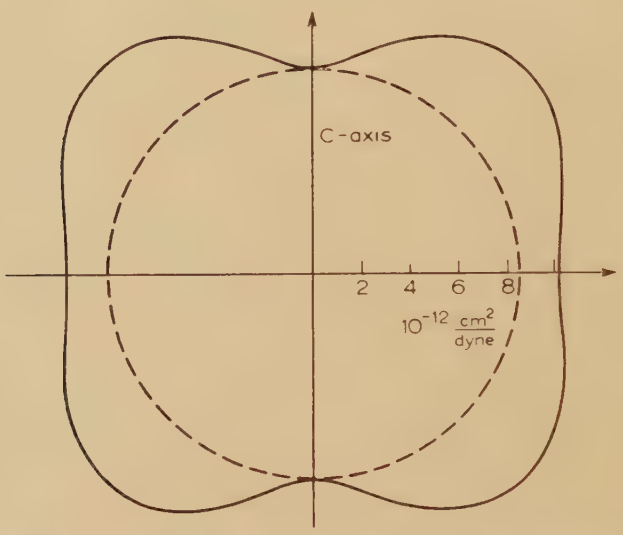
L = length of bar
d = diameter of rod or plate
h = thickness of plate
ρ = density of ice
λ = wavelength
m and n are integers

$\alpha, \beta, \gamma, \delta$ are correction coefficients for the finite diameter of the bars, and the finite thickness of the plates.

After Bass *et al.* (1957).

from the observed resonant frequencies in terms of other coefficients. The general accuracy of the experimental measurements appears to be limited by errors in the orientation of the crystals, by possible evaporation of the crystal during the experiment and by the effect of the mechanical coupling of the transducers on the resonant frequencies of the crystals. The vibrations were excited and detected by means of small Rochelle salt crystals, coupled through synthetic bristles (or steel needles) which were in contact with the specimens. The latter were turned on a lathe from single crystal regions of a large ice crystal which had been optically examined between crossed polaroids and by Tyndall's ice flower method. Grains boundaries are clearly shown up by optical interference patterns and the *c*-axis direction could be located to less than 0·1° ; the angle between the axis of the rod specimen (or the normal to the plate) and the crystallographic axis as given in table 2 was always less than 1°.

Fig. 1



Elastic coefficient S'_{11} as function of angle between *c*-axis and axis of rod (after Bass *et al.* 1957)

In fig. 1 the coefficient S'_{11}, defined in table 2, is plotted as a function of the angle the rod makes with the *c*-axis, the following transformation being employed :

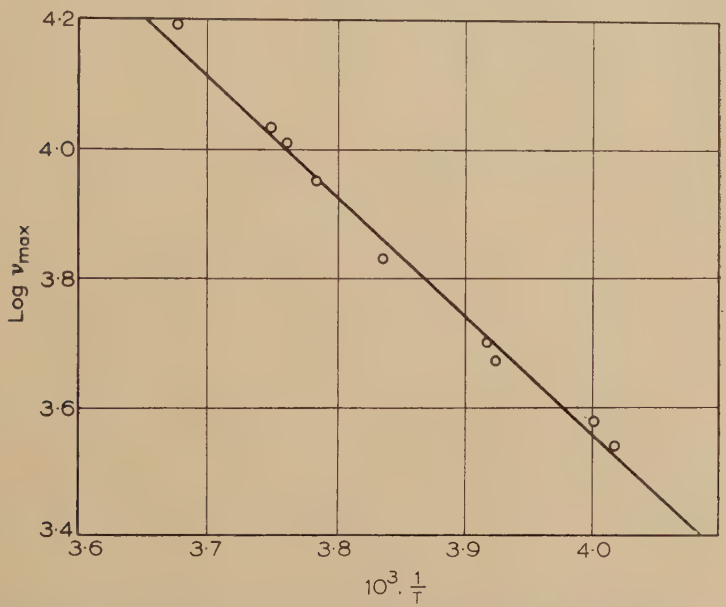
$$S'_{11}=S_{33}\cos^4\psi+S_{11}\sin^4\psi+(S_{44}+2S_{13})\cos^2\psi\sin^2\psi.$$

The results obtained by Jona and Scherrer and by Bass and his colleagues are in good agreement, especially when it is remembered that accuracy is lost in the process of the conversion of the constants.

Green and Mackinnon (1956) have recently reported, in a brief communication, the use of an ultrasonic pulse technique to determine elastic constants

by measuring the velocities of longitudinal and shear waves along the *c*-axis of single crystals. They employed a ' sing-around ' circuit as developed by Cedrone and Curran (1954) and their single crystal specimens were in the form of cylinders about 15 to 20 cm long and 2·3 cm diameter. The crystals were grown in a necked glass tube immersed in a bath of water which was frozen from the top downwards, and x-rays were employed to determine their orientation. The results give C_{33} and C_{44} directly but C_{11}, C_{12} and C_{13} were deduced from Penny's theoretical relationships. The values obtained, although less accurate, are in good agreement with those obtained by Jona and Scherrer ; the values shown in table 1 have been kindly calculated by M. Baker using Green and Mackinnon's experimental data.

Fig. 2



Log (frequency of maximum damping) as function of inverse absolute temperature (after Kneser *et al.* 1955).

The damping of mechanical vibrations in ice crystals is normally quite small but Kneser *et al.* (1955) have shown the existence of a relaxation effect at mid- and high-audio frequencies. Kneser *et al.* measured the logarithmic decrement of the torsional oscillations of single crystals of ice in the form of rods about 5 cm long and 1 cm diameter. The frequency of maximum damping as a function of temperature was found to follow the Arrhenius relation $\omega_{max} = A \exp(-\phi/kT)$, where A is a constant, ϕ is the energy of activation, k is Boltzmann's constant and T is the absolute temperature. Figure 2 shows the plot of log $(\omega_{max}/2\pi)$ against $1/T$ yielding a value for ϕ of 0·37 electron volt. In a further

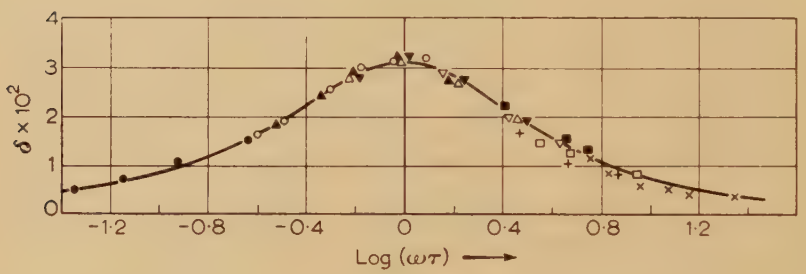
graph, fig. 3, all the results are shown to be represented by the equation

$$\delta = \delta_{\max} \cdot \frac{2\omega\tau}{(1+\omega^2\tau^2)}$$

where $\tau = (\omega_{\max})^{-1}$ is the relaxation time for maximum damping, whose value was $2{\cdot}9 \times 10^{-2}$. The Pauling (1935) model for ice provides an explanation for the existence of this relaxation in terms of a proton jump mechanism. It is interesting to note here that the activation energy concerned with the corresponding dielectric relaxation has been found to be 0·28 electron volt.

Results, as yet unpublished, similar to those of Kneser *et al.* have recently been obtained by Schiller (private communication) for various modes of vibration and for various crystallographic directions. The frequency at which maximum loss occurs and the energy of activation as found from these mechanical experiments are in close agreement with the corresponding quantities obtained in dielectric relaxation measurements.

Fig. 3



Curve representing the relation $\delta = \delta_{\max} \frac{2\omega\tau}{(1+\omega^2\tau^2)}$.

Frequency code (in Kc/s):

● = 0·69, ○ = 3·83, ▲ = 4·62, △ = 8·87, ▼ = 10·35, ▽ = 18·10, ■ = 23·87, □ = 30·6, + = 40·06, × = 80·74 (after Kneser *et al.* 1957).

I am indebted to Dr. Reiner Bass for the following theoretical analysis of the mechanical relaxation of single-crystalline ice.

It seems obvious to associate both relaxations with movements of the hydrogen atoms. In the mechanical case this may be done in two different ways. As a first possibility it can be assumed that an equilibrium exists between a large number of possible hydrogen arrangements and that this equilibrium is disturbed by a mechanical deformation of the crystal lattice. The rearrangement of the hydrogen atoms throughout the lattice then gives rise to the observed relaxation. A second possible mechanism is connected with the distribution of lattice defects such as doubly occupied and vacant bonds between neighbouring oxygen atoms. The presence of these defects was postulated by Bjerrum (1951) and

seems to be confirmed by the extensive dielectric investigation of Gränicher *et al.* (1957). Normally the probability of finding a given type of defect on a given bond would be approximately the same for all bonds. In the deformed lattice, bonds with a certain orientation would be preferred and the resulting rearrangement of the defects would cause the observed relaxation.

The different parts which are played by lattice defects in mechanism 1 (the rearrangement of hydrogen atoms throughout the lattice) and mechanism 2 (the local redistribution of the defects themselves) should be pointed out quite clearly. With mechanism 1 lattice defects can serve as ' catalysts ' in bringing about configurational changes by diffusion and their presence (in small numbers) can thus affect the relaxation time, but not the magnitude of the decrement. With mechanism 2, however, the magnitude of the decrement is proportional to the number of defects present.

Theoretical estimates of the maximum value of the decrement and its dependence on temperature and crystallographic orientation show decisively that mechanism 2 cannot be responsible for the observed relaxation. This can be seen from the following table in which the predictions for the two mechanisms are compared with the experimental results. + and − signs signify the presence or absence of a mechanical relaxation.

	Mechanism 1	Mechanism 2	Observed
Order of magnitude of decrement	10^{-1}	10^{-8}	3×10^{-2}
Temperature dependence	weak	strong	weak
Uniform dilatation			
Strain with rotational symmetry about *c*-axis, constant volume	−	+	−
Other types of deformation at constant volume	+	+	+

It would appear that the observed relaxation is due to mechanism 1 and the corresponding maximum value of the decrement has therefore been calculated in more detail. An important step is the choice of a simple but not too unrealistic model for the charge distribution in the lattice which enables the contribution of the hydrogen arrangement to the potential energy to be calculated. As a starting point the tetrahedral point charge model of Bjerrum (1951) for the H_2O molecule is used. To simplify this model further, each pair of charges of opposite sign occupying one hydrogen bond in the ice crystal is replaced by a point dipole situated in the centre of that bond. Every such dipole can assume either of two opposite directions along the bond, but of the four dipoles surrounding any one oxygen atom two always point towards the latter and two point

away from it. Interaction between adjacent hydrogen bonds only is considered and a dielectric constant ϵ is formally introduced for this interaction. The use of a dielectric constant $\epsilon = 3$ was suggested by Pitzer and Pollissar (1956) in order to account for changes of the electronic charge distribution of the free H_2O molecule under the influence of neighbouring molecules in the crystal lattice. It has a qualitative rather than a quantitative significance and can only be regarded as a crude approximation in the absence of a detailed knowledge of the charge distribution.

For the above model the potential energy of the lattice is independent of the hydrogen arrangement in the absence of mechanical strain. The same is true for the deformed lattice, as long as the strain tensor has rotational symmetry with respect to the *c*-axis. In more general cases, changes of the energy and entropy of the crystal can be expressed in terms of the strain tensor and a tensorial ordering parameter which characterizes the hydrogen arrangement. The resulting functions may then be used to calculate the mechanical dispersion and absorption. The following expression is obtained for the maximum value of the decrement in the above-mentioned case of a torsional vibration of a cylindrical specimen cut parallel to the *c*-axis.

$$\delta_{\max} = \frac{\pi}{2}\frac{\Delta C_{44}}{C_{44}} = \left(\frac{352}{9}\frac{\mu^2}{\epsilon V_0}\right)^2 \frac{\pi}{V_0 C_{44} kT}$$

where C_{44} = elastic constant ($= 3{\cdot}1 \times 10^{10}$ c.g.s. units), ΔC_{44} = dispersion of elastic constant C_{44}, μ = dipole moment of hydrogen bond ($= 0{\cdot}64 \times 10^{-18}$ c.g.s. units), and V_0 = volume of unit cell ($= 1{\cdot}3 \times 10^{-22}$ cm^3). At a temperature of about -20°C this yields

$$\delta_{\max} \begin{cases} = 3{\cdot}3 \times 10^{-1} \text{ for } \epsilon = 1 \\ = 3{\cdot}6 \times 10^{-2} \text{ for } \epsilon = 3 \end{cases}$$

compared with an experimental value of $\delta_{\max} = 3{\cdot}0 \times 10^{-2}$. The surprisingly good agreement between theory and experiment for a dielectric constant $\epsilon = 3$ may be regarded as accidental ; it seems likely, however, that an improved model for the charge distribution in the lattice would lead to a similar result.

It should be noted that the above theory does not imply any specific process by which the assumed configurational changes occur. Thus no information concerning the magnitude of the relaxation time or an energy of activation can be deduced. It would appear that the rate-determining process in the mechanical case as well as in the dielectric one is the diffusion of lattice defects (Bjerrum 1951, Gränicher *et al.* 1957).

It is of relevant significance to mention here that the mechanism of lattice defects gives rise to a second dispersion region in the dielectric loss factor (tan δ) at low frequencies, additional to the Debye maximum at high frequencies. This has been shown experimentally by Gränicert

et al. (1954) using polycrystalline ice in which the number of lattice defects was artificially increased by the addition of hydrofluoric acid. A similar low frequency relaxation was obtained in the mechanical case by Jellinek and Brill (1956) with polycrystalline ice. They obtained mechanical relaxation times of the order of 5 minutes or more ; this relaxation is not apparent in single crystals.

References

Barnes, W. H., 1935, *Proc. roy. Soc. Can.*, 111(3), **29,** 53.
Bass, R., Rossberg, D., and Ziegler, G., 1957, *Z. Phys.*, **149,** 199.
Bernal, J. D., and Fowler, R. H., 1933, *J. chem. Phys.*, **1,** 515.
Bjerrum, N., 1951, *Dan. Mat. Fys. Medd.*, **27,** No. 1.
Cedrone, N. P., and Curran, D. R., 1954, *J. Acoustical Soc. Amer.*, **26,** 9636.
Gränicher, H., Jaccard, C., Scherrer, P., and Steinemann, A., 1957, *Disc. Faraday Soc.*, No. 23, 50.
Gränicher, H., Scherrer, P., and Steinemann, A., 1954, *Helv. phys. acta*, **27,** 217.
Green, R. E., and Mackinnon, L., 1956, *J. Acoustical Soc. Amer.*, **28,** 1292.
Huggins, M. L., 1936, *J. Amer. chem. Soc.*, **58,** 694.
Jellinek, H. H. G., and Brill, R., 1956, *J. appl. Phys.*, **27,** 1198.
Jona, F., and Scherrer, P., 1952, *Helv. phys. acta*, **25,** 35.
Kneser, H. O., Magun, S., and Ziegler, G., 1955, *Naturwissenschaften*, **15,** 437.
Northwood, T. D., 1947, *Canad. J. Res.*, **25,** 88.
Pauling, L., 1935, *J. Amer. chem. Soc.*, **57,** 2680.
Penny, A. H. A., 1948, *Proc. Camb. phil. Soc.*, **44,** 423.
Pitzer, K. S., and Polissar, J., 1956, *J. phys. Chem.*, **60,** 1140.
Voigt, W., *Lehrbuch der Kristallphysik*, 1928 (Leipzig : Teubner).

Thermal Conductivities and Expansion Coefficients of Water and Ice

By R. W. Powell
National Physical Laboratory, Teddington

§ 1. Introduction

In this article the state of knowledge regarding two properties of water and ice, thermal conductivity and thermal expansion, will be reviewed, and attempts made to determine their most probable values and the directions in which further work appears desirable. Data for the heavy isotopic forms will be included when possible.

Water has naturally been one of the substances most widely studied, and, as the older investigations will have been considered when the International Critical Tables were in course of preparation, it is proposed to deal mainly with post-I.C.T. work.

§ 2. The Thermal Conductivity of Water : Range 0° to 90°c

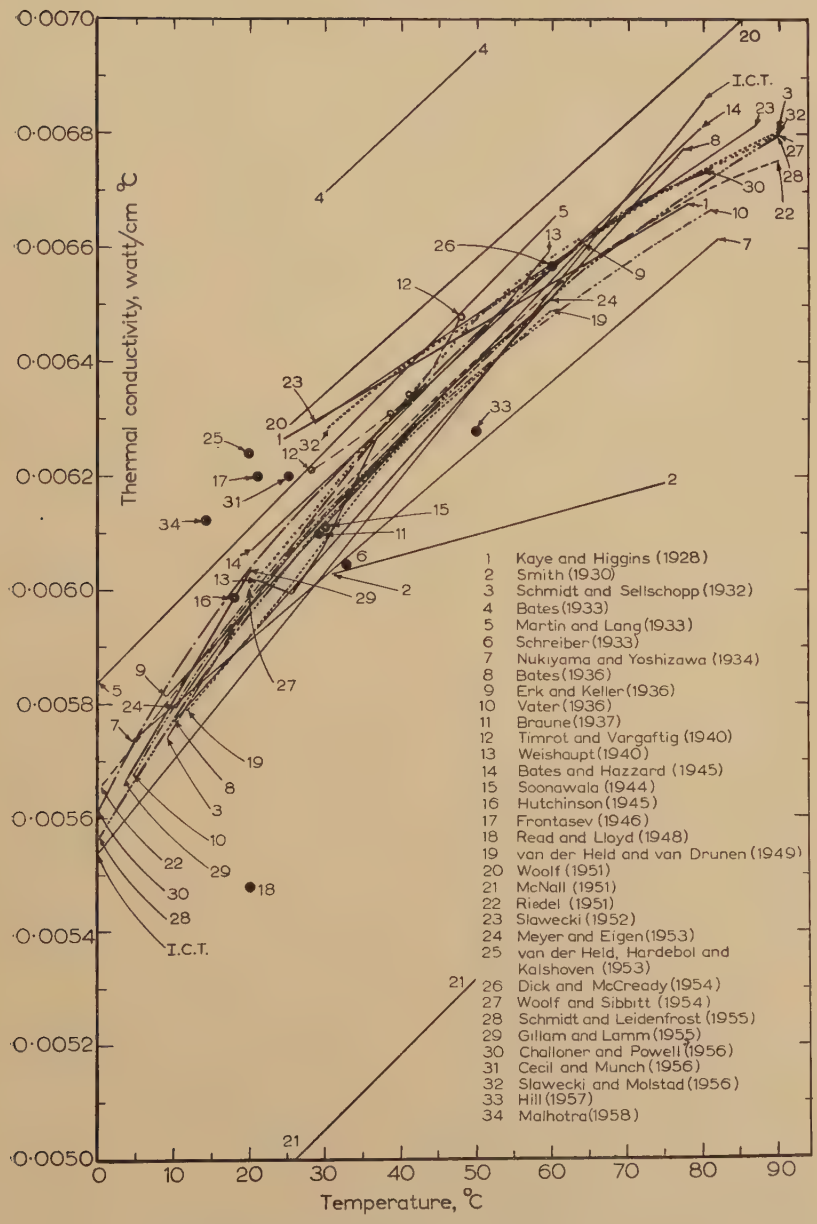
Thermal conductivity is a property which is not readily measurable to a high order of accuracy, and for which but few determinations have been made to better than 1%. In general, the main difficulty is the avoidance of heat leakage to or from the specimen. Such leakage becomes relatively more serious for materials of low thermal conductivity, and the thermal conductivity of water, despite being two to five times greater than that of most other liquids, is of the order of 1/650th of that of copper. With poor conducting solid materials, some compensation can be obtained by increasing the temperature difference and the area through which the measured heat flow is established, but with liquids, there is the added complication of convection, and this can become a source of error under these conditions. Appropriate reduction in the thickness of the liquid layer is required to prevent the incidence of convection, but the accuracy with which the thickness of the layer can be measured then tends to become a limiting factor.

In view of these general considerations, it is not surprising that considerable differences and error are apparent in many of the earlier determinations, and even in some of more recent origin.

Barratt and Nettleton (1929 a) were justifiably cautious when presenting the results for the thermal conductivities of liquids, and endeavoured to grade the reliability of the various workers into four categories, A to D. Grade A indicated a pronounced consensus of opinion, and their values for the thermal conductivity of water were allocated to this grade. Over the range 0° to 80°c they gave a linear relationship for the variation of the thermal conductivity, K_t, with temperature, t°c.

$$K_t = K_{20}[1 + \alpha(t - 20)].$$

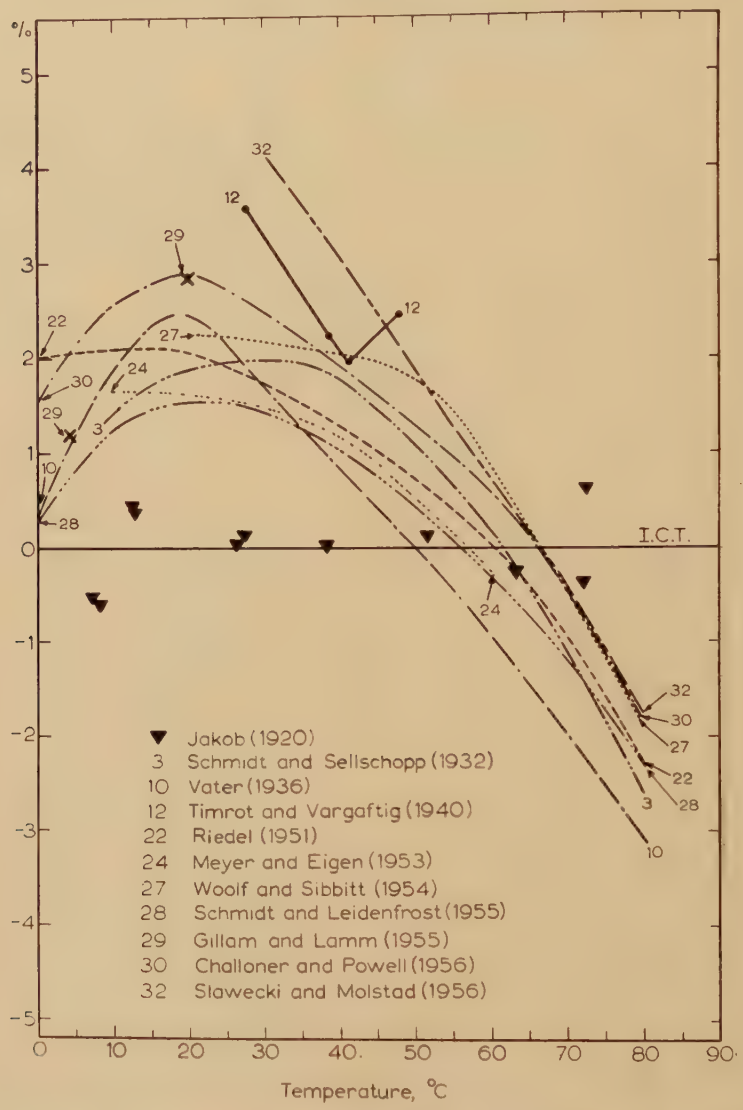
Fig. 1



Thermal conductivity of water, 0° to 90°C.

For K_{20} they proposed a value† of 0·00587 watt/cm °C, with a probable range of 0·00580 to 0·00595, that is, they allowed for an uncertainty of about ± 1·3% in this value. The temperature coefficient, α, is 0·00281.

Fig. 2



Percentage departure of selected values from I.C.T. values for water.

Barratt and Nettleton state that their values were mainly based on the work of Weber (1886), Jäger (1890), Milner and Chattock (1899), Lees

† watt/cm °C = J cm/cm² sec °C = 4.186 cal cm/cm² sec °C = 0·01163 kcal/m h °C = 0·0173 B.t.u. ft/ft² h °F.

(1898), Jakob (1920) and Bridgman (1923), but also refer to nine other workers. In point of fact, their line agrees almost exactly with that which Jakob gave as the best straight line through his own experimental points, namely

$$K_t = 0{\cdot}001325 \quad (1 + 0{\cdot}002984t)$$

where K_t is now expressed in cal cm/cm² sec °C.

The I.C.T.-line is reproduced in fig. 1, and, in the same figure an attempt has been made to include all subsequent results for the thermal conductivity of water over the temperature range 0° to 90°C. Owing to the number of such investigations the figure suffers from overcrowding. Nevertheless, it serves to show the general character of these results, and some important details will be considered subsequently.

The results of about six workers depart considerably, and can fairly safely be ignored, but those of the majority lie within about 2·5% of a mean curve.

The I.C.T.-line will be seen to pass through this region of maximum density at a temperature of about 60°C, but to be definitely lower at low temperatures and higher at high temperatures. Some of the difference appears to result from a marked curvature that is now apparent in many of these results, particularly in those of workers who made their investigations over a wide temperature range. The amount of curvature is relatively small except below 20°C and above 60°C, which explains why many workers fitted a straight line to their results. Also the thermal conductivities of most liquids had been found to vary linearly with temperature.

In fig. 2 an alternative method of plotting has been adopted for certain of the results, the percentage departure from the I.C.T.-values being plotted against temperature. In this figure Jakob's actual experimental values have been included. They show a scatter of about $\pm 0{\cdot}6\%$ from the I.C.T.-line. If the highest-temperature point is ignored, the remainder are seen to have a slight amount of curvature of similar type.

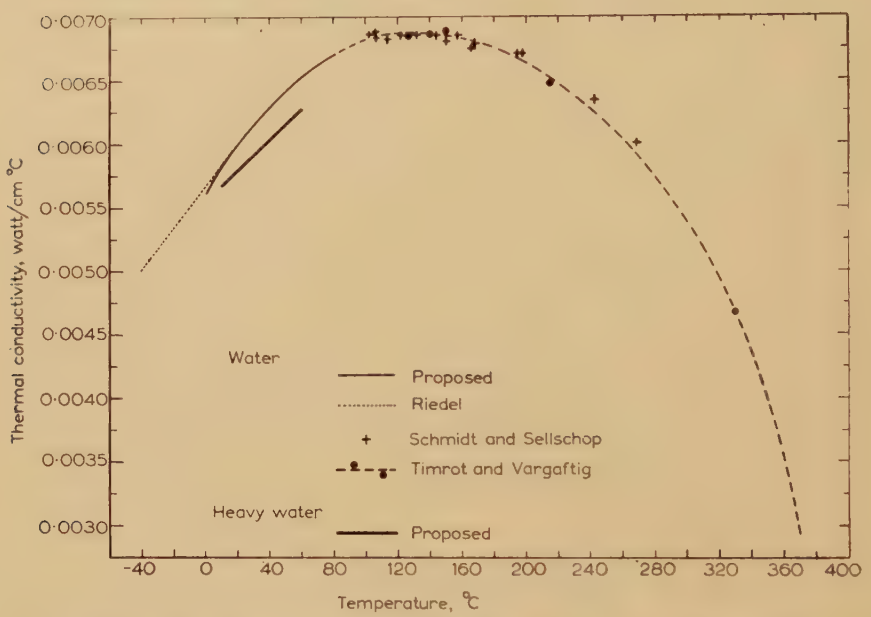
Schmidt and Sellschopp (1932), however, were the first workers definitely to obtain a curve rather than a straight line. Their work was distinctive in that by conducting their experiments in a closed stainless-steel pressure vessel, they were able to cover the temperature range 9° to 269°C. These complete results are plotted in fig. 3, and are seen to attain a maximum value at a temperature of about 130°C. This most striking result is in harmony with their values for the range 9° to 90°C, which are well satisfied by a continuation of the curve.

Timrot and Vargaftig (1940), are the only other workers to have made determinations on water at temperatures above 100°C. Their values are included in fig. 3 and are seen to be in general agreement with those of Schmidt and Sellschopp. More detailed consideration of this high-temperature range will be deferred until the lower temperature regime has been discussed.

For their determinations, Schmidt and Sellschopp used an apparatus of the concentric-cylinder type with the test liquid in an annular space only about 0·5 mm in width. Temperature differences of only about 1°C ensured freedom from convection, and the work appears to have been conducted with care.

Much more recently, Schmidt and Leidenfrost (1955) have used a similar apparatus, but one with a water film of about twice the thickness,

Fig. 3



Thermal conductivity of water and heavy water : proposed values.

and have obtained values for the range 20° to 83·5°C (extrapolated range, 0° to 100°C), which they state to have one-fifth the scatter of those of Schmidt and Sellschopp. The two mean curves agree closely, the greatest difference being in the region of 40°C, where Schmidt and Leidenfrost's values are some 0·8% lower.

Other workers who used the cylindrical type of apparatus were Woolf (1951), Woolf and Sibbitt (1954), Slawecki (1953) and Slawecki and Molstad (1956). Woolf's values as reported by Sakiadis and Coates (1954) are displaced above the curve given later by Woolf and Sibbitt, but their experimental points depart from their curve by up to 3%. The values due to the foregoing joint authors are also included in fig. 2.

Vater (1936) used a form of the plate method, where the water was held as a horizontal film about 1 mm thick between two rods of copper and surrounding guard cylinders, the heat flow being downwards through the system. Vater obtained somewhat different thermal conductivity

values according to whether the energy was determined from the electrical energy supplied, suitably corrected, or in terms of the gradient established in the copper rods. In view of uncertainties connected with the thermal conductivity assumed for these rods, it has been decided only to include the results from the first method in figs. 1 and 2.

Of the other workers who covered the full range of temperature and whose results are also included in fig. 2, Challoner and Powell (1956) used a more conventional form of the plate method, but with full thermal guarding and made determinations on films of 2 and 3 mm thickness, whilst Riedel (1940, 1951 a, 1954) has at various times made measurements with forms of both plate and cylindrical apparatus, as well as one in which the heat flows through a layer of liquid retained between concentric spheres. Agreement to within about 1% was obtained by Riedel for a wide range of liquids and temperatures, as shown by the results given in table 1.

Table 1. Values of Thermal Conductivity (watt/cm °C) obtained by Riedel in Three Types of Apparatus

Liquid	Temperature °C	Type of apparatus		
		Plate	Cylindrical	Spherical
Water	20	0·00600	0·00599	0·00595
Water	80	0·00670	0·00664	—
Acetone	20	$0{\cdot}00160_5$	$0{\cdot}00161_5$	$0{\cdot}00159_5$
n-Butyl alcohol	20	$0{\cdot}00153_5$	$0{\cdot}00153_5$	$0{\cdot}00152_5$
n-Butyl alcohol	80	$0{\cdot}00140_5$	0·00143	—
Benzene	20	$0{\cdot}00147_5$	$0{\cdot}00147_5$	$0{\cdot}00145_5$
Toluene	−80	$0{\cdot}00159_5$	$0{\cdot}00159_5$	—
Toluene	20	0·00135	0·00136	0·00135
Toluene	80	$0{\cdot}00117_5$	$0{\cdot}00118_5$	—
Carbon tetrachloride	20	$0{\cdot}00103_5$	$0{\cdot}00103_5$	$0{\cdot}00102_5$

This is an outstanding achievement and strongly supports the validity of the many determinations which Riedel has made both on pure liquids and on solutions. In another paper, Riedel (1949), a value of 0·00672 had been given for water at a temperature of 80°C, but the change is small and values at 60°C and below were unaffected. The following equation, converted to watt/cm °C units, was proposed by Riedel for the range 0° to 80°C:

$$K_t = 0{\cdot}00565 \quad (1 + 0{\cdot}00319t - 0{\cdot}0000103t^2).$$

The mean curves of these last mentioned workers are seen to agree to well within 1% over the whole temperature range. The results of Challoner and Powell and of Riedel (1951 b) for glycerine, ethyl alcohol and toluene also agree to within about 1·5% over their common temperature range of 0° to 70°C approximately.

Meyer and Eigen (1953) made measurements on a column of water 5 cm high and 3 cm in diameter, and heated from above to avoid convection. For the range 10° to 60°c their results are in general agreement with those already mentioned, and from 1·7 to 0·7% below those of Challoner and Powell. This is noteworthy in that others who have made use of thick layers, Bates (1933, 1936), Bates and Hazzard (1945) and Malhotra (1957) have obtained less consistent thermal conductivity values. Furthermore, both Challoner and Powell, and Meyer and Eigen have made determinations on heavy water, which are to be considered later.

It remains to mention methods of the hot-wire type. By using a taut electrically heated wire it is easy to ensure that the measured energy is little affected by end losses, but in the case of the usual steady-state version, the surrounding liquid layer needs to be kept small to avoid convection. Consequent dimensional uncertainties can influence the accuracy. Timrot and Vargaftig employed a method of this type for their determinations of the thermal conductivity of water and steam to high temperatures and pressures. Under saturation pressure Timrot and Vargaftig only published four values in the range now being considered. These values have been plotted in figs. 1 and 2, and are seen to lie on a curve of opposite sign to that obtained by other workers. They themselves appear to give little weight to these values, for, when tabulating values for the thermal conductivity of water under saturation pressure at intervals of 10°c, they give values in agreement with those of Schmidt and Sellschopp for the range 0° to 90°c. These tabulated values have therefore been omitted from figs. 1 and 2.

Weishaupt (1940), van der Held and van Drunen (1949), van der Held *et al.* (1953), Gillam and Lamm (1955) and Hill (1957) used variable state versions of the hot-wire method. Observations are made of the temperature–time curve for the wire when immersed in the liquid. The more recent experimenters have sought to avoid any restrictions on the thickness of the liquid layer by so limiting the duration of the measurements that convection currents are not formed. Gillam and Lamm required a time of the order of 20 seconds for their determination, which proved satisfactory for water at 4° and 20°c but not higher. These two values are seen to support the increased temperature coefficient which is evident for this range in four other curves of fig. 2.

Hill was primarily concerned with the development of a method applicable to transient conditions, and made a few trials on water, glycerol and medicinal paraffin. Although the duration of the experiment was only a few hundredths of a second and temperature increases of the order of 30 to 60°c were involved, his values were within a few per cent of accepted values for these liquids. In making this comparison a temperature of 50°c is quoted, but there would seem to be some uncertainty regarding the effective temperature in these experiments. His reported observations for water covered a range of 10%.

This completes the review of the main results plotted in fig. 1. Of those that are also included in fig. 2, the percentage departures from the I.C.T.–values for the five workers who covered the full range of temperature are tabulated below. A mean deviation is then derived and a new set of values calculated.

It will be seen that all the tabulated values for the range 10° to 80°C agree with the mean value to within 1%, and, in view of the variety of experimental methods which are included, it is felt that the values of thermal conductivity given in the last line of the table can be recommended.

At 0°C the value attributed to Riedel is 1·1% greater than the mean. This is rather disturbing, since Riedel is one of the two workers whose actual measurements have extended to 0°C. Furthermore, from observations to be considered in § 3, Riedel later raised his 0°C value from

Table 2. Comparison of Selected Values with I.C.T.-Values for the Thermal Conductivity of Water

Observer	Temperature (°C)								
	0	10	20	30	40	50	60	70	80
Percentage departure from I.C.T.-value									
Vater	(0·3)	1·9	$2·4_5$	1·7	0·8	0·0	−0·7	$-1·9_5$	−3·1
Riedel	2·0	2·1	$2·0_5$	$1·7_5$	1·3	$0·7_5$	$0·0_5$	−0·9	$-2·2_5$
Schmidt and Sellschopp	(0·3)	1·4	1·9	2·0	1·8	1·1	0·2	−1·1	−2·6
Schmidt and Leidenfrost	(0·3)	1·2	$1·5_5$	$1·4_5$	1·0	$0·4_5$	−0·3	−1·2	−2·3
Challoner and Powell	1·5	$2·5_5$	2·9	2·5	1·9	1·3	0·6	−0·4	−1·8
Average	0·9	$1·8_3$	$2·1_7$	$1·8_8$	$1·3_6$	$0·7_2$	$-0·0_3$	$-1·1_1$	−2·4
10^5 Thermal conductivity, watt/cm °C									
I.C.T.-value	554	$570·_5$	587	$603·_4$	620	$636·_3$	653	$669·_5$	686
Proposed value	560†	581	600	$614·_5$	$628·_5$	641	653	662	$669·_5$

() extrapolated value : † using weighted mean.

0·486 to 0·487 kcal/m h °C (0·00565 to 0·00566 watt/cm °C). It has therefore been decided to include Riedel's two values and to give double weight to the value of Challoner and Powell: that is, to give double weight to the determinations made closest to 0°C. In this way the value of 0·00560 watt/cm °C is obtained. More work appears desirable in the range 0° to 20°C. This receives further support in § 3.

§ 3. The Thermal Conductivity of Supercooled Water

Since water, in the absence of ice-promoting nuclei, can be cooled some 40°C below the normal freezing point, a knowledge of the thermal conductivity of supercooled water might occasionally be required. Information for this region is, however, rather scarce. Powell (1958)

has made reference to what appears to be the only direct determination of the thermal conductivity of water in the supercooled state. At a mean temperature of $-2°$c, and with the sample entirely below the normal freezing point there was stated to be no marked change in the thermal conductivity. Incidentally, a similar result had been reported earlier by Challoner and Powell for a sample of heavy water when supercooled by about the same amount. In neither case was there any definite evidence for any departure from the normal curve of thermal conductivity against temperature on entering the supercooled region.

Riedel (1950) has obtained a similar result from indirect measurements. The thermal conductivities of aqueous salt solutions were determined for various concentrations at temperatures of 20°, 1·5°, $-10°$, $-20°$, $-30°$ and $-40°$c. The salts studied were KCl to $-10°$c, NaCl to $-20°$c, $MgCl_2$ to $-30°$c and $CaCl_2$ to $-40°$c. For each temperature the thermal conductivity of water was derived by plotting thermal conductivity against salt concentration and extrapolating to zero salt concentration. The values which Riedel obtained, expressed in kcal m h °c are given in table 3.

Table 3. Thermal Conductivity of Water as derived by Riedel from Determinations on Aqueous Salt Solutions

Temperature (°c)	20	10	0	−10	−20	−30	−40
Thermal conductivity (kcal m h °c)	0·515	0·501	0·487	0·473	0·459	0·445	0·431
100 × Thermal conductivity (watt/cm °c)	0·599	$0·582_5$	0·566	0·550	0·534	$0·517_5$	0·501

The method was certainly justified at the two temperatures above 0°c, where the thermal conductivity of water was already known, but at lower temperatures, where the results were relatively few and somewhat scattered, the amount of extrapolation becomes large, and the values less certain. Riedel's values for the range 20° to $-40°$c obtained in this way are shown as a dotted line in fig. 3. These also suggest that no marked change in thermal conductivity occurs on passing to the supercooled state. It was on the basis of these results that Riedel made the previously mentioned increase in the 0°c value from 0·486 to 0·487 kcal/m h °c. There seems, however, little justification for this change, and, indeed the author reverted to 0·486 in a later paper, Riedel (1951 b). From an examination of Riedel's results for aqueous salts it would seem that he might equally well have retained the original 0°c value and extrapolated the points for lower temperatures to a continuation of this slightly lower curve. However, any change produced in this way would appear to be small compared with the difference between

Riedel's line for supercooled water and that indicated by the continuation of the present proposed curve into this region. From fig. 3 it can be appreciated that this difference becomes serious as the temperature is reduced, and exceeds any uncertainty involved in Riedel's extrapolation. Another rather disturbing aspect is also revealed. At normal temperatures the thermal conductivity of aqueous salt solutions decreases as the salt concentration is increased, and it is to be expected that the same would hold for lower temperatures. For a calcium chloride brine containing 30% by weight of the salt, Riedel gives at -40°C a thermal conductivity value of 0·410 kcal/m h °C (0·00477 watt/cm °C) which is almost the same value as the present proposed curve for water would indicate if extrapolated linearly from 10° through 0° to -40°C. It follows that a continuation of the proposed curve to -40°C would lead to values that are even lower than Riedel's observed value for a highly concentrated salt at that temperature.

The foregoing discrepancy is a serious one. The acceptance of Riedel's brine results suggests that a continuation of the proposed curve in the way considered is unlikely. Yet Riedel found a smooth continuation into the supercooling region, so the doubts that have now arisen extend up to the 0° to 20°C range. Too little weight may have been given to Riedel's data in the analysis of the previous section. Meyer and Eigen's results lend some support to this view, but, unfortunately, their curve stops short at 10°C.

There is need for further determinations to be made on water at temperatures below 20°C and as far as possible into the supercooled region.

§ 4. Thermal Conductivity of Water: Range 90° to 370°C

As already mentioned, only Schmidt and Sellschopp and Timrot and Vargaftig have published results for the thermal conductivity of water at temperatures above 100°C. The results of both pairs of workers, obtained at the saturation vapour pressure are plotted in fig. 3. For the range 100° to 200°C they are seen to be in good agreement and to indicate a broad maximum. The curve shown as a broken line represents the values that Timrot and Vargaftig have tabulated at intervals of 10°C for the thermal conductivity of water under saturation pressure, and can be accepted as representative of the present state of knowledge for water above its normal boiling point.

The line lies just over 1% below Schmidt and Sellschopp's experimental points. This is a remarkably good agreement for such extreme conditions, but, as previously mentioned, some adjustment appears to have been made at lower temperatures in favour of the data of Schmidt and Sellschopp. The position will be strengthened when a further set of measurements is made in this upper temperature range. The successful avoidance of convection troubles must become increasingly difficult as the critical region is approached.

§ 5. Influence of Pressure on the Thermal Conductivity of Water

Timrot and Vargaftig appeared to be mainly interested in studying the influence of high pressures on the thermal conductivity. From the results plotted in fig. 3, together with three determinations at 300 atmospheres pressure and four at 400 atmospheres, they published a table of values at 10°c intervals, of which selected values are given in table 4. In this table, the bracketted values are those suggested in table 2 as probable values for the lower temperature range.

For the higher temperatures and pressures the values of Timrot and Vargaftig should be adopted for the present.

Table 4. Timrot and Vargaftig's Data Showing the Effect of Pressure on the Thermal Conductivity of Water

Temperature (°c)	Thermal conductivity, watt/cm °c				
	Saturation pressure	100 Atm pressure	200 Atm pressure	300 Atm pressure	400 Atm pressure
0	0·00552 (0·00560)†	0·00555	0·00558	0·00563	0·00568
40	0·00634 ($0·00628_5$)†	$0·00638_5$	0·00644	0·00650	0·00656
80	$0·00674_5$ ($0·00669_5$)†	0·00680	0·00685	0·00691	$0·00696_5$
100	0·00683	0·00690	0·00695	0·00701	0·00707
150	0·00684	0·00692	0·00699	$0·00707_5$	$0·00715_5$
200	0·00663	0·00672	$0·00679_5$	0·00690	0·00700
250	0·00618	0·00625	$0·00636_5$	0·00648	0·00660
300	0·00540	0·00542	0·00561	$0·00580_5$	0·00597
350	0·00400	—	$0·00417_5$	$0·00459_5$	0·00494
370	0·00293	—	—	0·00379	0·00437

† These figures are from table 2.

Bridgman (1923) is responsible for the only other set of measurements that have been reported for water at pressures above normal. His method involved radial heat flow, but has been criticized by Riedel (1951 a) for inadequate allowance for end losses. Bridgman's determinations were made at temperatures of 30° and 75°c and to much higher pressures than those of Timrot and Vargaftig. At 30°c, Bridgman's results indicate an increase in thermal conductivity of about 0·6% for a pressure increase of from 1 to 100 atmospheres, whereas Timrot and Vargaftig found an increase of 0·8%. At the higher temperature a comparable difference is to be noted between the results of these workers.

§ 6. The Thermal Conductivity of Heavy Water

Three groups of workers have reported determinations of the thermal conductivity of heavy water, and they all agree that the thermal conductivity of heavy is about 3% lower than that of normal water.

Bonilla and Wang (1951) for the range 15° to 60°C reported the thermal conductivity of heavy water to average 97·3% of that of water. Meyer and Eigen obtained values for a sample consisting of 95% D_2O + 5% H_2O which were about 3% less than their own values for water. Challoner and Powell studied a sample stated to contain 99·95% of D_2O, and from their tabulated values the thermal conductivity is seen to vary from about 1·3% less than their value for water at 0°C to 5% less at 80°C. The lowest temperature reached was 1·9°C, for which the sample was entirely in the supercooled state. There was again no marked deviation of this point from the general trend.

Table 5. The Thermal Conductivity of Heavy Water

$10^5 \times$ Thermal conductivity, watt/cm °C						
Observer	Temperature (°C)					
	10	20	30	40	50	60
Meyer and Eigen	561·$_6$	577·$_6$	593·$_5$	607	620	632·$_5$
Challoner and Powell	569	579	589·$_5$	600	610	620
Average	565·$_5$	578·$_5$	591·$_5$	603·$_5$	615	626
Percentage of value proposed for water						
	97·3	96·4	96·2$_5$	96·0	95·9$_5$	95·9

In table 5, two sets of values have been tabulated for their common temperature range. Those of Meyer and Eigen have been read from their published curve and converted to 100% D_2O. Average values which are also included are seen to agree with the individual values to within about 1%. The last line of the table shows these average values expressed as percentages of the proposed values for water given in table 2.

For the range 10° to 60°C the mean value for the thermal conductivity of heavy water is 96·3% of the proposed value for normal water. This is 1% less than Bonilla and Wang's value for much the same temperature range.

These average values are represented by the thick line in fig. 3. Howieson (1957) gives a curve to 290°C. The extrapolated portion above 82°C is from 5 to 4% below the curve of fig. 3 for water.

§ 7. The Thermal Conductivity of Ice

The International Critical Tables contain two values for the thermal conductivity of ice which differ by 5%. At 0°c Schofield and Hall (1927) selected a value of 0·022 watt/cm °c, whereas Van Dusen (1929) gave a value of 0·0209 watt/cm °c. The latter suggested the linear relation

$$K = 0{\cdot}0209 \quad (1 - 0{\cdot}0017t)$$

for values of temperature, t, ranging from 0° to −170°c. It appears that this equation approximately represents the experimental results of Lees (1905), an author not mentioned by Schofield and Hall.

Barratt and Nettleton (1929 b), when considering the thermal conductivities of non-cubic crystalline compounds, remark that the thermal conductivity of single crystals of ice has not been studied: indirect evidence, especially from orientation of crystals, indicates A to be less than C, but can give no estimate of A/C, where A and C are the thermal conductivities measured along the principal crystal directions.

Lees employed a method involving radial heat flow, the specimen being formed by filling a brass tube with air-free distilled water and allowing the sample to freeze from below by inserting the base of the tube in liquid air. Also mounted in this tube and parallel to the axis were two glass tubes which became frozen into the ice at a known distance apart. Each tube was fitted with platinum wire heaters and resistance thermometers. The whole system was lowered to liquid-air temperature, and measurements were made as the temperature slowly returned to normal. These involved supplying heat alternately to the heaters in the two tubes and using the platinum thermometers to determine the temperatures at two known positions. Lees made the assumption that the brass tube was an isothermal surface, and presented a detailed analysis for evaluating the thermal conductivity of the contained solid. Ice was one of eight substances examined in this way by Lees. His experimental results for the range −182° to −16°c are plotted in fig. 4. The line given by Van Dusen is also reproduced, and will be seen to be well satisfied by Lees' results for all but the lowest portion of the temperature range.

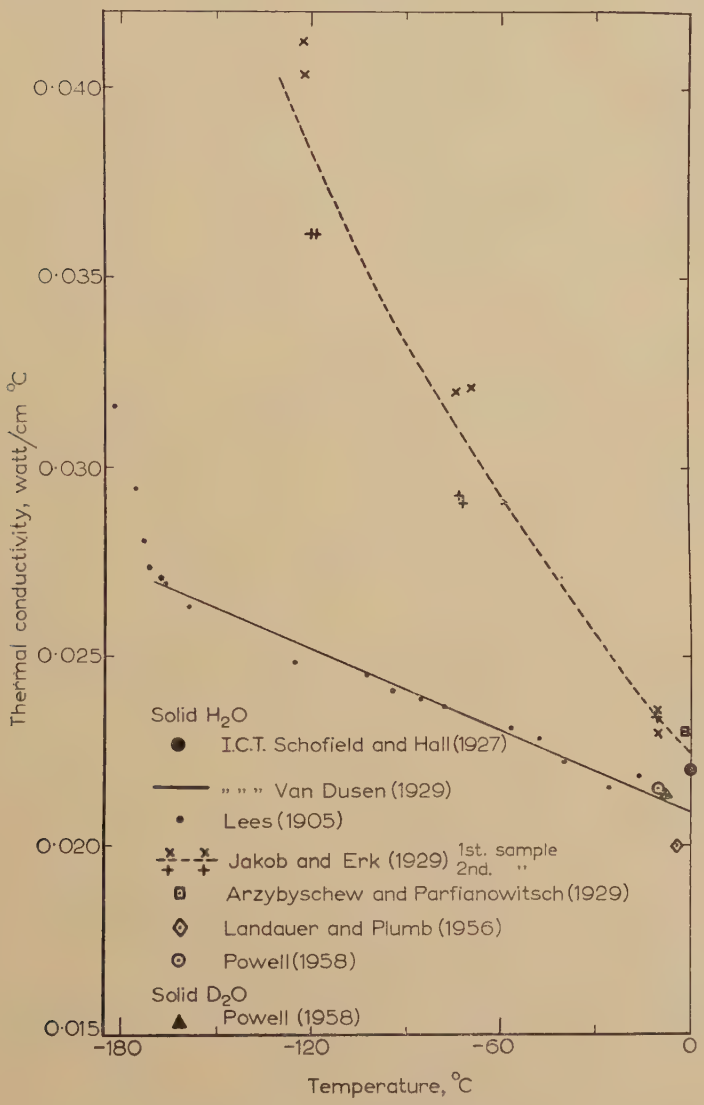
About the time that the International Critical Tables were published the next two determinations of the thermal conductivity of ice appeared.

Arzybyschew and Parfianowitsch (1929) derived a value of 0·0230 ± 0·003 watt/cm °c at an unspecified temperature close to 0°c. They allowed an ice layer to form on a cooled copper plate, and derived the thermal conductivity of the ice from observations of the variation of temperature with time as recorded by a thermocouple located at a point in the overlying liquid.

Jakob and Erk (1929), at temperatures of about −10°, −70°, and −120°c, made determinations on discs of ice, 11·7 cm in diameter retained between two copper discs, the upper one being heated. In their first experiments the temperature drop established across the sample was determined from temperature observations made with thermocouples

attached to the two copper discs. These experiments gave values which were much too low and decreased with decrease in mean temperature. The measured temperature differences were found to be too great due to

Fig. 4



Thermal conductivity of ice

the inclusion of temperature discontinuities at the two ice–copper interfaces. Their final results, which are plotted in fig. 4 were obtained, when the thermocouples were embedded in thicker ice discs at known positions.

For discs of respectively 17·0 and 16·5 mm thickness these temperature measurements showed that the isotherms within the ice were curved, suggesting that the contact was poorer at the edges than at the centre of the discs. The method of treating the results was modified to allow for these observed conditions, but the heat flow in the ice was clearly somewhat distorted, and the values can hardly be regarded as entirely satisfactory. At −120°c departures of about 6% are to be observed from the smooth curve drawn through the results for the two discs.

None of the samples so far mentioned has been examined crystallographically, so there is always a possibility that some of the differences in the results may be due to differences in the orientation of the samples with reference to the direction of heat flow. It is, however, unlikely that the large differences between the results of Lees and of Jakob and Erk can be explained in this way.

The next reference to work on the thermal conductivity of ice comes from Russia, where Shuleikin *et al.* (1931) used a variable-state method to study the influence of entrained gas on the thermal conductivity of ice. The actual method was a modification of one due to Malmgren, but they appear to have experienced some difficulty, as, for ice of maximum density and containing no gas, they adjusted their values to agree with the value obtained by Arzybyschew and Parfianowitsch. Their work cannot therefore be regarded as making any independent contribution to knowledge so far as the thermal conductivity of air-free ice is concerned. Mineral water containing carbon dioxide gas was used to produce ice of high gas content. Both the density and thermal conductivity of the ice were found to be linear functions of the gas content. The maximum gas content obtainable was 0·147 g cm^3, for which they obtained a reduction in ice density of 12·7% and in thermal conductivity of about 30%.

Vlassov and Uspenski (1931) employed a similar method at about −13°c to study the thermal conductivity of ice when subjected to hydrostatic pressures of up to 100 atmospheres. They reported some surprisingly high values for porous ice of large carbon-dioxide content. Thermal conductivities of nearly four times the normal value were obtained at pressures of 50 atmospheres and more, and these high values tended to persist after the pressure had been reduced. On the other hand, similar tests on gas-free ice of maximum density gave a fall in thermal conductivity with increase in pressure, values 23, 33 and 35% below normal being obtained at pressures of 50, 75 and 100 atmospheres respectively.

Landauer and Plumb (1956) were the first to make thermal conductivity determinations on single crystals of ice. They have described some comparative measurements which were made at about −4°c in two identical plate apparatuses on ice single crystals measuring approximately 4·5 × 4·5 × 1·3 cm, and having the heat flow parallel to the *c*-axis in one apparatus and perpendicular to it in the other. The samples studied included

laboratory-grown single crystals of ice, glacial monocrystals, commercial ice and glass. The surfaces of the samples were milled and lapped, and liquid films or silicone grease were used to improve the thermal contacts between the ice and the copper hot and cold plates.

The authors state that their absolute values for the thermal conductivity of ice varied from about 0·016 to 0·020 watt/cm °C, and the upper value has been plotted in fig. 4.

The average of all results indicated the thermal conductivity to be about 5% greater parallel to the *c*-axis than normal to this direction. The accuracy when determined by tests made on glass and identical ice specimens was about 3%. The conclusion was drawn that, if a difference in thermal conductivity exists for the different crystal directions, it is less than 8%. More accurate experiments will be necessary to specify the anisotropy with greater precision.

For the various types of ice examined by Landauer and Plumb no definite differences were found.

The validity of a suggestion made by Lliboutry (1955), that preferred growth of ice with the *c*-axis in the direction of freezing could be accounted for by its anisotropic conductivity is considered improbable. Indeed, the further suggestion is made that there is now evidence indicating that lake ice does not have a strong preferred direction of growth.

Powell has reported that the guarded hot-plate apparatus used by Challoner and Powell for water has been used for a few preliminary observations on water and heavy water in the solid phase. On slowly cooling water, freezing occurred at a temperature of about −2·4°C, and this was accompanied by a marked reduction in the temperature difference across the sample, but the value first obtained for the thermal conductivity of ice was far too low. This low value could result from the presence of an interfacial resistance of the type noted by Jakob and Erk, or from displacement of the hot plate by the solidifying water. Additional heat was therefore applied to the hot plate and its temperature brought to just above the melting point of the ice. As soon as this occurred the supply of heat was reduced and freezing allowed to recur. This procedure was effective in giving higher thermal conductivity values. After cooling to lower temperatures the same procedure was again found to be necessary. Preliminary values obtained in this was at about −10°C for normal ice and heavy water ice have been plotted in fig. 4. This completes the information at present available.

It seems clear that the thermal conductivity of ice at 0°C is approximately four times that of water at that temperature. Whereas the I.C.T. value at 0°C has been generally confirmed as of the correct order of magnitude, the position is much less satisfactory at lower temperatures. The large differences between the results of Lees and of Jakob and Erk call for consideration.

The thermal conductivity of many crystalline materials has been found to be proportional to the reciprocal of the absolute temperature. This relation is more nearly satisfied by the data of Jakob and Erk.

An independent assessment can also be obtained from consideration of the other substances tested in the same way by Lees. Only one, namely naphthalene, appears to have been studied over a comparable range of temperature by another observer. The thermal conductivity of naphthalene has been determined by Eucken (1911) as one of a number of materials for which reasonably satisfactory results appear to have been obtained. On comparing the two sets of data for naphthalene, it is seen that at temperatures of $-60°$ and $-120°$C Lees' values are respectively 13% and 31% lower than those of Eucken. From fig. 4 it will be seen that for ice Lees' values are again lower by rather comparable amounts, 21% at $-60°$C and 34% at $-120°$C.

These two considerations appear to throw doubts on Lees' values. A probable cause could be the development of cracks within his specimens. Jakob and Erk's values are definitely to be preferred. Even so these are not entirely satisfactory, and there is an obvious need for further investigations to be undertaken, both to confirm these conclusions and to provide the more precise values that are required for single crystals of ice.

§ 7. The Thermal Conductivity of Solid D_2O

The single preliminary observation referred to in § 6 and plotted in fig. 4 appears to be all that is available regarding the thermal conductivity of heavy-water ice. This gave a value comparable with that of normal ice, and it is again clear that very careful work will be required before a definite answer can be given regarding any differences between the thermal conductivities of the two forms of ice. These determinations will also need to be carried out using single crystal specimens so that questions of anisotropy can be resolved.

§ 8. The Density of Water and the Coefficient of Cubical Expansion

Rather than dealing directly with the coefficient of cubical expansion of water the density will be considered. This quantity, or its reciprocal, the specific volume, is more frequently tabulated, and the thermal expansion coefficient for any desired temperature interval can readily be derived from tables of either quantity.

Stott and Bigg (1928) were responsible for the tables of density and specific volume given for water in the International Critical Tables.

Their values for the range 0° to 40°C, which were given to seven places of decimals and at 0·1°C intervals, have frequently been used as the basis for comparative determinations on other liquids. The values were stated to be the means of those reported by Thiesen *et al.* (1900) and Chappuis (1907), and the differences were also tabulated.

For the range 40° to 100°C values taken from the work of Thiesen (1918) are given at 1°C intervals and to five places of decimals. For supercooled water values, based on determinations by Mohler (1912), are given to four decimal places at 1°C intervals down to $-13°$C.

On the basis of work by Chappuis (1910), the density of water saturated with air was stated to be $0{\cdot}000003_0$ g/ml less than the density of air-free water over the range 5° to 8°C.

It is now desirable to consider the above values in the light of subsequent work.

Whereas Thiesen *et al.* had found that their density values for the range 0° to 40°C could be satisfied by a four-constant formula, Chappuis had used three separate cubics in temperature, t, for the range of density values from 0° to 40°C. In view of this Tilton and Taylor (1937) re-examined Chappuis' experimental data and found them to be rather better fitted by a very similar four-constant formula:

$$1-d=\frac{(t-3{\cdot}9863)^2}{508929{\cdot}2}\,\frac{t+288{\cdot}9414}{t+68{\cdot}12963}$$

where d is the density in g/ml at t°C. The table of density values prepared from this equation shows only minor changes from Chappuis' original table.

The main new determination has been by Smith and Keyes (1934), who, on the basis of an extensive investigation conducted to high temperatures and pressures, published tables giving the specific volumes of water at 10°C intervals from 0° to 360°C at saturation vapour pressure and at various pressures up to 350 atmospheres. Towards the lower temperatures some differences are noticeable between these values and those of the I.C.T. They amount to 27 and 24 parts in 10^5 at 10°C and 20°C respectively.

The International Steam Tables (1935) include values for the specific volume of water based on the results of Thiesen *et al.*, Chappuis, and Smith and Keyes. In consequence of these differences, the I.S.T. values differ from the ICT values by almost the stated tolerance of 5 parts in 10^5 over the range 0° to 40°C.

Chang and Tung, in the course of comparative measurements made on heavy water have obtained results for normal water in the temperature range 50° to 100°C which agree with those of Thiesen to within 3 parts in 10^5.

Reference should also be made to Antonoff (1940) and Antonoff and Conan (1949) who have suggested the presence of kinks in the curve for water of density against temperature. In the region of 50·5°C, where the departure was stated to amount to 4 parts in 10^5, Kretschmer (1951) found no deviation, and concluded that the density of water must lie on a smooth curve to within 3 parts in 10^6 over the range 50° to 60°C.

It is interesting to note that Kux (1955) has quite recently prepared tables for the density of water from 0° to 60°C which are in agreement with those of Stott and Bigg.

§ 9. The Density of Heavy Water

According to Stokland *et al.* (1938) heavy water attains a maximum density of 1·10596 g/ml at 11·23°C, whereas normal water attains its

maximum density of 1 at 3·98°c. The main workers to make determinations of the density of heavy water over wide ranges of temperature have been Chang and Chien (1941) to 50°c, Chang and Tung (1949) to 101·4°c, Schrader and Wirtz (1951) to 100°c, Heiks *et al.* (1954) to 250°c and Grossman-Doerth (1955) to 150°c. The values obtained by Heiks *et al.* would seem to be rather less accurate, but those of the other workers show good agreement over their common ranges.

According to Riesenfeld and Chang the densities of water and heavy water become equal at about 370°c, that is at the critical temperature.

A survey of the thermodynamic and transport properties of heavy water has been made by Whalley (1958), which includes molar volumes and ratios of the molar volumes of heavy to normal water to 370°c at 10°c intervals.

§ 10. The Thermal Expansion of Ice

When considering ice in the International Critical Tables, Clarke (1928) gives the density at 0°c as $0{\cdot}9168 \pm 0{\cdot}0005$ g/ml, whilst for the linear expansion coefficient he reproduces curves obtained by Andrews (1886) and Sawyer (1911). These two curves have been reproduced in fig. 5, where they will be seen to differ appreciably from the results of other workers available at that time. Those of Struve (1850), Petterson (1883), Nichols (1899), Vincent (1902) and Dewar (1902) have also been included in this figure, together with two later sets of results. The latter appear to be in reasonably good agreement over their common range.

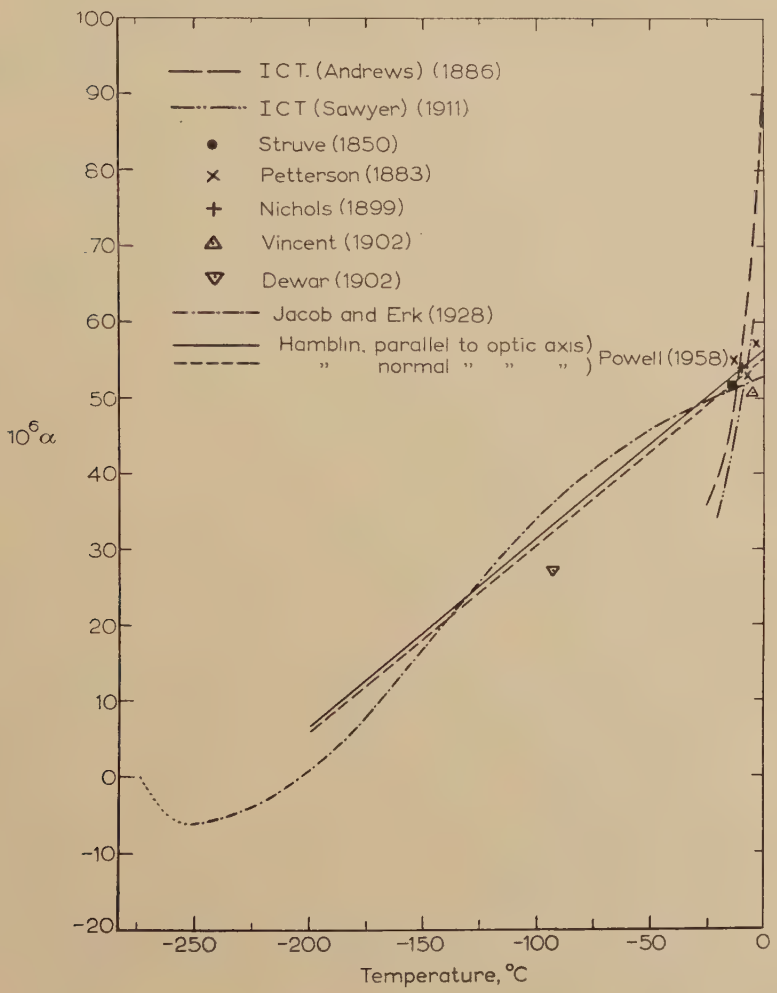
Jakob and Erk (1928) made measurements using a dilatometer on three rods of ice that had been frozen in paper tubes. They remarked that before testing, the rods were clear and free from air bubbles with the exception of some small air bubbles in the centre of the rod. After testing, transverse cracks inclined to the axis, developed, but the rod was not noticeably weakened. The values obtained for the rods differed a little amongst themselves and the reproduced curve represents their weighted mean values. At temperatures below -200°c the coefficient changed sign, and they extrapolated their curve to a value of zero at the absolute zero.

In discussing these results Jakob and Erk draw attention to a very similar type of variation which had been obtained by Grüneisen and Goens (1924) for a single crystal of zinc when measured in a direction at right angles to the crystal axis. They attempted an examination of one of their specimens in polarized light. Whilst no regular crystal orientation was apparent, they concluded that several individual crystals had grown radially and would therefore be similarly oriented with respect to their direction of measurement. They attributed the small differences in their results to possible crystal differences in their specimens.

Hamblin, as reported by Powell (1958), has determined the thermal expansion of ice down to liquid-nitrogen temperatures using single crystals. The original single crystals from which rods approximately 10 cm long

and 0·6 cm diameter were cut, were prepared by seeding and slowly cooling de-aerated water. They were tested by means of plane polarized light. The lengths were observed at different temperatures when the rods were mounted in a silica tube and an extension piece of silica made contact with a sensitive micrometer. From these observations and after

Fig. 5



Coefficient of linear thermal expansion of ice.

correcting for the expansion of silica the linear thermal expansion coefficients were found to decrease linearly with decrease in temperature over the range studied. The values for the direction parallel to the optic axis of the crystal being the greater by approximately 1·8% at 0° and by 10% at −200°c.

The corresponding measurements for heavy water ice have yet to be undertaken.

References

Andrews, T., 1886, *Proc. roy. Soc.*, **40,** 544.

Antonoff, G., 1940, *J. phys. Chem.*, **48,** 80.

Antonoff, G., and Conan, R. J., 1949, *Science*, **109,** 255.

Arzybyschew, S., and Parfianowitsch, I., 1929, *Z. Phys.*, **56,** 441.

Barratt, T., and Nettleton, H. R., 1929 a, *International Critical Tables*, **5,** 227 ; 1929 b, *Ibid.*, **5,** 231.

Bates, O. K., 1933, *Industr. Engng Chem.*, **25,** 431 ; 1936, *Ibid.*, **28,** 494.

Bates, O. K. and Hazzard, G., 1945, *Industr. Engng Chem.*, **37,** 193.

Bonilla, C. F., and Wang, G. J., 1951, *Progress Rept.* December 1950–February 1951, Atomic Energy Div. Columbia Univ. & E. & I. Du Pont de Nemiors & Co., 17 pp. DP–12.

Braune, B., 1937, *Dissertation*, Univ. Leipzig.

Bridgman, P. W., 1923, *Proc. Amer. Acad. Arts Sci.*, **49,** 1941.

Cecil, O. B., and Munch, R. H., 1956, *Industr. Engng Chem.*, **48,** 437.

Chang, T. L., and Chien, J. Y., 1941, *J. Amer. chem. Soc.*, **63,** 1709.

Chang, T. L., and Tung, L. M., 1949, *Chin. J. Phys.*, **7,** 230.

Challoner, A. R., and Powell, R. W., 1956, *Proc. roy. Soc.* A, **238,** 90.

Chappuis, P., 1907, *Trav. Bur. int. Poids Mes.*, **13,** D 40 ; 1910, *Ibid.*, **14,** D 63.

Clarke, J. R., 1928, *International Critical Tables*, **3,** 43.

Dewar, J., 1902, *Proc. roy. Soc.*, **70,** 236.

Dick, M. F., and McCready, D. W., 1954, *Trans. Amer. Soc. mech. Engrs*, **76,** 831.

van Dusen, M. S., 1929, *International Critical Tables*, **5,** 216.

Erk, S., and Keller, A., 1936, *Phys. Z.*, **37,** 351.

Eucken, A., 1911, *Ann. Phys., Lpz.* (4), **34,** 185.

Frontasev, B. P., 1946, *Zh. Fiz. Khim.*, **20,** 91.

Gillam, D. G., and Lamm, O., 1955, *Acta chem. scand.*, **9,** 675.

Grossman-Doerth, U., 1955, *Z. Naturf.*, **10 a,** 799.

Grüneisen, E., and Goens, E., 1924, *Z. Phys.*, **29,** 141.

Heiks, J. R., Barnett, M. K., Jones, L. V., and Orban, E., 1954, *J. phys. Chem.*, **58,** 488.

van der Held, E. F. M., and van Drunen, F. G., 1949, *Physica*, **15,** 865.

van der Held, E. F. M., Hardebol, J., and Kalshoven, J., 1953, *Physica*, **19,** 208.

Hill, R. A. W., 1957, *Proc. roy. Soc.* A, **239,** 476.

Howieson, J., 1957, A. E. of Canada Ltd., Chalk River Project Research & Development, NEI—77, August, 5 pp.

Hutchinson, E., 1945, *Trans. Faraday Soc.*, **41,** 87.

International Conference on Steam Tables. The Third, 1935, *Mech. Engng*, **57,** 710.

Jäger, G., 1890, *Wien Sitzungsberichte der Kais Akad. der Wiss.*, **99,** (2a), 245.

Jacob, M., 1920, *Ann. Phys. Lpz.*, **63,** 537.

Jakob, M., and Erk, S., 1928, *Z. ges. Kälteind.*, **35,** 125 ; 1929, *Ibid.*, **36,** 229.

Kaye, G. W. C., and Higgins, W. F., 1928, *Proc. roy. Soc.* A, **117,** 459.

Kretschmer, C. B., 1951, *J. phys. Chem.*, **55,** 1351.

Kux, C., 1955, *Phys. chem. Tables Landolt and Bornstein*, **6,** (1) 101.

Landauer, J. K., and Plumb, H., 1956, *Snow, Ice and Permafrost Res. Establishment, Corps of Engrs U.S. Army, Wilmette, Ill., Res. Paper* No. 16, April, 4 pp.

Lees, C. H., 1898, *Phil. Trans*, A, **191,** 399 ; 1905, *Ibid.*, **204,** 433.

Lliboutry, L., 1955, *C.R. Acad. Sci., Paris.*, **240,** 1449.

Malhotra, B. R., 1957, *Mod. Refrig.* **60,** 497.

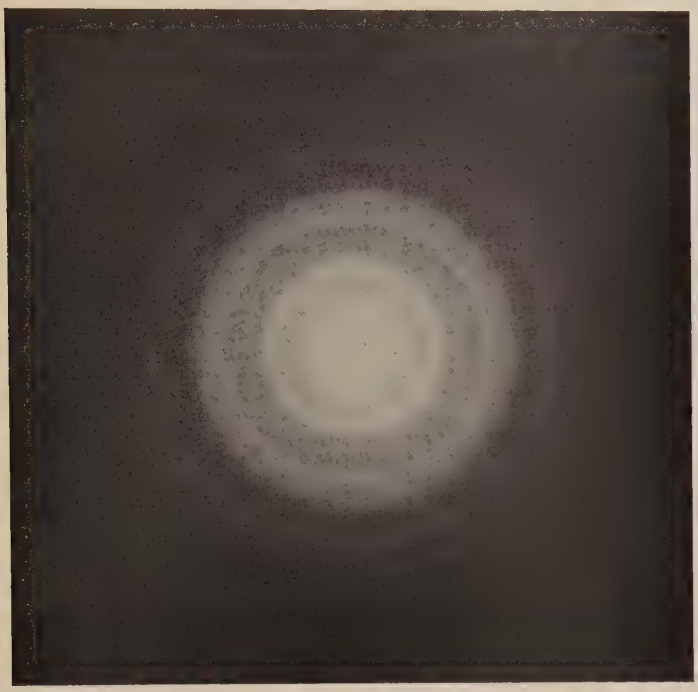
Martin, L. H., and Lang, K. C., 1933, *Proc phys Soc. Lond.*, **45,** 523.

McNall, P. E., 1951, *Dissertation*, Dept. Mech. Engng, Univ. of Purdue.

Meyer, F., and Eigen, M., 1953, *Z. Naturf.*, **8 a,** 500.

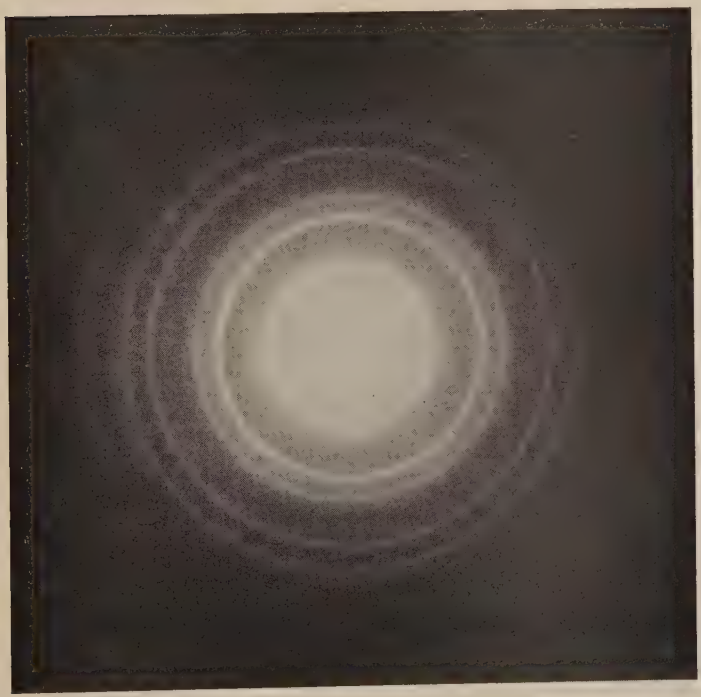
Milner, S. R., and Chattock, A. P., 1899, *Phil Mag.*, **48,** 46.
Mohler, J. F., 1912, *Phys. Rev.*, **35,** 236.
Nichols, E. L., 1899, *Phys. Rev.*, **8,** 184.
Nukiyama, S., and Yoshizawa, Y., 1934, *J. Soc. mech. Engrs Japan*, **37,** 347.
Petterson, O., 1883, *Vega Expedition*, Stockholm, Vol. 2.
Powell, R. W., 1958, *Proc Roy Soc*, A (To be published).
Read, J. H., and Lloyd, D. M. G., 1948, *Trans. Faraday Soc.*, **44,** 721.
Riedel, L., 1940, *Forsch. IngWes.*, **11,** 340 ; 1949, *Chem.-Ing.-Tech.*, **21,** 340 ; 1950, *Z. Kältetechnik*, **2,** 99 ; 1951 a, *Chem.-Ing.-Tech.*, **23,** 321 ; 1951 b, *Ibid.*, **23,** 465 ; 1954, *Arch. tech. Messen*, **1,** 273.
Riesenfeld, E. H., and Chang, T. L., 1936, *Z. phys. Chem.* B, **33,** 120.
Sakiadis, B. C., and Coates, J., 1954, *Bull. La. St. Univ. Exp. Sta.*, No. 48.
Sawyer, W. H., 1911, *Proc. Maine Soc. Civil Engrs.*, **1,** 27.
Schmidt, E., and Leidenfrost, W., 1955, *Forsch. IngWes.*, **21,** 176.
Schmidt, E., and Sellschopp, W., 1932, *Forsch. IngWes.*, **3,** 277.
Schofield, F. S., and Hall, J. A., 1927, *International Critical Tables*, **2,** 315.
Schrader, R., and Wirtz, K., 1951, *Z. Naturf.*, **6 a,** 221.
Schreiber, W. H., 1933, *Dissertation*, Tech. Hochschule Karlsruhe.
Shuleikin, V. V., Rosakov, N. I., and Rybchikov, V. A., 1931, *J. Geophys. U.S.S.R.*, **1,** No. 1–2, 179.
Slawecki, T. K., 1953, *Chem. Engng Progr.*, **49,** 49.
Slawecki, T. K., and Molstad, M. C., 1956, *Industr. Engng Chem.*, **48,** 1100.
Smith, J. F. D., 1930, *Industr. Engng Chem.*, **22,** 1246.
Smith, L. B., and Keyes, F. G., 1934, *Proc. Amer. Acad. Arts Sci.*, **69,** 285.
Soonawala, M. F., 1944, *Indian J. Phys.*, **18,** 71.
Stokland, K., Ronaess, E., and Tronstad, L., 1938, *Trans. Faraday Soc.*, **35,** 312.
Stott, V., and Rigg, P. H., 1928, *International Critical Tables*, **3,** 24.
Struve, W., 1850, *S. Forschr. phys.*, **6,** 48.
Thiesen, M., 1918, *Wiss. Abh. phys. tech. Reichsanst.*, **4,** 32.
Thiesen, M., Scheel, K., and Diesselhorst, H., 1900, *Wiss. Abh. phys., Tech. Reichsanst.*, **3,** 68.
Timrot, D. L., and Vargaftig, N. B., 1940, *J. tech. Phys., Moscow*, **10,** 1063.
Tilton, L. W., and Taylor, J. K., 1937, *J. Res. Natl. Bur. Stand.*, **18,** 205.
Vater, H., 1936, *Dissertation*, Leipzig University.
Vincent, J. H., 1902, *Proc. roy. Soc.*, **69,** 422.
Vlassov, L. I., and Uspenski, P. N., 1931, *J. Geophys., U.S.S.R.*, **1,** No. 1–2, 185.
Weber, H. F., 1886, *Repert. Phys.*, **22,** 116.
Weishaupt, J., 1940, *Forsch. IngWes.*, **11,** 20.
Whalley, E., 1958, *Proceedings of Joint Conference on Thermodynamics and Transport Properties of Fluids* (IUPAC and Inst. Mech. Engrs), (to be published).
Woolf, J. R., 1951, *Dissertation.* Dept. Mech. Engng Univ. of Purdue.
Woolf, J. R., and Sibbitt, W. L., 1954, *Industr. Engng Chem.*, **46,** 1947.

Fig. 1



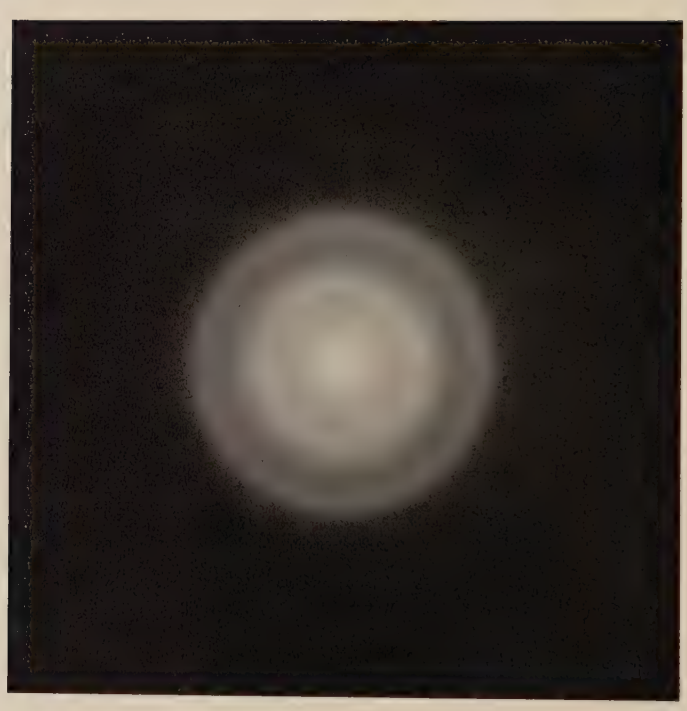
Electron diffraction pattern from hexagonal ice.

Fig. 2



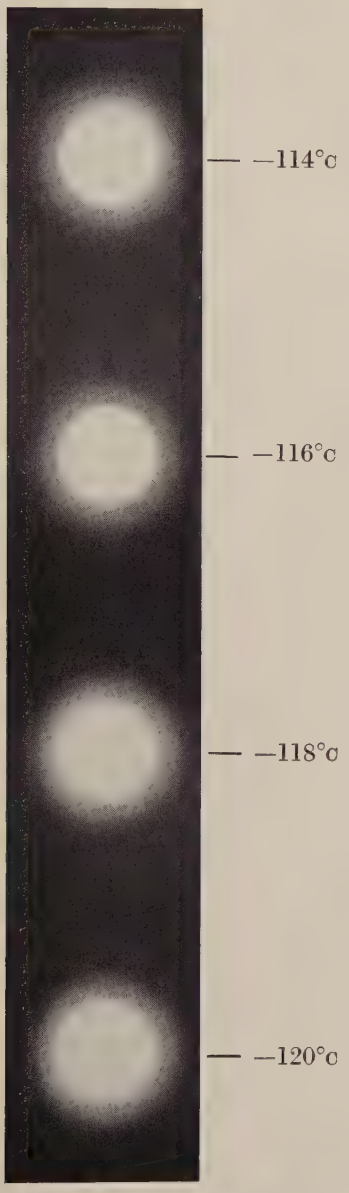
Electron diffraction pattern from cubic ice.

Fig. 3



Diffuse ring pattern from deposits made below −140°C.

Fig. 4



Diffraction patterns showing transition from diffuse to sharp (cubic) ring system.

Fig. 5



Reflection pattern obtained from a thick layer of the cubic form of heavy ice deposited on cleaved galena. The deposit has a preferred orientation with the [110] direction perpendicular to the surface of the galena.

Fig. 1



Hexagonal prismatic columns containing funnel-shaped cavities from isolated cirrus clouds at −50°C. (From Weickmann 1947.)

Fig. 2



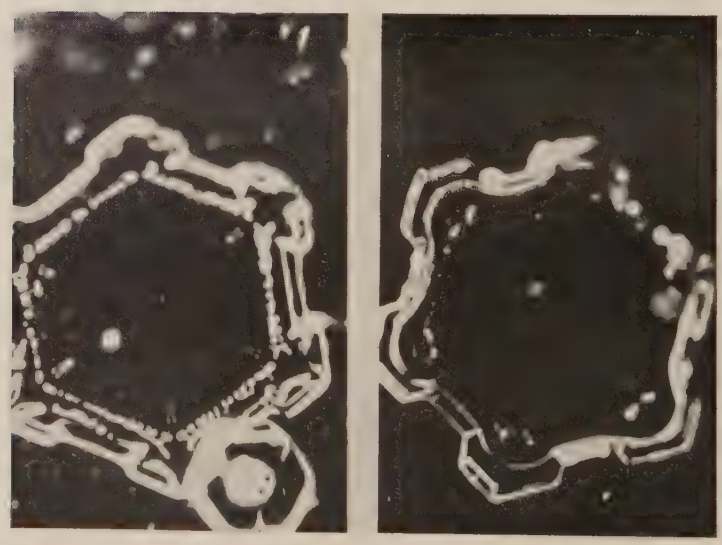
Clusters of hollow prisms from isolated cirrus at −44°C. (From Weickmann, op. cit.)

Fig. 3



Complete prismatic crystals, some with pyramidal faces, from cirrostratus at −26°C. (From Weickmann, op. cit.)

Fig. 4



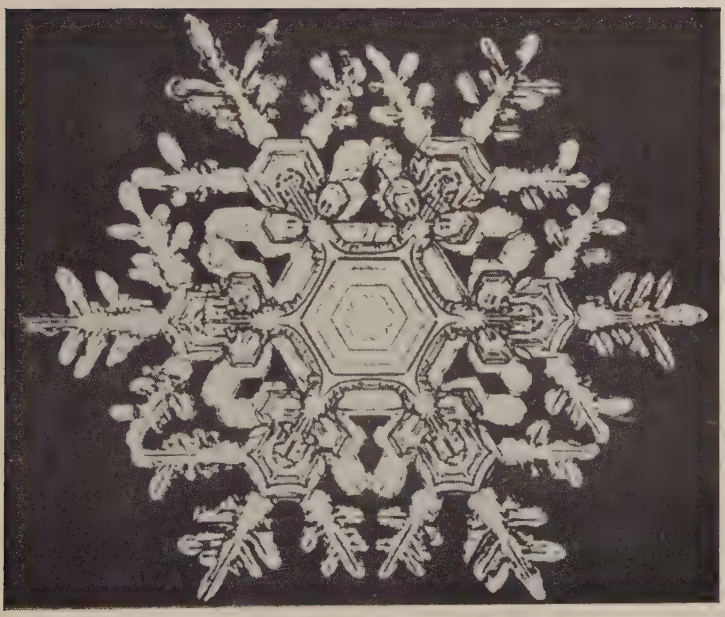
Thin hexagonal plates.

Fig. 5



A sector plate crystal.

Fig. 6



A hexagonal plate which has developed into a richly-branched (dendritic) stellar crystal. (From Bentley and Humphreys 1931.)

Fig. 7



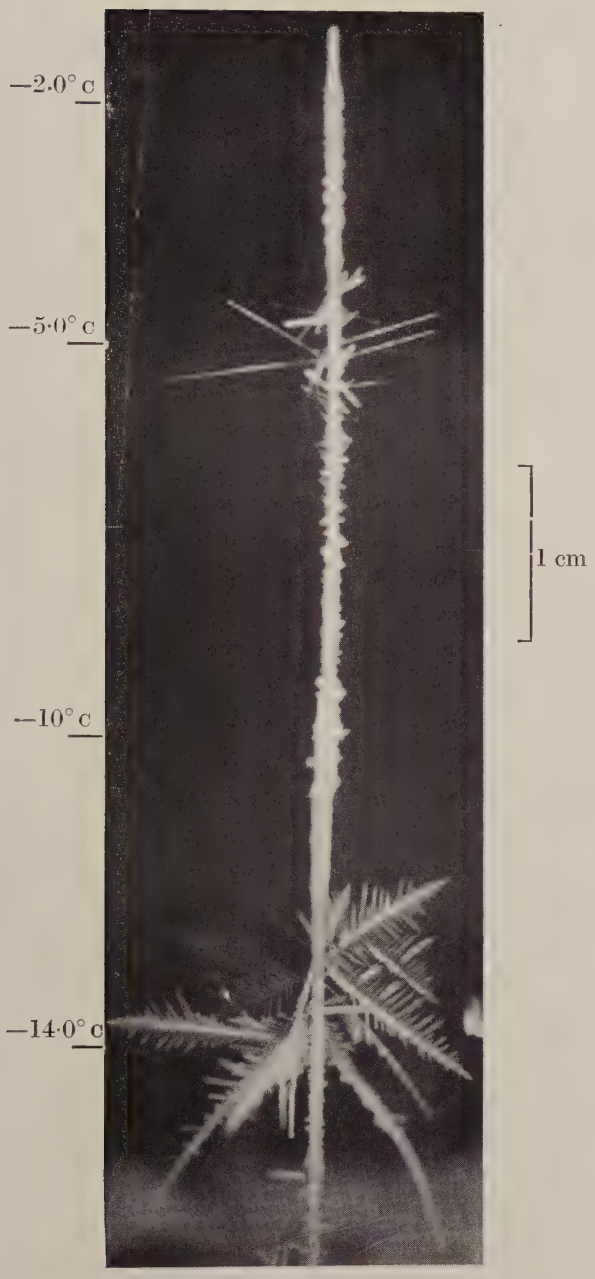
Needle-like crystals. (From Nakaya and Hasikura 1934.)

Fig. 8



A hexagonal column capped with hexagonal plates. (From Bentley and Humphreys 1931.)

Fig. 11



The variation of crystal habit along a part of the fibre in the diffusion chamber. The temperature varies from −2°c to −20°c with the saturation ratio everywhere exceeding 2·0. The sequence is plates→ needles→ hollow prisms→ plates→ dendrites.

Fig. 12



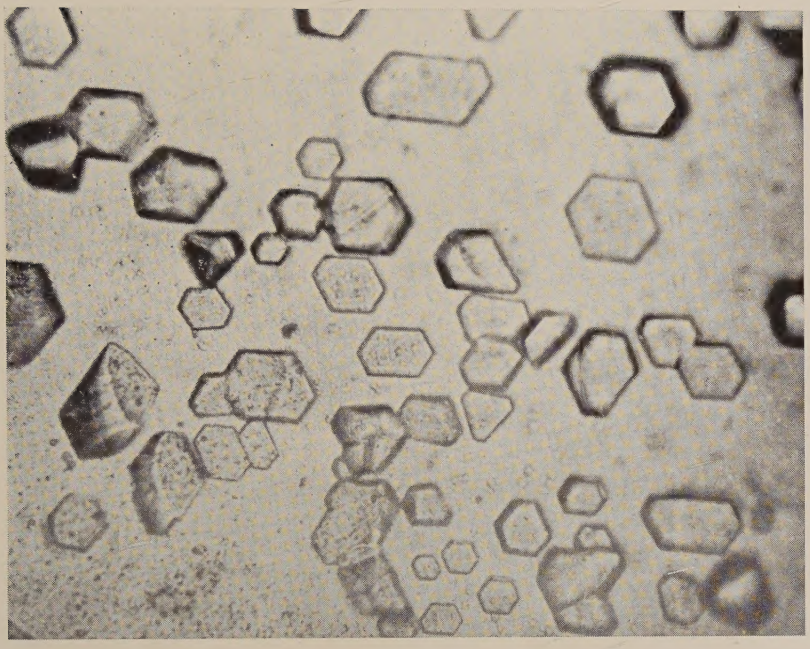
Needles grown at about $-4{\cdot}5^{\circ}$C developed plates on their ends when transferred into a new environment at about $-1{\cdot}5^{\circ}$C.

Fig. 13



Crystals showing multiple changes of habit viz: needles → plates → hexagonal cups → needles as the result of being moved successively from -4°C → -13°C → -8°C → -4°C.

Fig. 14



The oriented growth of hexagonal plate-like ice crystals on the basal plane of a single crystal of silver iodide at $-20°$C.

JUN 8 1958
FILED IN STACKS

A new International Journal

Molecular Physics

Editor: H. C. LONGUET-HIGGINS, F.R.S.
Associate Editor: J. H. VAN DER WAALS

Editorial Board:

J. Bjerrum, *Copenhagen*; G. Careri, *Padua*; C. A. Coulson, *Oxford*; F. H. C. Crick, *Cambridge*; P. J. W. Debye, *Cornell*; D. Hadzi, *Ljubljana*; O. Hassel, *Oslo*; W. Heitler, *Zürich*; J. O. Hirschfelder, *Wisconsin*; D. F. Hornig, *Princeton*; J. A. A. Ketelaar, *Amsterdam*; J. G. Kirkwood, *Yale*; R. Kronig, *Delft*; J. W. Linnett, *Oxford*; A. Liquori, *Rome*; Dame Kathleen Lonsdale, *London*; P-O. Löwdin, *Uppsala*; M. Magat, *Paris*; W. Moffitt, *Harvard*; R. S. Mulliken, *Chicago*; A. Münster, *Frankfurt*; L. J. Oosterhoff, *Leiden*; L. E. Orgel, *Cambridge*; J. A. Pople, *Cambridge*; I. Prigogine, *Brussels*; R. E. Richards, *Oxford*; J. S. Rowlinson, *Manchester*; G. S. Rushbrooke, *Newcastle upon Tyne*; L. E. Sutton, *Oxford*; H. W. Thompson, *Oxford*; B. Vodar, *Bellevue, Paris*.

Contents of April, 1958

Wave Functions for the Methane Molecule. By Ian M. Mills, Department of Theoretical Chemistry, Cambridge University

Vibrational Intensities in Methane. By Ian M. Mills, Department of Theoretical Chemistry, Cambridge

The absorption Spectra of Aromatic Carbonium Ions in HF solution. By G. Dallinga, E. L. Mackor and A. A. Verrijn Stuart, Koninklijke/Shell-Laboratorium, Amsterdam, (N. V. De Bataafsche Petroleum Maatschappij)

Concentration Quenching in Fluorescent Acene Solutions. By A. Dammers-de Klerk, Laboratory for General and Inorganic Chemistry, University of Amsterdam, The Netherlands

Electronic Spectra of Alternant Hydrocarbon di-negative Ions. By P. Balk, S. De Bruijn and G. J. Hoijtink, Chemical Laboratory of the Free University, Amsterdam

Electron Spin Densities in Alternant Hydrocarbon Mono-negative and Mono-positive Ions and in Odd Alternant Hydrocarbon Radicals. By G. J. Hoijtink, Chemical Laboratory of the Free University, Amsterdam.

A Contribution to the Theory of the Exchange Narrowing of Spectral Lines. By R. A. Sack, Department of Theoretical Chemistry, University of Cambridge, and British Rayon Research Association, Manchester

The Effect of Quadrupole Relaxation on Nuclear Magnetic Resonance Multiplets. By J. A. Pople, Department of Theoretical Chemistry, University of Cambridge

Molecular Orbital Theory of Aromatic Ring Currents. By J. A. Pople, Department of Theoretical Chemistry, University of Cambridge

A Molecular Orbital Treatment of the Vinyl Chloride Molecule. By M. Simonetta, G. Favini and S. Carrà, Physical Chemistry Department, University of Milan, Italy

Open Shell Calculations for the Two- and Three-Electron Ions. By R. P. Hurst, J. D. Gray, G. H. Brigman and F. A. Matsen. Departments of Chemistry and Physics, University of Texas, Austin

Paramagnetism in Molecular Compounds. By H. M. Buck, J. H. Lupinski and L. J. Oosterhoff, Division of Theoretical Organic Chemistry, Leiden University

Price per part £1 5s. 0d., plus postage

Subscription per volume (4 issues) £4 15s. 0d. post free, payable in advance

Printed and Published by

TAYLOR & FRANCIS LTD

RED LION COURT, FLEET STREET, LONDON, E.C.4

Orders originating in U.S.A. and Canada should be sent to the Academic Press Inc., 111 Fifth Avenue, New York, 3, N.Y., U.S.A.